

DISPLACEMENT OF WATER FROM A TITANIUM DIOXIDE
SURFACE BY AN ORGANIC LIQUID

A thesis submitted for the degree of
Doctor of Philosophy of the University of London
and the
Diploma of Imperial College

by

RICHARD STRATTON-CRAWLEY

Department of Mineral Resources Engineering,
Royal School of Mines,
Imperial College,
London University.

August, 1977

'TO ALL TO WHOM THESE PRESENTS SHALL COME ' (1)

ABSTRACT

The limitations of the froth flotation process at very fine particle sizes have been discussed and the methods of overcoming them by the use of non-polar oils reviewed.

An investigation has been made of the extraction of sub-micron TiO_2 (rutile) particles from an aqueous phase into an organic phase. The surfactants used were a homologous series of alkyl sulphates with 12, 14, 16 and 18 carbon atoms in their hydrocarbon chains and hexadecyltrimethylammonium bromide (CTAB). Various oil phases were employed but the system most extensively investigated was rutile/water/benzene. In addition to extraction tests studies were also made of the interfacial conditions required for extraction.

Extraction of rutile into oil with CTAB occurred when the oil/water interfacial tension was below a certain critical value and the contact angle approached 180° . The same was not true with the alkyl sulphates, although a contact angle of 180° was still required. Interaction between water dissolved in the oil and the highly charged alkyl sulphate-coated rutile surface is suggested as the reason for the difference in the extraction conditions with CTAB and alkyl sulphate.

Results are presented that show that the adsorption of surfactants at the rutile/water interface is consistent with Coulombic attraction and chain-chain associations (hydrophobic bonding) at high adsorption densities.

Evidence is presented that shows that with long-chain alkyl sulphates dimerization occurs in solution and this complicates interpretation of interfacial tension data. Furthermore under similar conditions armoring of an oil drop can occur so that an apparently oleophilic rutile surface gives an oleophobic response to a captive drop.

ACKNOWLEDGEMENTS

I wish to express my sincere thanks to Dr. H.L. Shergold for his invaluable guidance and encouragement during the last three years.

I should also like to express my gratitude to Dr. J.A. Kitchener and my colleagues in the Royal School of Mines for many useful discussions.

I am indebted to the Science Research Council for financial assistance provided during the course of this work.

Finally, I should like to thank Mary, who put up with my bad moods when experiments went wrong, and Caroline, who deciphered my handwriting and typed this thesis.

	<u>Page</u>
ABSTRACT	1
ACKNOWLEDGEMENTS	2
LIST OF CONTENTS	3
LIST OF FIGURES	7
LIST OF TABLES	10
1. <u>INTRODUCTION.</u>	12
1.1 Froth flotation: displacement of water from a solid surface by air.	13
1.2 Floatability of fine particles.	16
1.3 Recovery processes involving oil.	18
1.3.1 Collector extender flotation.	19
1.3.2 Emulsion flotation.	19
1.3.3 Spherical agglomeration.	20
1.3.4 Oil flotation.	21
1.3.5 Pigment flushing.	23
1.4 Aim of project.	25
2. <u>INTERFACIAL CHEMISTRY OF THE SYSTEM, OXIDE/WATER/OIL.</u>	27
2.1 Theory of emulsions.	28
2.1.1 Stabilization of emulsions by surface-active agents.	28
2.1.1.1 Macroscopic theories of stability.	28
2.1.1.2 Structural theories of stability.	29
2.1.1.3 Electrical theories of stability.	30
2.1.2 Stabilization of emulsions by solid emulsifiers.	30
2.2 Electrical phenomena at the oxide/water interface.	31
2.3 Adsorption of surfactants at the oxide/water interface.	35
3. <u>EXPERIMENTAL.</u>	40
3.1 Materials.	41
3.2 Extraction studies.	44

	<u>Page</u>
3.3 Electrokinetic studies.	46
3.3.1 Electrophoresis.	46
3.3.2 Experimental procedure.	47
3.4 Adsorption measurements.	48
3.4.1 Experimental procedure.	48
3.4.2 Alkyl sulphate analysis.	48
3.4.3 CTAB analysis.	50
3.5 Contact angle measurements.	51
3.5.1 Apparatus.	51
3.5.2 Experimental procedure.	51
3.6 Surface/Interfacial tension measurements.	52
3.6.1 General.	52
3.6.2 Apparatus.	53
3.6.3 Experimental procedure.	54
4. - 6. <u>RESULTS AND DISCUSSION.</u>	56
4. <u>SOLID/WATER INTERFACE.</u>	57
4.1 Electrokinetic studies.	57
4.1.1 System modified by alkyl sulphates.	57
4.1.2 System modified by CTAB.	65
4.2 Adsorption studies.	68
4.2.1 Adsorption of alkyl sulphates at the rutile/water interface.	68
4.2.2 Adsorption of CTAB at the rutile/water interface.	75
4.2.3 Effect of supporting electrolyte on adsorption of CTAB at the rutile/water interface.	79
5. <u>SOLID/WATER/OIL SYSTEM.</u>	80
5.1 Extraction studies.	80
5.1.1 Systems modified by alkyl sulphates.	80
5.1.1.1 Effect of hydrocarbon chain length.	80

	<u>Page</u>
5.1.1.2 Effect of organic phase.	87
5.1.1.3 Effect of additives.	97
5.1.1.4 Effect of agitation intensity.	97
5.1.1.5 Effect of phase volume.	97
5.1.1.6 Reversibility of extraction.	98
5.1.2 Systems modified by CTAB.	98
5.2 Contact angle measurements.	101
5.2.1 Effect of alkyl sulphate concentration on the contact angle.	101
5.2.2 Effect of oil phase on the contact angles in systems modified by alkyl sulphates.	107
5.2.3 Contact angles in systems modified by CTAB.	109
6. <u>OIL/WATER INTERFACE</u>	112
6.1 Interfacial tension measurements.	112
6.1.1 Effect of sodium alkyl sulphates on the benzene/water interfacial tension.	112
6.1.2 Effect of sodium alkyl sulphates on the air/water surface tension.	118
6.1.3 Effect of potassium and lithium alkyl sulphates on the benzene/water interfacial tension.	118
6.1.4 Interfacial tension between various oils and water in systems modified by alkyl sulphates.	123
6.1.5 Effect of CTAB on the oil/water interfacial tension.	124
6.1.6 Adsorption at the oil/water interface.	126
7. <u>GENERAL DISCUSSION</u>	130
7.1 Displacement of water from a solid surface by an oil : Theoretical considerations.	131

7.2	Adsorption at the rutile/water, water/oil and rutile/oil interfaces in relation to extraction of particles into the oil phase.	134
7.3	Work of adhesion of oil drops to the rutile surface.	137
7.4	Displacement of water from a solid surface by organic liquid.	139
7.4.1	Systems modified by CTAB.	139
7.4.2	Systems modified by alkyl sulphates.	142
8.	<u>CONCLUSIONS</u>	145
	REFERENCES.	149

	<u>LIST OF FIGURES</u>	<u>Page</u>
2.1	Stern-Grahame model of the solid/water interface in (a) the absence and (b) the presence of specific adsorption.	36
	
3.1	Calibration curves for the spectrophotometric determination of the alkyl sulphates.	49
3.2	Calibration curve for the spectrophotometric determination of CTAB.	49
	
4.1	Zeta-potential of rutile as a function of pH.	58
4.2	Zeta-potential of rutile as a function of pH at various SOS concentrations.	59
4.3	Zeta-potential of rutile as a function of SOS concentration at various pH values.	59
4.4	Zeta-potential of rutile as a function of SDS concentration at various pH values.	61
4.5	Zeta-potential of rutile as a function of STS concentration at various pH values.	61
4.6	Zeta-potential of rutile as a function of alkyl sulphate concentration at pH 3.1.	64
4.7	Zeta-potential of rutile as a function of pH at various CTAB concentrations.	66
4.8	Zeta-potential of rutile as a function of CTAB concentration at various pH values.	66
4.9	Adsorption isotherms of SOS on rutile at various pH values.	69
4.10	Adsorption isotherms of alkyl sulphates on rutile at pH 3.1.	70
4.11	Adsorption isotherms of CTAB on rutile at various pH values.	76
4.12	Adsorption isotherm of CTAB on rutile at pH 10.5.	78
4.13	Adsorption isotherms of CTAB on rutile in the presence of supporting electrolyte at pH 6.3.	78
	
5.1	Response of system : rutile/water/n-heptane modified by SDS.	81

	<u>Page</u>
5.2 Response of system : rutile/water/n-heptane modified by STS.	82
5.3 Response of system : rutile/water/n-heptane modified by SHS.	83
5.4 Response of system : rutile/water/n-heptane modified by SOS.	84
5.5 Response of system : rutile/water/benzene modified by SDS.	88
5.6 Response of system : rutile/water/benzene modified by STS.	89
5.7 Response of system : rutile/water/benzene modified by SHS.	90
5.8 Response of system : rutile/water/benzene modified by SOS.	91
5.9 Response of system : rutile/water/cyclohexane modified by SOS.	93
5.10 Response of system : rutile/water/diethyl ether modified by SOS.	94
5.11 Response of system : rutile/water/isobutyl methyl ketone modified by SOS.	95
5.12 Response of system : rutile/water/n-dodecanol modified by SOS.	96
5.13 Response of system : rutile/water/n-heptane modified by CTAB.	99
5.14 Response of system : rutile/water/benzene modified by CTAB.	100
5.15 Effect of alkyl sulphate concentration on contact angles of benzene on rutile at pH 3.1.	103
5.16 Comparison of contact angles of benzene on rutile and adsorption densities at the solid/water interface for SDS, STS and SHS at pH 3.1.	106
5.17 Contact angles of benzene on rutile at pH 3.1 as a function of alkyl sulphate adsorption density.	106
5.18 Effect of STS concentration on contact angles of various organic liquids on rutile at pH 3.1.	108
5.19 Comparison of contact angles of benzene on rutile and adsorption density of CTAB at the solid/water interface at pH 10.5.	110

5.20	Contact angles of benzene on rutile at pH 10.5 as a function of CTAB adsorption density.	110
.		
6.1	Effect of pH on the interfacial tension of the benzene/alkyl sulphate solution interface.	113
6.2	Interfacial tension between benzene and water as a function of sodium alkyl sulphate concentration.	113
6.3	Conductivity of SDS solutions in the presence and absence of benzene.	117
6.4	Interfacial tension between benzene and water as a function of sodium alkyl sulphate chain length at various temperatures.	117
6.5	Surface tension of water as a function of sodium alkyl sulphate concentration.	119
6.6	Interfacial tension between benzene and water as a function of (a) potassium alkyl sulphate concentration and (b) lithium alkyl sulphate concentration.	121
6.7	Interfacial tension between benzene and water as a function of surfactant concentration for (a) dodecyl, (b) tetradecyl and (c) hexadecyl sulphate salts.	122
6.8	Interfacial tension between benzene and water as a function of CTAB concentration.	125
.		
7.1	Model of the system, water/oil/solid.	131
.		

<u>LIST OF TABLES</u>		<u>Page</u>
3.1	XRF analysis of rutile powder.	41
3.2	Oil phases employed.	45
	
4.1	Critical hemimicelle concentration (C_{HMC}) for alkyl sulphates at pH 3.1.	65
4.2	Critical hemimicelle concentration and the first inflexion point in the adsorption isotherms of alkyl sulphates on rutile at pH 3.1.	72
	
5.1	Key to response diagrams.	80
5.2	Classification of oil phases according to their effect on extraction in the system, rutile/water/oil modified by alkyl sulphates.	92
5.3	Classification of oil phases according to their effect on extraction in the system, rutile/water/oil modified by CTAB.	101
5.4	Sessile contact angles of various oils on rutile in the presence of 10^{-4} M CTAB at pH 10.5.	111
	
6.1	Interfacial tension between various oils and alkyl sulphate solutions, and, the response of rutile particles in each system.	124
6.2	Interfacial tension between various oils and CTAB solution, and, the response of rutile particles in each system.	126
6.3	Adsorption densities of surfactants at the benzene/water interface.	128
	
7.1	Surface potential at the benzene/water interface in the presence of SDS, STS and CTAB.	136
7.2	Work of adhesion of water and benzene on rutile as a function of STS concentration at pH 3.1.	138
7.3	Work of adhesion of water and benzene on rutile as a function of CTAB concentration at pH 10.5.	138
7.4	Work of adhesion of water and various oils on rutile in the presence of (a) 6×10^{-4} M STS at pH 3.1 and (b) 10^{-4} M CTAB at pH 10.5.	140

	<u>Page</u>
7.5 Viscosities of various organic liquids at 25 C (165).	143
7.6 Dipole moments of various organic liquids (263).	143
7.7 Solubility of water in various organic liquids at 25° C.	144

.....

CHAPTER 1
INTRODUCTION

1.

INTRODUCTION

1.1 Froth flotation : displacement of water from a solid surface by air

The displacement of water from a solid surface by air has long been utilized in the minerals industry in the process known as selective froth flotation. The process consists of a multicomponent suspension through which air bubbles are allowed to rise and attach to the valuable mineral component. Selectivity is attained by modification of the surface conditions on the mineral to be floated such that a bubble-particle aggregate is formed. Finally, the mineral laden bubbles rise to the surface of the suspension where they are separated off and the products recovered.

The phenomenon of bubble attachment to a solid surface is described by Young's equation (2). For the ideal equilibrium conditions at the solid/liquid/vapour contact line

$$\gamma_{SV} = \gamma_{SL} + \gamma_{LV} \cos \theta \dots \dots \dots (1)$$

where γ_{SV} , γ_{SL} and γ_{LV} are the interfacial tensions of the solid/vapour, solid/liquid and liquid/vapour interfaces, and θ is the contact angle.

The free energy change per unit area associated with attachment of the bubble to a solid surface is given by

$$\Delta G = \gamma_{SV} - \gamma_{SL} - \gamma_{LV} \dots \dots \dots (2)$$

or, substituting for $(\gamma_{SV} - \gamma_{SL})$ from Young's equation

$$\Delta G = \gamma_{LV} (\cos \theta - 1) \dots \dots \dots (3)$$

Thus, any bubble which produces a finite contact angle on a solid surface reduces the net free energy of the system i.e. contact is thermodynamically favourable. Under these conditions the surface is said to be hydrophobic. Conversely, if the contact angle is zero, contact is thermodynamically unfavourable and the surface is hydrophilic.

For a finite value of the contact angle it follows that the following condition must be fulfilled

$$\gamma_{SV} - \gamma_{SL} < \gamma_{LV} \dots \dots \dots (4)$$

This relationship has been used by certain authors (3) (4) to describe the thermodynamic conditions for flotation. Most minerals are hydrophilic, and the contact angle can therefore be increased by decreasing $(\gamma_{SV} - \gamma_{SL})$. Addition of amphipathic surfactants can be used for this purpose.

The decrease in surface or interfacial tension upon adsorption of surfactant at an interface is given by Gibbs' equation (5)

$$d\gamma = - \sum_i \Gamma_i d\mu_i \dots \dots \dots (5)$$

where, Γ_i = surface excess of component i, in moles cm^{-2} .

μ_i = chemical potential of component i.

A similar expression has been derived by Guggenheim (6).

In dilute surfactant solutions equation 5 becomes

$$d\gamma = - RT \sum_i \Gamma_i \cdot d \ln C_i \dots \dots \dots (6)$$

where, C_i = concentration of component i.

It has been argued (4) (7) (8) (9) that an increase in the contact angle must be explained by the decrease of the mineral/air interfacial tension, a decrease which is larger than the decrease in the mineral/liquid interfacial tension. In terms of the surface excess of the surfactant components at the two interfaces, the condition is fulfilled when

$$\Gamma^{SV} > \Gamma^{SL} \dots \dots \dots (7)$$

Given that the thermodynamic conditions are favourable for the displacement of water from a solid surface by air, the attachment process also depends on kinetic parameters. The kinetics of flotation are concerned with the rate at which particles are transferred from the suspension to the froth, and are very dependent on particle size as will be shown later. The mechanism of particle capture may be

subdivided into two stages:

- (i) bubble-particle collision, and
- (ii) bubble-particle attachment.
- (i) Bubble-particle collision.

The initial mechanism of bubble-particle collision is basically a hydrodynamic phenomenon. The probability of collision is dependent on the relative motions of the bubble and particle and on the size and inertia of the particle (10) (11).

Derjaguin and coworkers (12) (13) have postulated an alternative mechanism which could be present, the diffusiophoretic effect. The theory proposes that there is an intermediate stage between collision and attachment where long-range surface forces of dynamic origin are present. According to the theory, adsorbed surfactant ions are swept to the rear of a bubble rising through a suspension and as a result ionic concentration gradients are set up on the bubble surface. The bubble then becomes surrounded by an electrolyte diffusion layer which results in an electric field of the unequal mobility of the surfactant anions and cations. Particles entering this field are attracted or repelled to or from the bubble surface according to the charge of their own electrical double layer. The electric field surrounding the bubble extends up to $10 \mu\text{m}$ from the surface (14) and has an intensity of up to $3 \times 10^6 \text{ Vm}^{-1}$ (15). Experimental evidence has been reported (16) to substantiate the existence of this phenomenon, but its importance in flotation systems is not yet clear (17).

- (ii) Bubble-particle attachment.

Following the collision between a bubble and particle, a thin liquid film still separates them. For attachment to occur, the film must thin and rupture, and then recession of the water from the hydrophobic solid surface must rapidly take place.

The rupture and recession of the film must occur in the time in

which the particle is in close contact with the bubble. The duration of contact has been shown to be a few milliseconds only (18). If the 'induction time' necessary for attachment is longer than the duration of particle-bubble contact, flotation will not occur. There is a close relationship between induction time and practical flotability (19) and it has become a useful tool for determining the kinetics of attachment (20-23).

The mechanism of thinning, rupture and recession of the wetting film has been the subject of investigation. Philippoff (24) considered that an air bubble was an elastic body and that particles colliding with it caused elastic deformation. Adhesion between the bubble and particle must occur during the deformation or when the bubble regained its original shape the particles would be ejected from the surface. This phenomenon has been observed for large particles (>200 mesh) but not for finer particles (25) (26).

The interactions that lead to the thinning and rupture of liquid films have been extensively investigated and will not be examined in detail here. The primary forces involved (27) are London dispersion forces, forces due to overlapping double layers of the particle and bubble, and forces arising from hydration of the solid surface. Additionally, the buoyancy and internal pressure of the bubble contribute to thinning, but are generally small compared to other forces (28).

The forces involved in thinning and rupture have been analysed using the concept of 'disjoining pressure' (29). This parameter includes all the surface forces and is taken to be positive when the film resists thinning.

1.2 Flotability of fine particles

The problems involved in the flotation of fine particles have

been the subject of extensive reviews (30) (31). Many workers have shown that there is an optimum size for flotation, generally 20-70 μ m (24), depending on the characteristics of the ore being treated. Below this optimum size flotation rate decreases with decreasing size.

The experimental studies on the effect of particle size on flotation rate are varied and give conflicting results. Tomlinson and Fleming (32) found that under 'free' flotation conditions the rate decreased with the square of the particle diameter, whereas under 'inhibited' conditions the rate was independent of particle size. This work was, however, carried out under ideal conditions and its relevance to practical flotation is, therefore, uncertain. Gaudin, Schuhmann and Schlechten (33) showed that the flotation rate of galena with potassium ethyl xanthate as collector was proportional to particle size down to 5 μ m, but below this size it became constant. A logarithmic relationship between rate and particle size was found by Morris (34) when floating a copper concentrate. Bushell (35), investigating the flotation of quartz with n-decyl amine acetate, found that flotation rate was independent of particle size for particles smaller than 150 mesh. Finally, no relationship was observed by de Bruyn and Modi (36) between the flotation rate of quartz with dodecylammonium acetate and particle size at coarse sizes. Their results did, however, indicate a linear relationship at small sizes.

Attempts to develop a theoretical relationship between flotation rate (k) and particle size (r) have been similarly conflicting. Sutherland (11), assuming a direct encounter hypothesis, derived the equation

$$K = \frac{K_1 \cdot r}{K_2 + r} \dots \dots \dots (8)$$

where, K_1 and K_2 are constants. Effects of particle inertia and gravity were assumed to be negligible. Sutherland also showed that the results of Gaudin and coworkers (33) fitted the model, but agreement

was probably fortuitous.

Derjaguin and Dukin (12) argued on theoretical grounds that below a certain critical particle size contact with a bubble would not be made because the particle would be swept away in the streamlines. At intermediate sizes 'diffusiophoretic' forces determine whether or not adhesion would be attained. The critical particle size was not calculated by Derjaguin and Dukin, but Meloy (37) claimed that the theory predicts that all particles finer than $10\mu\text{m}$ should float at the same rate. This is, however, not substantiated by practice and results show a steady decrease in flotation rate with particle size down to $1\mu\text{m}$ (38) (39).

Various methods have been used to improve the efficiency of flotation of fine mineral particles (50) (31). The addition of neutral oils in various amounts in flotation - related processes is one such method and is discussed in the next section.

1.3 Recovery processes involving oil

The use of flotation-related processes utilizing an oil phase is not new. Patents for the oil flotation process date back to 1860 (1). Renewed interest in such techniques has occurred as the need to achieve higher recovery of fine particles has increased.

An oil in water dispersion is energetically more favourable than that of air in water. High oil/water interfacial areas can, therefore, be generated by such emulsions and a corresponding smaller mean drop size results. Systems using an oil phase have the advantage of high probability of particle-drop collisions and also a large interfacial area for particle attachment. In addition, oil droplets have an increased momentum compared with air bubbles, which should favour particle-oil droplet collision.

The processes include collector extender flotation, emulsion

flotation, oil agglomeration, oil flotation and pigment flushing.

The processes differ according to the oil/solid ratio and whether air bubbles are present or not.

1.3.1 Collector extender flotation

Collector extender flotation utilizes the least amount of oil (0 - 1.5 kg/tonne ore). The method involves conditioning the mineral with collector and oil at high pulp density and then floating the hydrophobic component. The purpose of the oil is to aid the distribution of the collector and to increase the hydrophobicity of the collector-coated particles.

Collector extender flotation has been applied to the flotation of feldspar and phosphate ore (40) but in both cases desliming was found to be necessary. Roberts (41) found that desliming was unnecessary when floating sulphidized malachite and azurite with xanthates and 0.2 kg. gas oil/tonne ore. Similarly, Kihlstedt (42) showed that collector extender flotation was insensitive to slime content when floating hematite with a tall oil/fuel oil emulsion. Recovery and grade were improved and tall oil consumption reduced when high fuel oil admixtures were used.

Of interest is the work of Lin and Metzger (43) who floated quartz with dodecyl ammoniumchloride as collector using bubbles of paraffinic gases (ethane, propane and butane). The gases coadsorbed with the collector, increasing the hydrophobicity of the mineral particles, and the rate of flotation and recovery increased.

1.3.2 Emulsion flotation

Emulsion or agglomeration flotation uses larger quantities of oil than collector extender flotation (1 - 100 kg/tonne ore). The process has been applied directly to minerals whose surface properties are such

that they are not readily wetted by water (44). Neutral oils have also been used in conjunction with collectors in the flotation of manganese (45) (46) (47), ilmenite (48) (49) (50), hematite (51) (52) and apatite (53) ores.

The effect of the neutral oil in emulsion flotation is unclear. Karjalahti (53) and Fahrenwald (54) considered that the role of the oil was to adhere to the hydrophobic particles which then formed a selective agglomerate. Intensive conditioning at high pulp density was a prerequisite for this to occur. Lapidot and Mellgren (50), however, showed that flocculation of hydrophobic mineral particles occurred whether a neutral oil was present or not. They concluded that the neutral oil increased the hydrophobic nature of the particle and improved the dispersion of the collector. Livshits and Kuz'Kin (55) have suggested that the hydrophobicity of the mineral surface is unaltered by the addition of a neutral oil, and that its main effect is to decrease the induction time of mineral particles in contact with air bubbles. This effect is attributed to the additional capillary force of the oil film under an air bubble. Some authors (49) (50) maintain that coarse and fine particles can be treated together by emulsion flotation. The work of Lapidot and Mellgren (50) and Karjalahti (53), however, showed that recovery of the valuable mineral increased when deslimed feed was used.

As with collector extender flotation, the oil is generally added as an emulsion, and no separate oil phase is apparent at the end of the process. In both cases the hydrophobic particles or agglomerates are floated by conventional froth flotation techniques.

1.3.3 Spherical agglomeration

Spherical agglomeration involves conditioning a ground ore at high pulp density with a suitable collector so that the valuable

component is rendered hydrophobic, and then collecting the collector-coated mineral with oil. Mixing with the oil is carried out in such a way that the mechanical action provided ensures that oil-continuous spherical pellets containing the hydrophobic component are formed. The condition of the mineral surface must be such that a contact angle greater than 90° is formed i.e. the mineral is preferentially wetted by the oil phase. In the process, the amount of oil used is 2 - 6% of the aqueous pulp volume, and is not apparent as a separate phase at the end of the process.

Puddington and coworkers have investigated the process extensively (56) (57) (58). Mineral systems that have been concentrated by the oil agglomeration process on a laboratory scale include tin (59) (60), gold (61), coal (62) (63), titanium (64), barite (65) and iron (66) (67) ores.

The process has been applied on an industrial scale to the removal of soot in waste water from oil gasification plants (68).

1.3.4 Oil flotation

In all the previous processes the quantity of oil used has been such that no separate oil phase is visible at the end of the separation. Recently, considerable work has been carried out to develop a process that utilizes sufficiently large amounts of oil that a separate oil phase is formed. In this process, called oil or two-liquid flotation, oil is directly substituted for air in the flotation process, oil droplets collecting the hydrophobic component in the pulp instead of air bubbles.

The principle upon which the process is based is the stabilization of emulsions by solid particles (Section 2.1). According to von Reinders (69) three situations may occur in the system oil/water/solid:

1. $\gamma_{SO} > \gamma_{WO} + \gamma_{SW}$ the solid will be dispersed in the aqueous phase.

2. $\gamma_{SW} > \gamma_{SO} + \gamma_{WO}$ the solid will be dispersed in the oil phase.

3. $\gamma_{WO} > \gamma_{SO} + \gamma_{SW}$, or if none of the three interfacial tensions is greater than the sum of the other two, the solid will concentrate at the oil/water interface.

If the interfacial tension between the three phases are modified by use of suitable surfactants such that for a particular mineral component condition 3 is satisfied, it should be possible to concentrate mineral particles at the oil/water interface.

Schulman and Leja (65) investigated the stabilization of emulsions by barium sulphate particles, with alkyl sulphates and other surfactants. When the contact angle was below 90° oil-in-water emulsions were formed, and water-in-oil emulsions were obtained when the contact angle was greater than 90° . These results are consistent with the observation (71) that the phase preferentially wetting the solid will be the continuous phase. At high concentrations of long-chain surfactant the contact angle approached 180° and some barium sulphate particles became dispersed in the oil phase. Takakuwa and Takamori (72) used the fact that phase inversion occurs when the contact angle exceeds 90° in a study of the flotation of galena.

Oil flotation has been applied to many mineral separations on a laboratory and pilot plant scale (73). Shergold and Mellgren (74) (75) applied the process to the separation of fine hematite and quartz particles, using iso-octane as the oil phase and either alkyl sulphates or alkyl amines as collector. Lai and Fuerstenau (76) concentrated fine alumina particles at the iso-octane/water interface using sodium dodecyl sulphate as collector. Similarly, Raghavan and Fuerstenau (77) concentrated $0.2 \mu\text{m}$ hematite particles by oil flotation using potassium octylhydroxamate to control the wettability of the hematite particles. Coleman and coworkers (78) successfully used a two-liquid technique to

extract calcite from ground shale. It has been suggested (79) that the process may also be applied to the concentration of sulphide minerals and diamonds.

Studies have also been made on the application of oil flotation to the recovery of cassiterite slimes (80) (81) (82). Slime fraction losses are considerable in the treatment of tin ores (81). Zambrana and coworkers (81) (82) have developed a continuous oil flotation method for the treatment of minus 10 μm cassiterite with gasoleine as the oil phase and Aerosol 22 as collector. The authors reported recovery of about 80% of the cassiterite in the rougher concentrate with a grade of 6.5% Sn. Cleaner concentrate grades of approximately 14% Sn at recoveries of about 60% were obtained.

Oil flotation has been applied to the removal of impurities, such as anatase, rutile and iron oxide, from minus 5 μm Kaolin clay (83) (84). A pilot plant for the process has been developed by English China Clays Ltd. (85) using kerosene as the oil phase and oleic acid as collector.

The major disadvantage of the oil flotation process is the formation of stable emulsions. Breaking the emulsions to recover the mineral and oil is necessary and is often difficult on a large scale (30).

1.3.5 Pigment flushing

Pigment flushing is a process by which a pigment is transferred directly from an aqueous phase into an organic phase. The process is extensively used in the paint and printing ink industries and has the advantage of avoiding drying and grinding into an oil to obtain a satisfactory oil-based dispersion. Whilst numerous patents exist on the process (a chronological list of U.S. patent has been tabulated by Langstroth (86)), there is a lack of predictive theory of flushing

and dispersion stability in non-aqueous media (87).

The essential requirement for the process to take place is that the contact angle should be as small as possible (measured through the oil phase) (88). Two types of surface treatment are used to render pigments more oleophilic. In the first method an oil-soluble or oil-wettable film is deposited on the solid surface by double decomposition in aqueous medium (89). A water-soluble surfactant (usually anionic) is precipitated on the pigment by a suitable precipitant (e.g. heavy metal salt, cationic surfactant, etc.,). In some cases the interfacial tension of the precipitated film against water is greater than the original pigment surface and at the same time its interfacial tension against oil is lower (88).

The second method involves the adsorption of an amphipathic ion with the paraffin-chain orientated towards the aqueous phase (90). The surfactant acts by lowering the solid/oil interfacial tension rather than increasing the solid/water interfacial tension (88).

Bass (91) claimed that a good flushing agent was; cationic, soluble in water, a flocculating agent in aqueous media and a dispersing agent in non-aqueous media. Anionic surfactants tend to be precipitated under acid conditions and in the presence of heavy metal ions that are present in pigment slurries. Flocculation of the oleophilic particles in the aqueous phase aids the flushing process, but as a result some water is inevitably carried into the oil phase and flushing is usually, therefore, not 100% efficient. The flushing agent should also not act as an emulsifying agent (92) otherwise the flushing process is impaired.

The mechanism of the flushing process has been described by Apps (93). Addition of an oil phase leads to emulsification and the generation of a large interfacial area. Pigment particles near the interface transfer into the oil layer as the contact angle tends to

zero. The initial oil-in-water emulsion passes to an unstable water-in-oil emulsion which breaks down. The viscous oil globules coalesce and the oil and water phases separate.

Gomm et al (94) considered the thermodynamics of the flushing process and estimated the wettability of small particles by an 'apparent boundary tension' method. These authors found that when precipitated anionic surfactants are used as the flushing agent the equilibrium water wettability of the pigment is increased. Flushing, they suggest, occurs due to the free energy arising during the dissolution of the oil-soluble surface coating which overcomes the increase in water wettability. Some associated water is inevitably carried into the oil phase with the pigment. The fundamentals of the process, particularly the degree of oil-wettability, however, have not been determined and pigment flushing still remains an empirical process.

1.4 Aim of project

Mineral separation processes involving an oil phase are based on the establishment of a hydrophobic surface coating and the exploitation of that condition with a flotation-related technique. The extraction of the mineral particles completely into organic phase, analogous to pigment flushing, has not been investigated in detail, although it has been observed (70) (95). Such a process might provide the basis for the selective separation of mineral particles.

It has been inferred that a contact angle of 180° (measured through the aqueous phase) is required before extraction occurs. This corresponds to the thermodynamic condition that

$$\gamma_{SW} > \gamma_{SO} + \gamma_{WO} \dots \dots \dots (9)$$

The nature of the surfactant and the conditions required to obtain this condition are not known.

It was the objective of this work to establish whether or not

mineral particles could be extracted into an organic phase and to determine the conditions required for the displacement of water on a mineral surface by a second immiscible liquid. Particular attention was made to the effect of surfactant type and structure, and oil type, structure and polarity on the oleophilicity of the solid.

The solid phase selected for the investigation was chemically precipitated titanium dioxide (rutile). It was chosen because it has a well characterized surface with a z.p.c. in the region pH 4 - 6 which means that the effects of both anionic and cationic surfactants could be studied. Furthermore, rutile is a commercial pigment and the results obtained might be of interest to both the mineral and pigment industries.

CHAPTER 2
INTERFACIAL CHEMISTRY OF THE SYSTEM,
OXIDE/WATER/OIL

2 INTERFACIAL CHEMISTRY OF THE SYSTEM, OXIDE/WATER/OIL

2.1 Theory of emulsions

When two immiscible liquids are shaken together an emulsion is generally formed which consists of one liquid phase intimately dispersed in the other in the form of droplets. Two types of emulsion may exist in an oil and water system, oil-in-water (O/W) or water-in-oil (W/O) emulsions. The droplet phase is called the disperse or internal phase and the matrix is the continuous or external phase. Emulsions possess a minimal stability which may be accentuated by such additives as surface-active agents, macromolecular compounds and finely-divided solids. The complexity of emulsion systems is such that a detailed description of the phenomenon is beyond the scope of this thesis and for this the reader is referred to the monograph of Becher (96). In view of the importance of emulsions in oil/water systems, however, a brief review of the factors determining emulsion stability is given below.

2.1.1 Stabilization of emulsions by surface-active agents

2.1.1.1 Macroscopic theories of stability

Much of the early work on emulsions was concerned with the effect of the nature and concentration of the emulsifier on the type of emulsion formed (97) (98) (99). Theories of emulsion stability proposed were based on the geometry of the adsorbed emulsifier ion (100) or the lowering of interfacial tension caused by the surfactant (101).

Bancroft suggested two theories relating the nature of the emulsifying agent to the type of emulsion formed which have some usefulness. The original theory (102) postulated that the phase in which the emulsifier was more soluble would be the continuous phase. Bancroft and Tucker (103) later restated the theory pointing out that the inter-

facial film was duplex in nature, that is there were two interfacial tensions present on each side of the interface. Thus, the internal phase was on the side of the film with the higher interfacial tension. The work of Clowes (99) supported the theory.

2.1.1.2 Structural theories of stability

Recent developments in the theory of emulsion stability have emphasized the importance of the properties of the interfacial film. Schulman and coworkers (104) (105) (106) have shown that stable emulsions are formed when strong penetration complexes are formed between species in both the water and oil phases. The interfacial film resulting from such complex formation must possess great strength and resistance to rupture. The interfacial tension must also be a minimum (107) so that dispersion of the oil in the water phase involves as small an increase in free energy as possible. The theory of interfacial complex formation also correlates with the effect of surface viscosities on stability of emulsions (108). The mechanism by which the interfacial film resists coalescence appears to be that desorption of the emulsifying agents from the interface is hindered upon compression of the film (109).

Summarizing the requirements for the stabilization of emulsions by ionic surfactants, Gilbert (110) stated four postulates;

- (1) an interfacial film must form which acts as either a mechanical or electrical barrier to coalescence,
- (2) molecular interaction between molecules at the interface giving rise to a complex interfacial film must occur,
- (3) the interfacial film must be in equilibrium with both phases,
- (4) the physico-chemical structure of the interfacial film depends on the
 - a) distribution of surfactant molecules between the two phases,

- b) nature of the hydrocarbon chain and polar group in the surfactant,
- c) presence of additives in the aqueous phase,
- d) temperature and physical factors,
- e) phase volume ratio.

2.1.1.3 Electrical theories of stability

Oil droplets dispersed in water have a net negative charge (111) (112). The origin of the charge is that cations, having greater primary solvation sheaths, are more strongly attracted to the bulk solution than anions. At the interface, therefore, there is an excess of anions (113). Cations will also be repelled by the dipolar field at the interface.

In the absence of emulsifiers the electrical double layer in the aqueous phase is so small, that two oil drops will coalesce when brought together (114). In the presence of ionic emulsifiers, however, the adsorbed monomolecular surfactant film leads to a large electrical double layer at the interface which imparts stability to the emulsion. Generally, under these conditions, the double layer on the aqueous side of the interface is so large that the double layer on the organic side may be neglected (115). This being so, the DLVO theory (116) (117) for stability of lyophobic colloids can be applied to the stability of emulsions.

2.1.2 Stabilization of emulsions by solid emulsifiers

If a solid particle is partially wetted by the two immiscible liquid phases constituting an emulsion, the particle will take up a stable position at the liquid-liquid interface. Coalescence of emulsion droplets will be inhibited, therefore, as work has to be done to displace the particle from the interface. The action of solids can be

determined simply in terms of the value of the oil-water contact angle on the solid.

Pickering (118) was the first worker to suggest that the condition for the formation of O/W emulsions was that the solid was more readily wetted by the water than by the oil. In support of this conclusion, Briggs (119) observed that ferric hydroxide, arsenic sulphide and silica led to O/W emulsions with kerosene and benzene, whilst carbon black, rosin and lanolin stabilized W/O emulsions.

Solids having a moist gelatinous and basic structure are generally more efficient emulsifiers (120) (121) (122) than dry granular ones. It has also been shown (123) that with a given solid, the type of emulsion formed was dependent on the technique of shaking.

The thermodynamic criteria describing the distribution of solids between two mutually insoluble liquids according to Von Reinders (59) have already been mentioned (section 1.3.4). In the case where solid collects at the liquid-liquid interface and thus stabilizes emulsions, Young's equation may be applied in the form

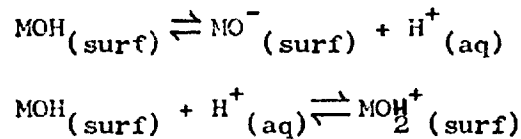
$$\gamma_{SO} - \gamma_{S:} = \gamma_{WO} \cos\theta \dots \dots \dots (1)$$

If $\gamma_{SW} > \gamma_{SO}$ then $\cos\theta$ is positive and $\theta < 90^\circ$, and the major portion of the solid will be in the aqueous phase. Similarly if $\gamma_{SO} < \gamma_{SW}$, $\theta > 90^\circ$ and the particle will be largely in the oil phase. Thus, it would appear that the phase which has the larger interfacial area will be the external phase. The work of Schulman and Leja (70) confirmed this theory.

2.2 Electrical phenomena at the oxide/water interface

An electrical charge arises at the solid/solution interface upon immersion of a solid in aqueous solution. The major portion of a metal oxide surface is composed of relatively polarizable oxide ions

interspersed with oxygen ions bridged to metal ions, rather than the less polarized metal ions (124). Thus, for simple oxide minerals, such as rutile, hydration of the solid surface followed by adsorption or dissociation of hydrogen ions from the surface hydroxyls has been postulated as the source of the surface charge (125). The hydration step is an attempt by the exposed surface atoms to complete their coordination shell of nearest neighbours. The mechanism may be written



Thus, hydrogen and hydroxyl ions are potential determining ions for oxides in aqueous media, together with the lattice ions.

At all values of pH there will be a distribution of positive, negative and neutral sites on the oxide surface (126) and at a certain pH there will be no net charge on the surface. This pH is called the zero point of charge (z.p.c.). The z.p.c. varies between oxides and is dependent on the appropriate cationic charge and radius (127).

Alternative surface charging mechanisms have been reviewed by MacKenzie (128). The adsorption of charged hydroxo complexes of the form $\text{M}(\text{OH})_{\text{n}}^{z-\text{n}}$ has been proposed by Parks and De Bruyn (129). The concentration of these complexes in solution is pH controlled and therefore electrokinetic measurements do not permit selection between this and the above mechanism. Parks (127) further suggested that frequently observed discrepancies between the z.p.c. and isoelectric point (as measured by electrokinetic methods) are due to the adsorption of polynuclear hydroxo complexes which are slow to equilibrate in solution.

The dependence of the surface potential (ψ_0) on aqueous solution composition is given by the Nernstian expression

$$\psi_0 = \frac{kT}{ze} \cdot \ln a/a_0 \dots \dots \dots (2)$$

where, k = Boltzmann constant.
 T = absolute temperature.
 z = valence of potential-determining ion.
 e = electronic charge.
 a = activity of the potential-determining ion.
and a_c = activity of the potential-determining ion at the z.p.c.

The electrical double layer, comprising the surface charge and counter ions, was originally investigated by Helmholtz (130) and the concept later modified by Gouy (131) and Chapman (132). These authors considered that the distribution of ions in solution in a direction normal to the surface was given by the following form of the Boltzmann equation

$$n_i = n_o \exp (-z_i e \Psi / kT) \dots \dots \dots (3)$$

where, n_i = concentration of ions (i) at a point where the potential is Ψ .
 n_o = concentration of ions in the bulk solution.

Using the Poisson equation relating the electrical potential and the space charge density they showed that

$$\sigma = \sqrt{\frac{2 \epsilon \kappa e k T}{\pi}} \cdot \sinh \frac{z e \Psi_o}{2 k T} \dots \dots \dots (4)$$

where, σ = surface charge.
 ϵ = dielectric constant.
 n = total concentration of symmetrical indifferent electrolyte.
 Ψ_o = total double layer potential.

When the potential is so small ($\ll 25\text{mV}$) that the exponentials may be expanded, equation 4 becomes

$$\sigma = \frac{\epsilon \chi}{4 \pi} \cdot \Psi_o \dots \dots \dots (5)$$

where, χ = Debye-Huckel function, $\left[\frac{8 \pi n z^2 e^2}{\epsilon k T} \right]^{\frac{1}{2}}$. i.e. the reciprocal of the ionic radius, which is a measure of double layer thickness.

For small values of Ψ_o , the potential at a distance x from the surface can be shown to be

$$\Psi_x = \Psi_o e^{-\chi x} \dots \dots \dots (6)$$

Equation 6 shows that the potential falls exponentially to zero

as the distance from the solid surface is increased.

For a point far from a surface of high potential i.e. $\frac{ze\psi_0}{kT} \gg 1$
 and $\frac{ze\psi_x}{kT} \ll 1$,

$$\psi_x = \frac{4kT}{ze} \cdot \beta \cdot e^{-\lambda x} \dots \dots \dots (7)$$

where, $\beta = \frac{\exp(ze\psi_0/2kT) - 1}{\exp(ze\psi_0/2kT) + 1} \dots \dots \dots (8)$

This treatment of the double layer has three shortcomings;

- (1) the dielectric constant is assumed to be independent of distance from the solid surface. As the dielectric constant of water is known to vary with electric field strength (133), this assumption is clearly not valid.
- (2) ions are assumed to be point charges. This leads to unreasonably high local ion concentrations calculated from equation 3.
- (3) the surface charge is assumed to be smeared over the surface rather than in the form of discrete ions.

Stern (134) extended the theory of Gouy and Chapman by introducing two modifications. He considered that the region near the surface could be divided into two layers, the first consisting of an inner, compact double layer and the second a diffuse Gouy layer. The boundary between the two layers was postulated as the closest a hydrated counter-ion could approach to the surface. This plane of closest approach of counter-ions is called the Stern plane. Stern further allowed for a specific 'chemical' interaction between the ions and the surface i.e. within the Stern layer. Thus, equation 3 must be modified to contain work terms other than those arising from the electrical potential difference, that is

$$n_i = 2rn_0 \exp \left(\frac{-(ze\psi_s - \phi)}{kT} \right) \dots \dots \dots (9)$$

where, r = radius of ion.

ψ_s = potential at the Stern plane, calculated from Gouy-Chapman theory.

ϕ = term allowing for specific 'chemical' forces which exist

between the adsorbed species and the solid surface.

A further improvement on the theory was made by Grahame (135), who took into account the two types of ion present in the Stern layer, namely the hydrated counter-ion and the specifically adsorbed ion. In Grahame's model the specifically adsorbed ion was assumed to be dehydrated and closer to the surface than the other ion. Thus, Stern's concept of a single layer of immobile ions with their centres in one plane was replaced by two parallel planes associated with each type of ion. The two layers are usually called 'inner' and 'outer' Helmholtz planes.

The diagrams given by Grahame (135) which represent the variation of potential in the double layer when specific adsorption is present, and a schematic representation of the double layer are shown in Fig.

2.1.

An interesting model of the rutile/solution interface was proposed by Berubé and De Bruyn (136) in which specific adsorption of inorganic ions in the double layer was related to their disrupting or promoting influence on the structural order of the water molecules in the surface region. Strong specific adsorption, they concluded, was to be expected by those ions which favour structure promotion e.g. Li^+ , Na^+ , and the potential-determining ions, H_3O^+ and OH^- .

2.3 Adsorption of surfactants at the oxide/water interface

The mechanism of adsorption of surfactants at the oxide/water interface has been reviewed by other authors (137). Fuerstenau and coworkers (138) (139) used the Stern-Grahame model of the electrical double layer to explain the adsorption of alkyl-ammonium ions at the quartz/water interface and alkyl sulphonates at the alumina/water interface. They showed that the collector ions were adsorbed as counter-ions in the double layer at low concentrations, but as the

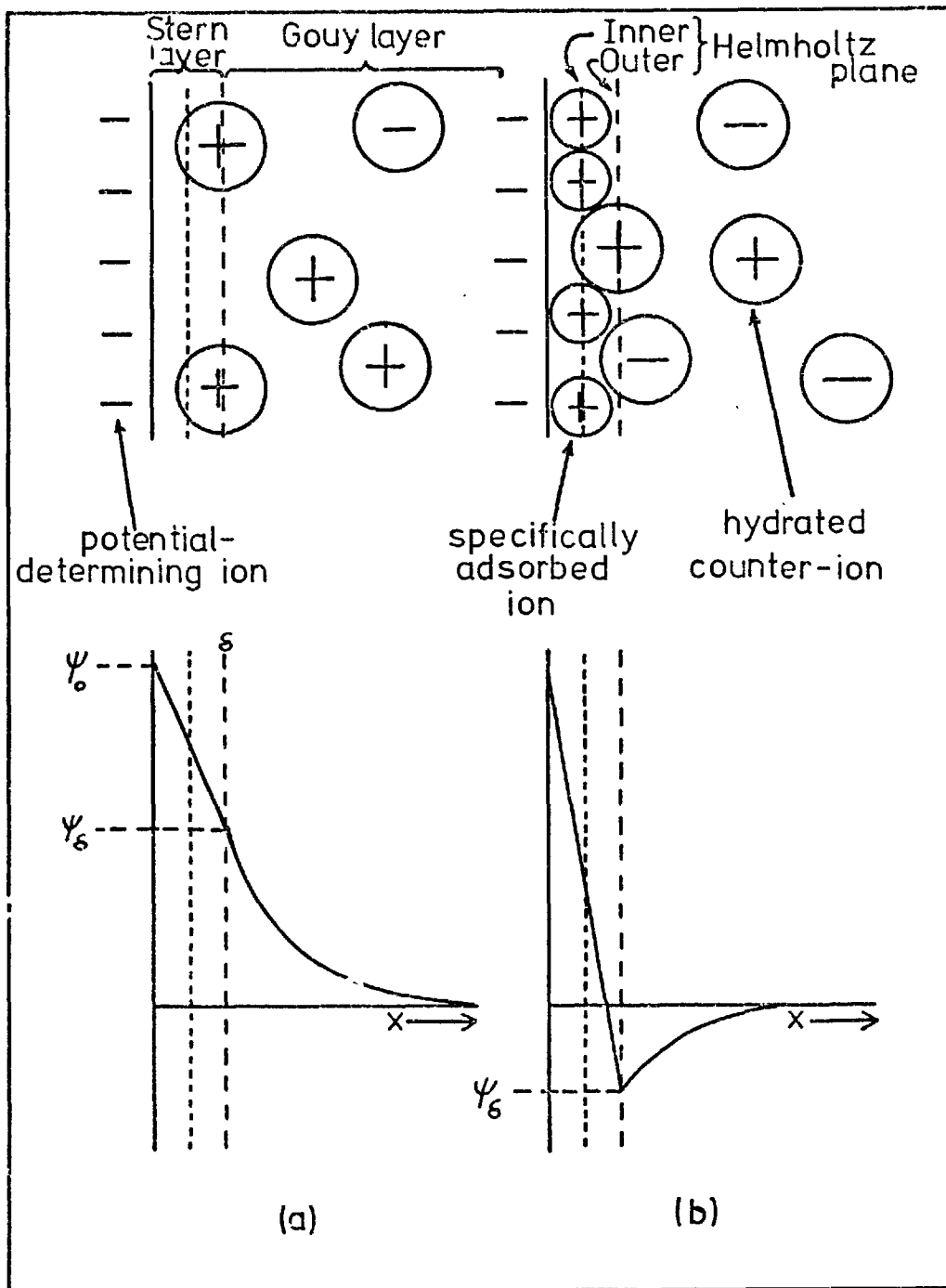


Fig. 2. 1. Stern-Grahame model of the solid/water interface in (a) the absence and (b) the presence of specific adsorption.

adsorption density increased lateral association occurred through interaction of the hydrocarbon chains and the ions become specifically adsorbed. The associated adsorbed species at the surface, termed 'hemimicelles', are the two-dimensional equivalents of the bulk micelle, and have been observed to occur at about $1/100$ of the critical micelle concentration. The lowering of free energy of the system upon adsorption of this kind is given by

$$\Delta G^{\circ}_{ads} = \Delta G^{\circ}_{coul} + \Delta G^{\circ}_{CH_2} \dots \dots \dots (9)$$

$$= ze\psi_s + n\phi_{CH_2} \dots \dots \dots (10)$$

where, ΔG°_{coul} = electrostatic contribution to total free energy.

$\Delta G^{\circ}_{CH_2}$ = interaction due to association of hydrocarbon chains of adsorbed collector ions at the interface.

n = number of CH_2 groups in hydrocarbon chain.

and ϕ_{CH_2} = hydrophobic contribution per mole of CH_2 groups removed from water upon association.

The contribution of the cohesive energy per mole of CH_2 groups has been evaluated to be approximately $-KT$, which is in agreement with values obtained from solubility data and micelle formation (140).

When an ion exhibits specific chemical affinity for the solid surface, e.g. fatty acids at the oxide/water interface (141) (142), an additional term has to be included in equation 10, viz

$$\Delta G^{\circ}_{ads} = ze\psi_s + n\phi_{CH_2} + \Delta G^{\circ}_{chem} \dots \dots \dots (11)$$

where, ΔG°_{chem} = free energy due to formation of covalent bonds with the surface.

Thus, if ΔG°_{chem} is finite, the ion will be adsorbed even if ψ_s is zero or has the same sign as the adsorbing ion. Other free energy terms may be included in equation 11 to account for contributions of solvation effects on the polar head of the surfactant and solid, hydrogen bonding, etc., but generally these can be ignored.

A different approach to the phenomenon of adsorption has been made by Cases and coworkers (143) (144) (145) who considered adsorption as a condensation process on either an homogeneous or inhomogeneous surface. Their treatment showed that isotherms could be predicted on the basis of the nature of the solid surface. For an homogeneous surface where no lateral binding occurred between collector chains the isotherm (a plot of fractional surface coverage versus degree of under-saturation of collector in aqueous solution) would have a small finite slope at low surface coverage followed by an infinite slope up to monolayer coverage as condensation takes place. In the case where hydrocarbon chain interactions occurred, the slope at 0.5 monolayer coverage would have a finite value, but the isotherm would nevertheless be sigmoidal in shape. The authors also showed that for inhomogeneous surfaces, the adsorption isotherm should have a constant slope up to monolayer coverage. On an inhomogeneous surface, when the surface is composed of areas whose adsorption energies are different, the collector will condense area by area and a stepwise isotherm is predicted. Experimental isotherms of long chain alkylammonium chloride adsorption on biotite were presented and shown to have two distinct regions. The first had a finite slope which they concluded was due to condensation on an inhomogeneous surface. The second region had an infinite slope which they considered to be due to adsorption onto the first layer i.e. an homogeneous surface.

Fuerstenau (146) has criticized this approach on the grounds that the assumption made in the derivation of the theoretical isotherms that entropic effects involved in the adsorption from solution are similar and equal to that involved in the adsorption from the gaseous state is erroneous. Water structure at the solid/liquid interface plays a key part in adsorption, and any water molecule released on adsorption of collector would significantly increase the entropy of the system. It

is indeed probable that the weakening and destruction of the hydrated layers at the solid/liquid interface gives rise to the hydrophobic effect of collectors (147), rather than the effect due to dispersion forces between hydrocarbon chains of the collector in the adsorbed layer (148).

CHAPTER 3
EXPERIMENTAL

3.

EXPERIMENTAL

3.1 Materials

Specially prepared titanium dioxide (Tioxide R-SM2) was supplied by Professor G.D. Parfitt of Tioxide International. It had been obtained in the rutile form by heating the oxide at a high temperature. The crystals were elliptically-shaped, with a mean size of 0.18 μm as determined by electron microscopy. The manufacturer's specifications (149) showed that the rutile contained 0.25% ZnO, 0.24% P_2O_5 , 0.14% K_2O , all deliberately added before calcination, and 0.29% Nb_2O_5 which persists from the ore.

Before use, surface impurities, particularly residual sulphate remaining from the preparation process, were washed from the surface by extraction with hot water for 24 hours in a Soxhlet extraction apparatus. Additional washing resulted in no further sulphate removal from the rutile surface. The rutile was finally dried at 100°C.

A semi-quantitative X-ray fluorescence scan was carried out on the material and the results are shown in Table 3.1.

Table 3.1 XRF analysis of rutile powder

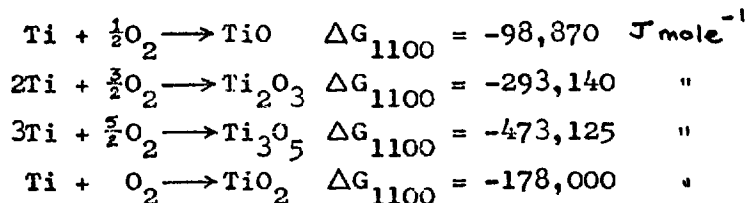
Major	Intermediate	Minor	Trace
5%	(0.5-5)%	(0.05-0.5)%	< 0.05%
Ti	Si	P	Ca
		S	Cr
		Cl	Mn
		K	Fe
		Zn	Sn

The specific surface area of the material determined by B.E.T. krypton adsorption, was 6.47 m^2g^{-1} .

For contact angle studies rutile plates were prepared by oxidizing a 25mm x 25mm x 1mm titanium metal foil supplied by

Goodfellows Metals Ltd. assaying 99.99% Ti. The foil was polished with rutile powder on a clean 'Selvyt' cloth under conductivity water until microscopic examination with reflected light revealed no surface scratches. The foil was then cut into sixteen 6mm x 6mm plates which were heated at 1000°C under clean oxygen for one hour in a tube furnace.

The products of the oxidation of titanium and the standard free energies of reaction (150) are given below,



All the oxides of titanium transform to titanium dioxide on heating (151). Titanium dioxide exists in three polymorphic forms, namely, anatase (tetragonal), brookite (orthorhombic) and rutile (tetragonal) (152). Anatase and brookite are both thermodynamically unstable (153) and transform to rutile. At low temperatures the transition is immeasurably slow, but above 730°C for the anatase-rutile transition (154) and 950°C for the brookite-rutile transition (155) the rate of transformation is rapid.

The oxidised layer on the titanium plates was confirmed as titanium dioxide (rutile) by X-ray diffraction analysis of the powdered surface coatings. Absorption peaks at 2θ angles were recorded and the d values corresponding to these angles calculated from the Bragg law. The diffraction pattern agreed very well with that previously reported (156).

The surfactants used in the conditioning and oil extraction tests were a series of alkyl sulphates (12 - 18 carbon atoms in the hydrocarbon chain) and cetyltrimethylammonium bromide. The sodium dodecyl sulphate (SDS) was a 'chemically pure' sample supplied by B. Newton Maine Ltd. Measurements of the conductivity in aqueous solutions of the SDS revealed that the critical micelle concentration (c.m.c.) was

8.20×10^{-3} M. This value is in good agreement with literature values (157). Samples of sodium tetradecyl sulphate (STS), hexadecyl sulphate (SHS) and octadecyl sulphate (SOS) were supplied by Cambrian Chemicals and all had purities of 98% (minimum).

The Krafft point (158) of long-chain alkyl sulphates (greater than 14 carbon atoms) is higher than 25°C and consequently the solubility was exceeded before the c.m.c. was reached under the experimental conditions used. The solubilities of the long-chain alkyl sulphates were determined by measuring the equilibrium surfactant concentration of the supersaturated surfactant solutions after they had been equilibrated for one week at room temperature. The solubilities were as follows: STS, 9.82×10^{-4} M; SHS, 2.07×10^{-4} M; and SOS, 3.87×10^{-5} M.

The cetyltrimethylammonium bromide (CTAB) was supplied by Koch-Light and had a purity of not less than 99%. The c.m.c. of CTAB determined by conductivity measurements, was 8.90×10^{-4} M which is in good agreement with literature values (159).

The Krafft points of the longer chain alkyl sulphates were determined by adding amounts of the surfactants equivalent to their approximate c.m.c. values (160) to known volumes of water. At room temperature the surfactants were insoluble but as the temperature was increased above the Krafft points dissolution occurred. The temperature was then slowly decreased and the points at which the solutions became cloudy were taken as the Krafft points. Values of 30°C , 46°C , and 61°C were obtained for STS, SHS and SOS respectively. These are in good agreement with values obtained by other workers (161).

Potassium and lithium salts of the alkyl sulphates were prepared by passing a solution of the sodium salt through a column of analytical grade 'Amberlite' ion exchange resin (IR-120 (H)), supplied by B.D.H. The resulting alkyl sulphuric acid was then neutralized potentiometrically with 'Analar' lithium or potassium carbonate.

The oil phases used in the course of the work are summarized in Table 3.2 with their structural formulae, purity and supplier, and interfacial tensions against pure water.

Before use the oils were passed through activated alumina columns until their interfacial tensions were in good agreement with literature values.

High purity conductivity water was used throughout the work. This was prepared by passing distilled water through a mixed-bed of ion exchange resin and then through a column of activated charcoal and finally redistilling under nitrogen. The conductivity of the water was less than $4.0 \times 10^{-6} \text{ohm}^{-1} \text{cm}^{-1}$ and bubble-persistence tests indicated that there were no surface-active impurities in the water. The surface tension of the water was $72.3 \pm 0.1 \text{ mNm}^{-1}$.

pH adjustments were made using solutions of 'Analar' HCl and NaOH. All other reagents were of 'Analar' grade.

3.2 Extraction studies

Preliminary extraction tests were carried out on the rutile/water/oil system to determine which surfactant types produced extraction of the rutile into the organic phase and under what conditions. Certain systems were then selected for more detailed studies.

In an extraction test 0.5g rutile was conditioned for 5 min with 20 ml surfactant solution at constant ionic strength and at the required pH. 6 ml oil was then added and the system conditioned for a further 5 min. All conditioning was carried out by shaking the suspensions in 150 ml stoppered flasks. At the end of conditioning the emulsions were allowed to stand and the position of the TiO_2 was noted. Particles in the organic phase were defined as extracted and those at the oil/water interface were said to be concentrated.

Initial tests indicated that extraction into the oil phase was





Oil	Structural formula	Grade	Supplier	Interfacial tension (mNm^{-1})
n-hexadecane	$\text{CH}_3(\text{CH}_2)_{14}\text{CH}_3$	puriss, 99.0%	Koch-Light	53.30(162)
n-heptane	$\text{CH}_3(\text{CH}_2)_5\text{CH}_3$	puriss, 99.0%	Koch-Light	50.77(162)
n-hexane	$\text{CH}_3(\text{CH}_2)_4\text{CH}_3$	puriss, 99.0%	Koch-Light	50.5 (157)
2,2,4-trimethylpentane (iso-octane)	$(\text{CH}_3)_3\text{C}\cdot\text{CH}_2\cdot\text{CH}(\text{CH}_3)_2$	pure, 99.5%	B.D.H.	49.7 (162)
hexahydrobenzene (cyclohexane)	$\text{CH}_2\cdot(\text{CH}_2)_4\cdot\text{CH}_2$, 	puriss, 99.0%	Koch-Light	49.6 (157)
1-octene	$\text{CH}_3(\text{CH}_2)_5\text{CH}:\text{CH}_2$	pure, 96.0%	Koch-Light	43.7 (157)
methylbenzene (toluene)	$\text{C}_6\text{H}_5\cdot\text{CH}_3$, 	analar	B.D.H.	36.0 (163)
benzene	C_6H_6 , 	analar	B.D.H.	34.1 (163)
1-hexene	$\text{CH}_3(\text{CH}_2)_3\text{CH}:\text{CH}_2$	puriss, 99.0%	Koch-Light	31.3 (157)
decahydronaphthalene (dekalin)	$\text{C}_{10}\text{H}_{18}$, 	g.p.r., 97%	B.D.H.	-
diethyl ether	$\text{CH}_3\text{CH}_2\text{OCH}_2\text{CH}_3$	puriss	Koch-Light	10.7 (165)
4-methylpentan-2-one (isobutyl methyl ketone)	$(\text{CH}_3)_2\text{CHCOCH}_3$	analar, 99.0%	B.D.H.	10.0 (163)
di-iso-propyl ether	$(\text{CH}_3)_2\text{CHOCH}(\text{CH}_3)_2$	pure	Koch-Light	17.9 (164)
1-dodecanol	$\text{CH}_3(\text{CH}_2)_{11}\text{OH}$	specialty pure, 99%	B.D.H.	-
ethyl acetate	$\text{CH}_3\text{CO}_2\text{CH}_2\text{CH}_3$	analar, 99.0%	B.D.H.	8.0 (163)
1-butanol	$\text{CH}_3(\text{CH}_2)_3\text{OH}$	analar	B.D.H.	2.0 (163)

Table 3.2 Oil phases employed

independent of the ionic strength. Further tests were, therefore, conducted in the absence of sodium chloride and this also removed problems associated with 'salting-out' effects.

5.3 Electrokinetic studies

3.3.1 Electrophoresis

The origin of the charge on an oxide particle immersed in water has been discussed and its importance in relation to the mechanism of adsorption of surfactants emphasized. The determination of the sign and magnitude of the surface charge is, therefore, of fundamental importance for studies of mineral-surfactant interaction. The zeta-potential (ζ) can be determined indirectly by the technique of microelectrophoresis which is particularly suitable for fine mineral particles (128).

The zeta-potential is related to the electrophoretic mobility of particles, that is the velocity of migration of the particles under unit potential gradient, by the Helmholtz-Smoluchowski equation (166) modified where necessary by Henry's correction factor for retardation (167). Thus,

$$u = \frac{\epsilon E \zeta}{6\pi\eta} \cdot f(\kappa a) \dots \dots \dots (1)$$

- where, u = electrophoretic mobility.
 ϵ = permittivity.
 E = electric field strength.
 η = viscosity of the medium.
 a = radius of particles.

and κ = Debye-Hückel function, i.e. the reciprocal of the double layer thickness.

The function $f(\kappa a)$ depends on the size, shape and orientation of the particles and its values, which vary between 1 and 1.5, are tabulated elsewhere (168).

Corrections for the effect of surface conductivity (169) and relaxation (170) (171) have also been made, but the approximations involved generally lead to an overestimation of these effects (172).

3.3.2 Experimental procedure

The electrophoretic mobility of the rutile particles was determined using a Rank Bros. particle microelectrophoresis apparatus (Mk. II). A standard suspension was prepared by dispersing 0.5g rutile in 500ml water. Aliquots of 0.1ml of the standard suspension were added to 100ml electrolyte solution at the required pH and allowed to equilibrate for 15 min. The suspension was then added to the electrophoresis cell and the mobility of the particles at the stationary levels (173) under a given voltage determined. In all, 10 particles were measured travelling in one direction and then another 10 in reverse.

The electrophoretic mobility was calculated from the equation

$$u = \frac{v \kappa \Delta}{I} \dots \dots \dots (2)$$

- where, v = particle velocity.
- κ = specific conductivity of suspension.
- Δ = cross-sectional area of cell.
- and I = current.

Equation (2) may be expressed more conveniently in the form,

$$u = \frac{v \cdot L}{V} \dots \dots \dots (3)$$

- where, V = applied potential.
- L = effective inter-electrode distance.
- $\quad = R\kappa\Delta$
- and R = resistance across cell.

The effective inter-electrode distance for the cell used in the course of this work was 8.73 cm.

The zeta-potential was obtained from the electrophoretic mobility by use of equation (1), which at 25°C reduces to,

$$\xi = 12.8U. u.f(\eta a) \dots \dots \dots (4)$$

where, ξ is measured in mV and electrophoretic mobility in $\mu\text{m}.\text{sec}^{-1}/\text{volt cm}^{-1}$.

3.4 Adsorption measurements

3.4.1 Experimental procedure

The adsorption tests were carried out in closed 150ml flasks, whose internal surfaces had been rendered hydrophilic by cleaning with nitric acid and ethanol. Preliminary experiments indicated that surfactant adsorption was a rapid process, and that no detectable difference in adsorption was obtained between equilibration periods of 15 min and 6 hours. Thus, 0.5g rutile was shaken with 40ml surfactant solution at a known pH for 15 min. On completion of conditioning, the solid was separated from the surfactant solution by centrifuging, and the pH and equilibrium concentration of the surfactant determined. The adsorption density was deduced from the difference between the surfactant concentration before and after adsorption. The reversibility of adsorption was established by using different amounts of rutile in the adsorption tests.

3.4.2 Alkyl sulphate analysis

The method used for the determination of the alkyl sulphates was that of Gregory (175) for anionic surfactants. The alkyl sulphate solutions were reacted with a copper triethylenetetramine complex in an alkaline medium of monoethanolamine and the resulting complex extracted into an isobutanol-cyclohexane mixture. Addition of diethylammonium diethyldithiocarbamate to the extracted complex produced a colour which was determined spectrophotometrically in a Unicam SP500.

The reagents were prepared in the following manner:

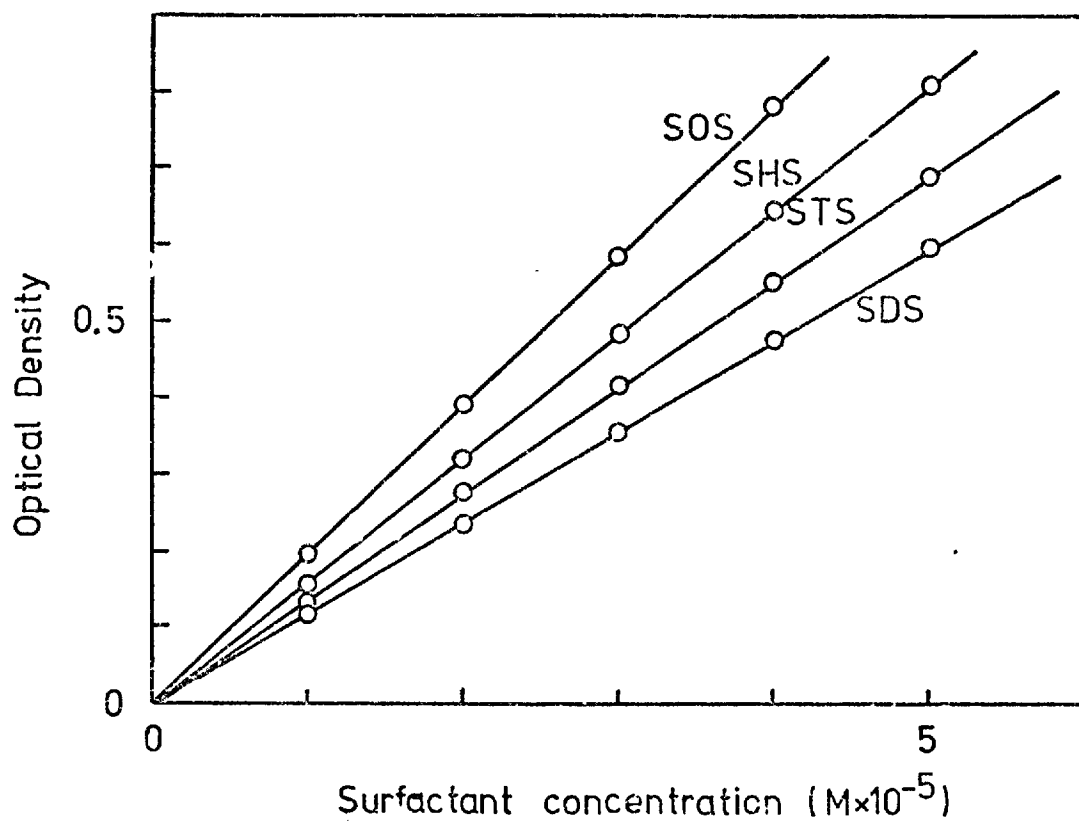


Fig. 3. 1. Calibration curves for the spectrophotometric determination of the alkyl sulphates.

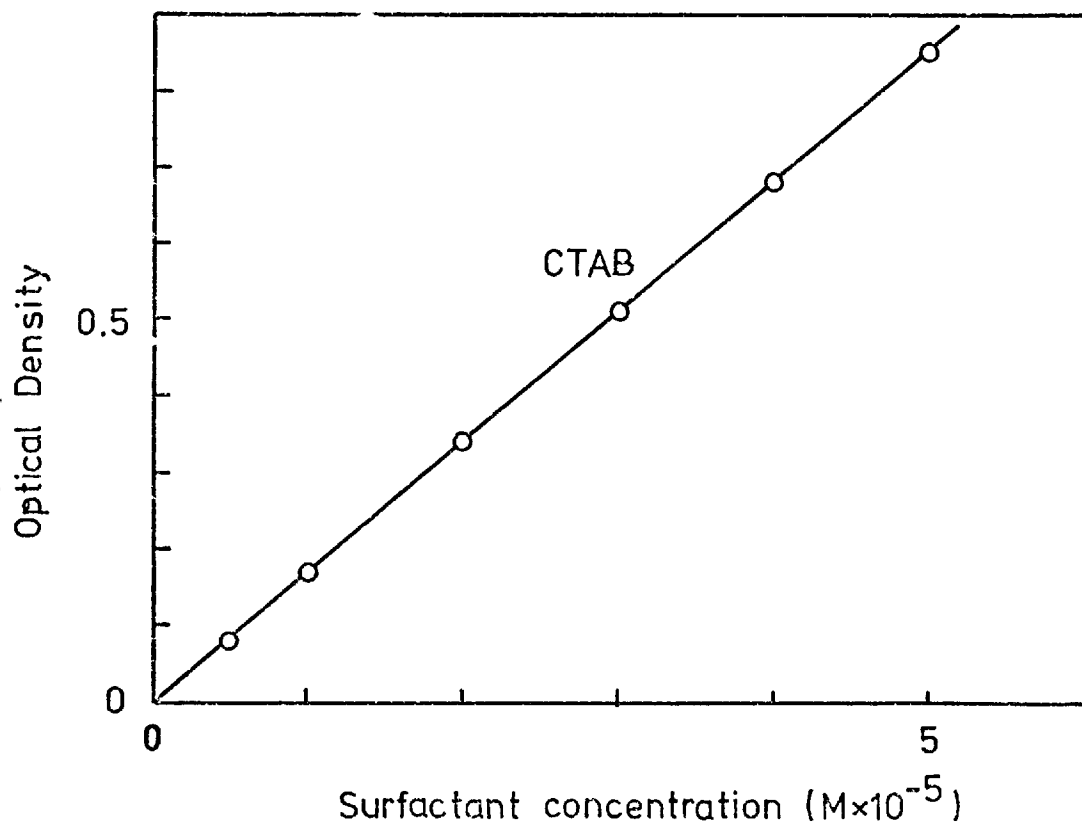


Fig. 3. 2. Calibration curve for the spectrophotometric determination of CTAB.

Copper triethylenetetramine: 25g copper (II) nitrate trihydrate was dissolved in 125ml water and a solution containing 16.25g triethylenetetramine in 125ml water slowly added. A solution containing 250ml monoethanolamine in 250ml water was then added and the whole made up to 1 litre with distilled water.

Isobutanol-cyclohexane extractant: 200ml isobutanol was mixed with 800ml cyclohexane.

Diethylammonium diethyldithiocarbamate solution: 2g diethylammonium diethyl-dithiocarbamate was dissolved in 100ml isobutanol. This solution was prepared fresh every two days.

In a determination 5ml copper complex and 10ml extractant were added to 25ml of the sample and the mixture rapidly inverted 100 times. The organic phase was then separated from the aqueous phase and mixed with two drops of carbamate solution. After the sample had been left to stand in the dark for 15 min, the optical density at a wavelength of $435m\mu$ was determined.

Calibration curves for the alkyl sulphates are shown in Figure 3.1.

3.4.3 CTAB analysis

CTAB was determined by complexing the quarternary ammonium salt with an acidified alcoholic solution containing a sulphnapthelein indicator, bromocresol green (176), after a method originally suggested by Mukerjee (177).

The indicator was prepared by dissolving 0.1g bromocresol green in 50ml ethanol, acidifying the solution with 0.5ml concentrated sulphuric acid and diluting to 100ml.

In a determination 5ml CTAB solution was added to 1ml indicator solution and the mixture diluted to 10ml. 5ml chloroform was then added and the mixture rapidly inverted 100 times. The monocetyl

trimethylammonium salt has a much higher solubility in chloroform than in water and was preferentially partitioned in the organic phase where its colour was determined spectrophotometrically at 416m μ .

The calibration curve for CTAB is shown in Figure 3.2.

3.5 Contact angle measurements

3.5.1 Apparatus

The contact angle apparatus consisted of a silica spectrophotometer cell held on the modified stage of a Beck 6000 microscope, mounted in the horizontal plane. Illumination was provided by a tungsten lamp in the same horizontal plane as the microscope and sample. Light passed through the cell at a small angle of incidence to the surface of the sample. The objective of the microscope was a 25mm lens and the eyepiece a Vickers 'Dick-wright slotted ocular' with a magnification of 10 X. Angles were measured ($\pm 0.1^\circ$) by rotating the eyepiece independently of the instrument to line up the cross-wires.

Oil droplets were formed and brought into contact with the sample surface by means of an 'Aglar' micrometer syringe mounted in the same vertical plane as the spectrophotometer cell. The syringe was mounted on an extension and could be moved vertically and horizontally by means of two 'Research Instruments' micromanipulators mounted in the respective planes. *The angle was measured through the aqueous phase.*

3.5.2 Experimental procedure

Prior to measuring the contact angles the aqueous surfactant solution was equilibrated with the organic phase by shaking and then separated from it by centrifugation. The aqueous phase was transferred to the sample cell and the organic phase added to the syringe. To avoid dilution effects the sample was transferred from a similar surfactant solution to the solution in the sample cell. In the case of

cationic surfactants, the sample cell was also conditioned in the surfactant solution prior to addition of the sample. Care was taken to ensure that the rutile surface was not exposed to air during the transfer from one solution to another.

An oil drop of fixed volume was formed on the tip of the micrometer syringe dipping in the aqueous medium. After an equilibration period of 5 min, the drop was brought into contact with the rutile surface, equilibrated, and then its volume increased by a known amount. After a further equilibration period the contact angle between the three phases was measured through the aqueous phase. This angle was termed the 'advancing angle'. The bubble volume was then returned to its original volume and the 'receding' contact angle measured. A preliminary series of tests showed that the contact angles obtained after 3 min equilibration were constant provided that the sample was conditioned with the surfactant solution for 15 min. Throughout the determinations equilibration periods of 5 minutes were therefore used.

Sessile drops were formed on the surface when the contact angles were large ($>125^\circ$). Under these conditions the equilibrium 'advancing' angle was measured, although some measurements of the equilibrium 'receding' angle of the sessile drop were also made by removing oil from the drop on the surface. The values obtained in the latter case were, however, dependent on the amount of oil removed. Angles tending to 180° were designated 180° even though it was appreciated that the work of adhesion of water to the solid could not be zero.

3.6 Surface/Interfacial tension measurements

3.6.1 General

The interfacial tensions between the various oil phases and surfactant solutions were determined for the purpose of

- (a) determining the influence of adsorption at the oil/surfactant solution interface on the displacement of water from the rutile surface by an organic liquid, and

(b) substituting the value of interfacial tension into the Young-Dupré equation for the work of adhesion of a liquid on a solid.

The determinations were made using the drop-volume method of Gaddum (178). The method consists of measuring the volume of a drop (and associated satellite drops) that breaks away from a capillary tip, and relating this volume to the surface or interfacial tension by an empirical relation. The origin of the relation is a force balance on a pendant drop, with the gravitational force mg being balanced by the surface or interfacial tension force $2\gamma r$. The equation becomes,

$$\gamma = \frac{\Delta\rho Vg}{r} \cdot F \dots \dots \dots (5)$$

- where, γ = surface/interfacial tension.
- $\Delta\rho$ = difference between density of the pendant drop and the density of the supporting medium.
- F = correction factor for deviation of the pendant drop from 'ideal drop'.
- V = volume of drop.
- r = radius of capillary tip.

The factor F is dependant on the ratio V/r^3 . Values of F have been tabulated by Harkins and Brown (179).

3.6.2 Apparatus

The apparatus was similar to that used by Adam (180) and consisted of a U-tube with one arm connected to a water manometer and the other housing a glass capillary which was attached to a micrometer syringe. The free end of the capillary was polished so that its cross-section was at right-angles to its length, and there were no edge imperfections when viewed at a magnification of 20 X. The outside diameter of the capillary was measured by travelling microscope and the mean diameter was 0.415 ± 0.001 cm.

The cationic surfactant, CTAB, was found to adsorb onto the glass

capillary rendering the surface oleophilic. This caused incomplete wetting of the capillary by the pendant drops of CTAB solution and invalidated the method. As a result, a U-shaped Teflon capillary was prepared and the oil drops were allowed to rise through the aqueous CTAB solutions. The correction factors are the same for both methods (181). The diameter of the Teflon capillary was 0.483 ± 0.001 cm.

All glassware was cleaned by nitric acid and ethanol until the surfaces were hydrophilic.

3.6.3 Experimental procedure

A 40ml sample of surfactant solution was shaken with 12ml oil in a 150ml flask for 15 min. Sufficient 0.1 M NaOH or HCl was added to give the required pH. The resulting emulsion was centrifuged and after separation of the two phases the pH of the aqueous phase was measured.

20ml aqueous phase was then pipetted into the U-tube and 6ml organic phase added to the arm containing the capillary. The syringe was filled with either aqueous surfactant solution or organic phase depending on whether the surfactant was alkyl sulphate or CTAB. The capillary tip was then placed in position just below the surface of the organic phase or, in the case of CTAB, 1 cm below the oil/water interface. A drop was formed on the capillary tip and the volume increased until the drop began to 'neck'. The drop was then left for an ageing period after which the volume was increased until the drop became detached. The procedure was repeated, and the difference in micrometer readings between the first and second drops corresponded to the volume of the drop. The drop volume used in the calculations was the mean of ten individual drop volume measurements. Preliminary tests indicated that an ageing period of 5 min was suitable for the drop to attain equilibrium with the surrounding phase. Similar drop formation times have been reported by other workers (182) (183).

Initially the syringe was refilled by raising or lowering the phase levels in the U-tube by use of the manometer. During the filling operation, however, some of the surrounding phase often entered the syringe and the tip became contaminated (182). The syringe was therefore subsequently refilled from equilibrated stock solutions.

Surface tension measurements of the alkyl sulphate solutions were carried out in a similar manner. In this case, however, the surfactant drops were dropped from the capillary in air.

All measurements were carried out at 25°C.

CHAPTERS 4 - 6
RESULTS AND DISCUSSION

4.1 Electrokinetic studies

4.1.1 System modified by alkyl sulphates

It has been reported (184) that the ageing of some oxides in distilled water produces changes in the zeta-potential. Preliminary tests with the rutile used in this work, however, showed that the zeta-potential was independent of ageing.

The potential determining role of hydrogen and hydroxyl ions for oxide minerals has been well established (c.f. section 2.2). The dependence of the zeta-potential of rutile on pH was, therefore, determined and the results are shown in Fig. 4.1. As the pH was increased, the positive zeta-potential decreased to zero at pH4.3, which corresponds to the iso-electric point (i.e.p.), and then became negative. Further increases in the pH produced even more negative zeta-potentials.

The zero point of charge (z.p.c.) of rutile was found to be pH5.3 by a solid titration method described by Cornell, Posner and Quirk (185). The difference between the z.p.c. and the i.e.p. can be attributed to the presence of small amounts of anionic impurity e.g. sulphate. Both values, however, are in the range of values reported for rutile (186), i.e. pH3.5 - pH6.7, although for rutile free from impurities the value of both z.p.c. and i.e.p. is reported to be at pH5.5 (185).

The electrokinetic behaviour of rutile in the presence of SDS as a function of pH at various surfactant concentrations is shown in Fig.

4.2. All the solutions were prepared at a constant ionic strength of 10^{-2} M controlled with NaCl. The zeta-potential against pH curves obtained at different SDS concentrations in the concentration range 10^{-8} M - 2×10^{-7} M were of a similar shape to that obtained in the

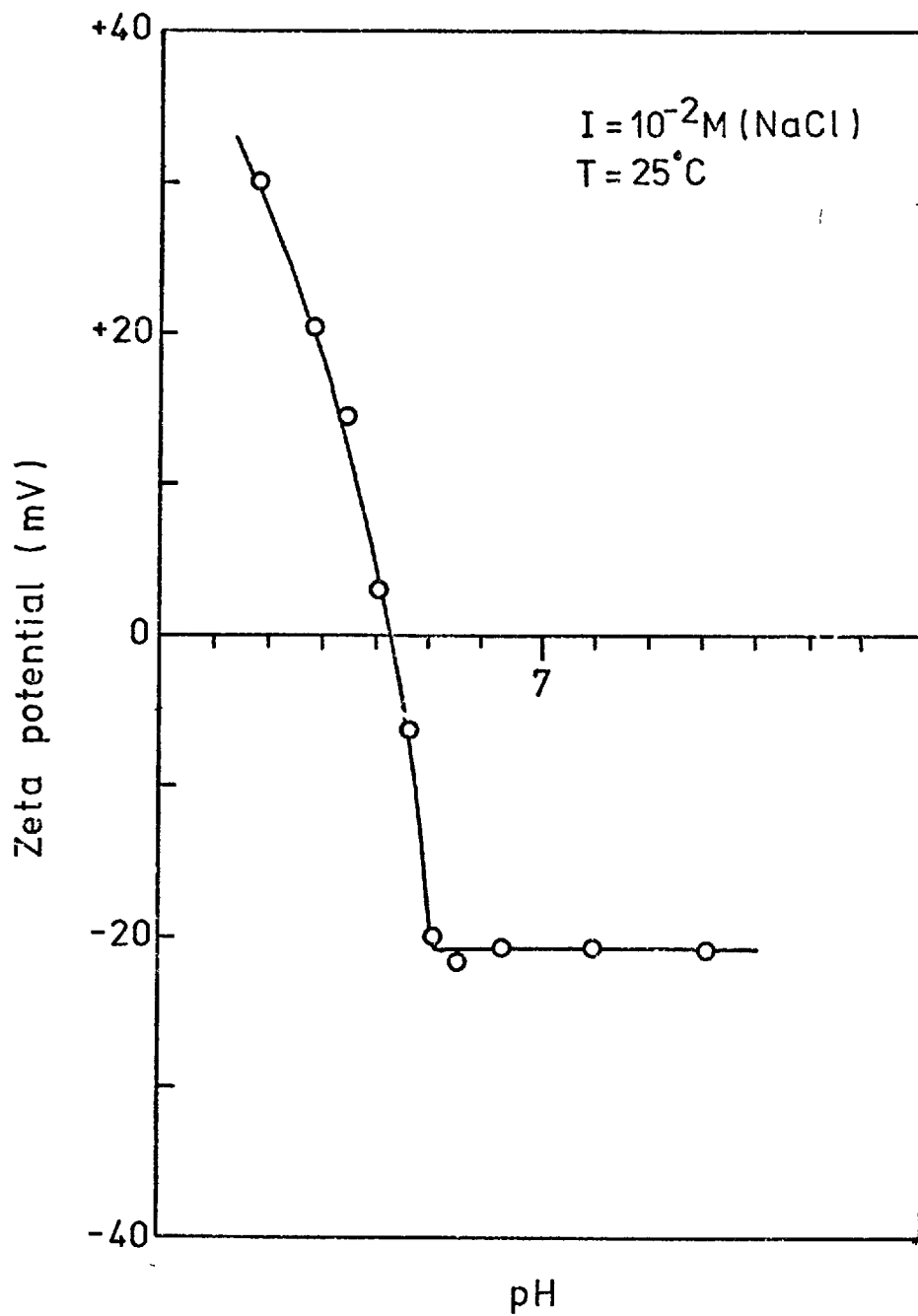


Fig. 4. 1. Zeta-potential of rutile as a function of pH.

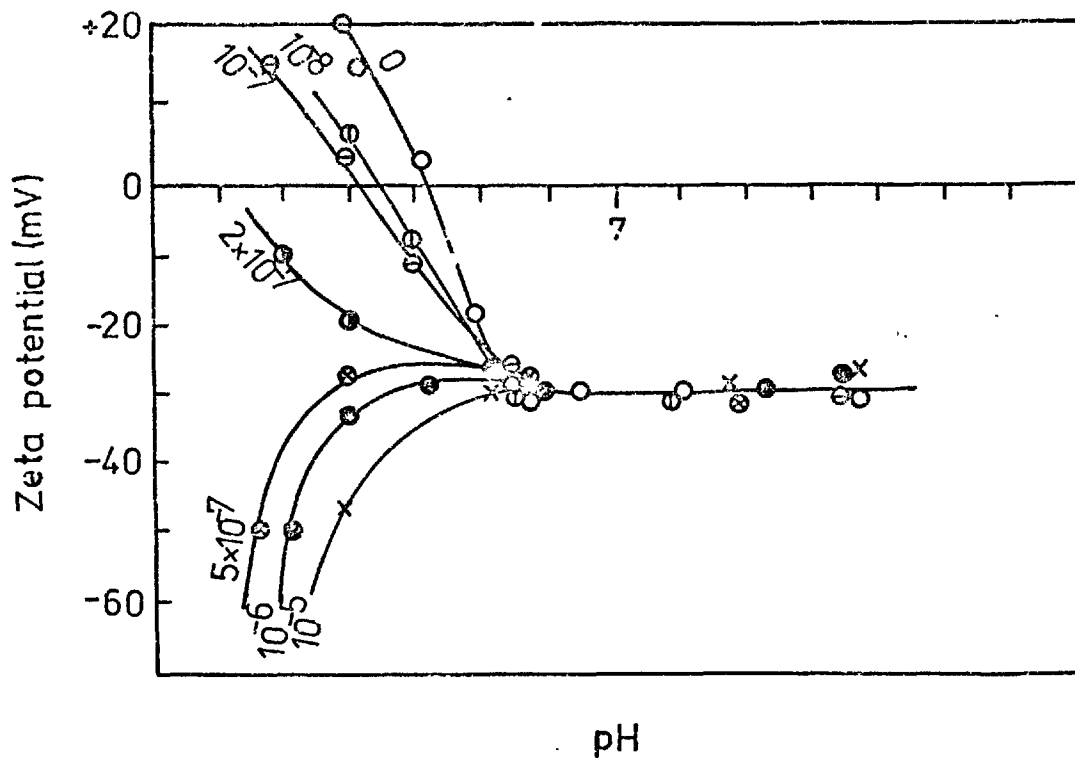


Fig. 4. 2. Zeta-potential of rutile as a function of pH at various SOS concentrations.

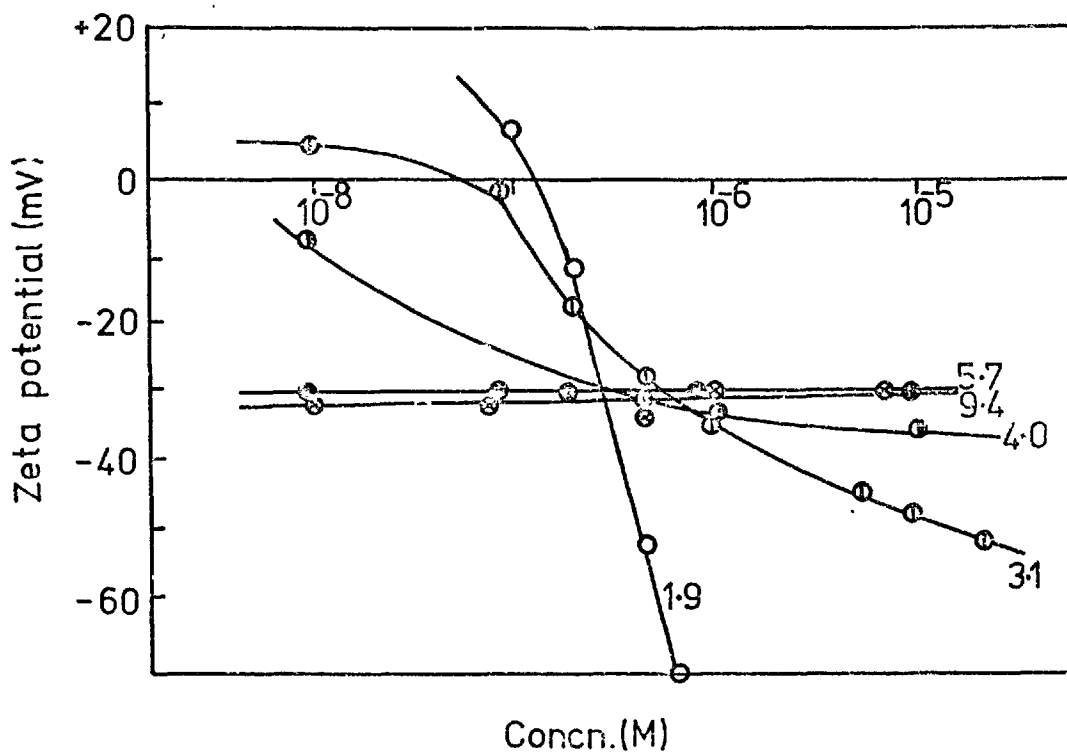


Fig. 4. 3. Zeta-potential of rutile as a function of SOS concentration at various pH values.

absence of surfactant, except that the pH at which the zeta-potential was reversed decreased with increasing concentration. At higher SOS concentrations the zeta-potential was negative at all pH values and in acid media it became increasingly more negative as the surfactant concentration was increased. Under the latter conditions the negative potential even exceeded that obtained at pH values above the i.e.p. in the absence of surfactant.

In the absence of specific adsorbent-adsorbate chemical interaction, there is no adsorption at the z.p.c./i.e.p. and the curves for all concentrations of surfactant pass through the z.p.c. of the oxide. In the present case, the shift in the pH at which the zeta-potential was reversed and the corresponding large negative potentials at pH 4.3 (the i.e.p.) in the presence of surfactant indicates a specific chemical affinity of the alkyl sulphate for the rutile surface.

The data from Fig. 4.2 has been replotted in Fig. 4.3 to show the dependence of rutile zeta-potential on the logarithm of SOS concentration at various pH values. Similar curves are shown in Figs. 4.4 and 4.5 for SDS and STS.

The abrupt charge reversal at low pH values is a result of the onset of hemimicelle formation, i.e. specific adsorption as a result of association of the hydrocarbon chains of the surfactant which is driven by entropy changes that arise from the structure of water (187). At pH values above the i.e.p., the alkyl sulphate acts as a ~~counter~~-ion in the electrical double layer, as evidenced by the independence of the zeta-potential of alkyl sulphate concentration at pH values 5.7 and 9.4.

The results presented are consistent with the adsorption of long-chain alkyl sulphate ions by Coulombic attraction to the positive rutile surface at low pH values, followed by a hydrophobic bonding interaction at higher adsorption densities. Rastogi and Srivastava (188) have presented further experimental evidence to support this mechanism of

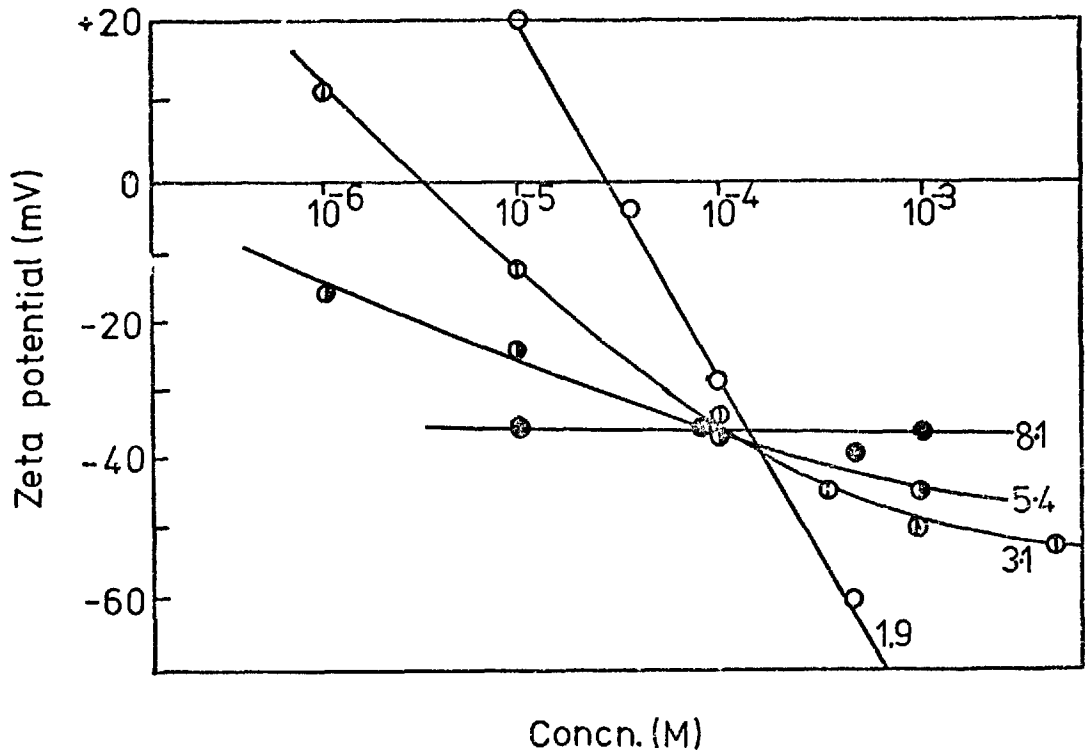


Fig. 4. 4. Zeta-potential of rutile as a function of SDS concentration at various pH values.

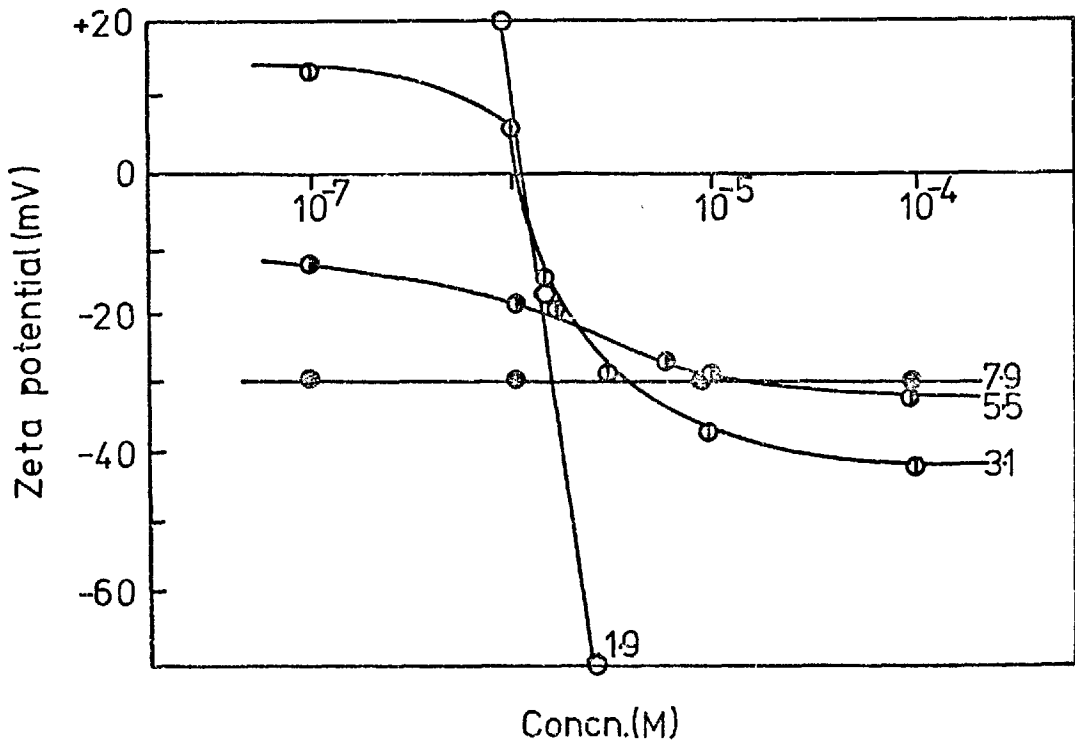


Fig. 4. 5. Zeta-potential of rutile as a function of STS concentration at various pH values.

adsorption. These authors showed that as SHS and SDS was adsorbed on rutile, two maxima occurred in the pH and conductivity curves (versus log surfactant concentration). The first maximum occurred at low surfactant concentrations and was ascribed to release of OH^- ions from the diffuse part of the double layer as a result of ion exchange with the alkyl sulphate ions. The second maximum occurred at concentrations approximately equivalent to zero zeta-potential where the authors concluded that hemimicellization and resulting adsorption into the Stern plane was responsible for the release of further OH^- ions.

The shift of the i.e.p. in the presence of surfactant in the present investigation indicates that the alkyl sulphates have some specific affinity for the rutile surface. It is difficult to imagine any specific chemical interaction between the alkyl sulphate ion and the rutile surface. Divalent sulphate ions are known to be specifically adsorbed on rutile (185), but it is unlikely that the same would apply to the monovalent sulphate ion of the surfactant. Parfitt and Wharton (189), investigating the stability of rutile particles in distilled water, noted that the zeta-potential of rutile became more negative in the presence of SDS at pH 5.5, which is above the i.e.p. of their sample (pH 4.5) i.e. where the surface potential was negative. They concluded that this was the result of an ion exchange reaction between the dodecyl sulphate anion and specifically adsorbed chloride ions. The authors quoted two references to support the hypothesis of specific chloride adsorption (190) (191). The work of Morimoto and Sakamoto (190) was quoted incorrectly however. These authors showed that in 1:1 electrolytes, although there was often evidence of specific adsorption of the cation, adsorption of the chloride ion was negligible. The results of Berubé and De Bruyn (136) on the capacitance of the rutile electrical double layer in the presence of various indifferent electrolytes confirmed that the chloride ion was not specifically adsorbed on

rutile. It seems likely that the results obtained by Parfitt and Wharton (189) were due to ion exchange between the dodecyl sulphate ion and residual chloride ions remaining on the rutile surface from the preparation process which involved the hydrolysis of redistilled titanium tetrachloride. Although an ion exchange reaction of the type postulated by Parfitt and Wharton would be consistent with the results obtained, such a mechanism seems doubtful.

Fig. 4.6 shows the dependence of rutile zeta-potential on the logarithm of surfactant concentration for the series of alkyl sulphates at pH 3.1 ± 0.1 in the absence of added sodium chloride. The arrows on the curves indicate the concentration of surfactant at which monolayer coverage was obtained for each chain length (c.f. section 4.2 Adsorption studies). The results are similar to those obtained by Wakamatsu and Fuerstenau (192) for a homologous series of alkyl sulphonates on alumina at pH 7.2. The curves show the importance of the $n\phi$ term in the equation

$$\Delta G_{\text{ads}} = ze\psi_0 + n\phi \dots \dots \dots (1)$$

which describes the free energy change on adsorption of surfactant.

For conditions of constant ψ_0 (i.e. constant pH), adsorption at a given surfactant concentration (reflected by a decrease in zeta-potential) increases with increasing chain length, as predicted by equation 1.

An estimate of the concentration of each surfactant at which the onset of hemimicellization occurs can be obtained from the curves. The onset of hemimicelle formation is reflected by an abrupt change in slope of the curves, and this point for each chain length is given in Table 4.1.

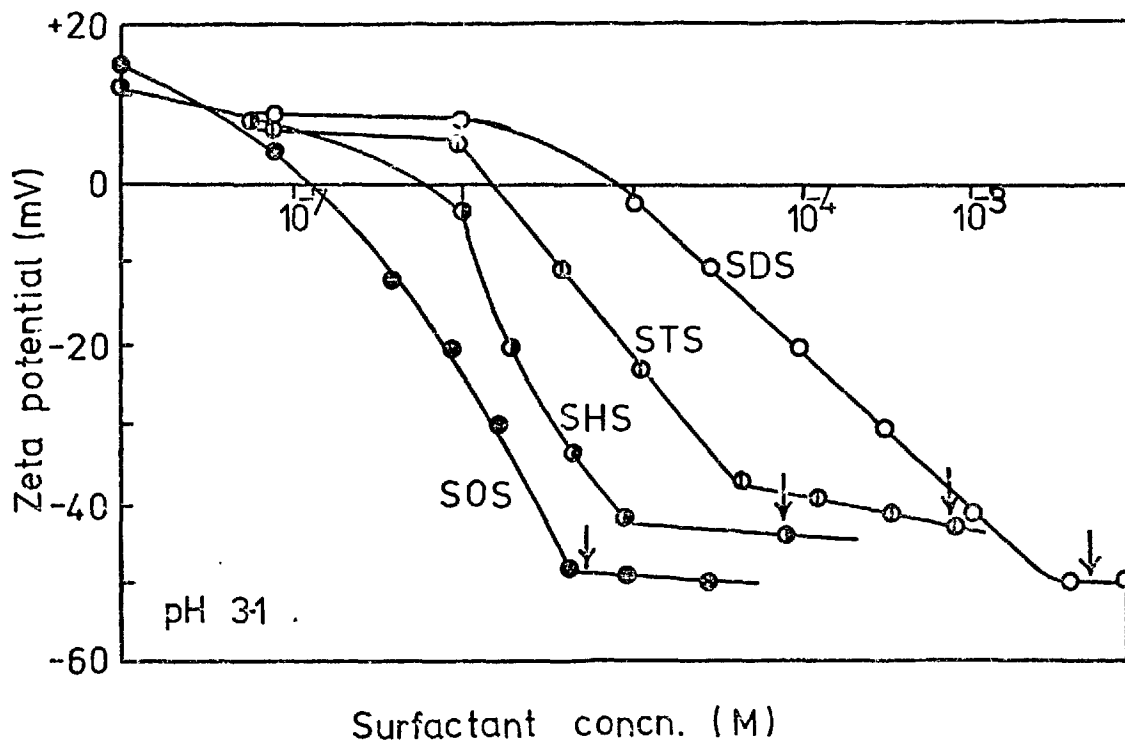


Fig. 4. 6. Zeta-potential of rutile as a function of alkyl sulphate concentration at pH 3.1.

Table 4.1 Critical hemimicelle concentration
(C_{HMC}) for alkyl sulphates at pH 3.1

Chain length (carbon atoms)	C _{HMC} (M)
12	3 x 10 ⁻⁶
14	10 ⁻⁶
16	3 x 10 ⁻⁷
18	4 x 10 ⁻⁸

When the zeta-potential of the rutile particles is zero, the Stern-Grahame expression for the adsorption of the surfactant is given by the following equation

$$n_s = 2rn_o \left(- \frac{N\phi}{RT} \right) \dots \dots \dots (2)$$

Putting equation 2 in logarithmic form and rearranging terms gives

$$\ln n_o - \ln \left(\frac{n_s}{2r} \right) = - \frac{N\phi}{RT} \dots \dots \dots (3)$$

Assuming that the effective fraction of CH₂ groups removed from water when the potential at the Stern plane is zero is independent of chain length, the graph of log n_o against N should be a straight line. This was, indeed, the case and from the slope of the line, the value of φ was calculated to be - 0.4 RT.

4.1.2 Systems modified by CTAB

The electrokinetic behaviour of rutile in the presence of CTAB as a function of pH at various CTAB concentrations is shown in Fig. 4.7. The curves obtained are analogous to those obtained with the alkyl sulphates. The zeta-potential versus pH curves in the concentration range 4 x 10⁻⁶ M - 10⁻⁵ were of a similar shape to that obtained in the absence of surfactant except that the pH at which the zeta-potential reversed increased with increasing CTAB concentration. At higher CTAB

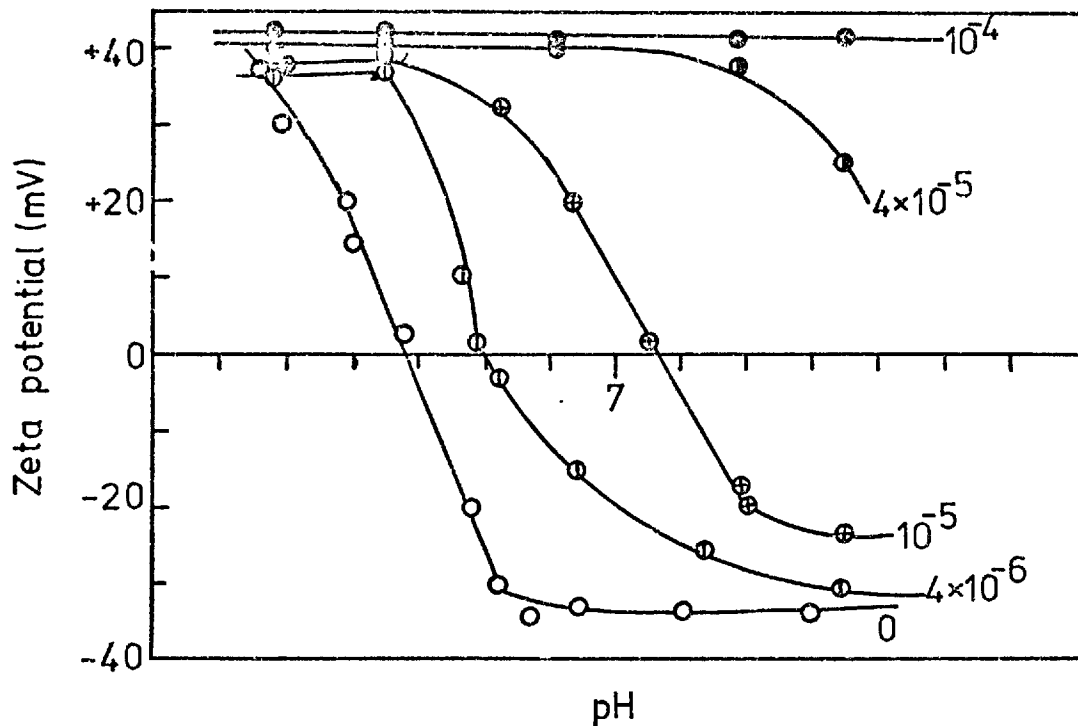


Fig. 4. 7. Zeta-potential of rutile as a function of pH at various CTAB concentrations.

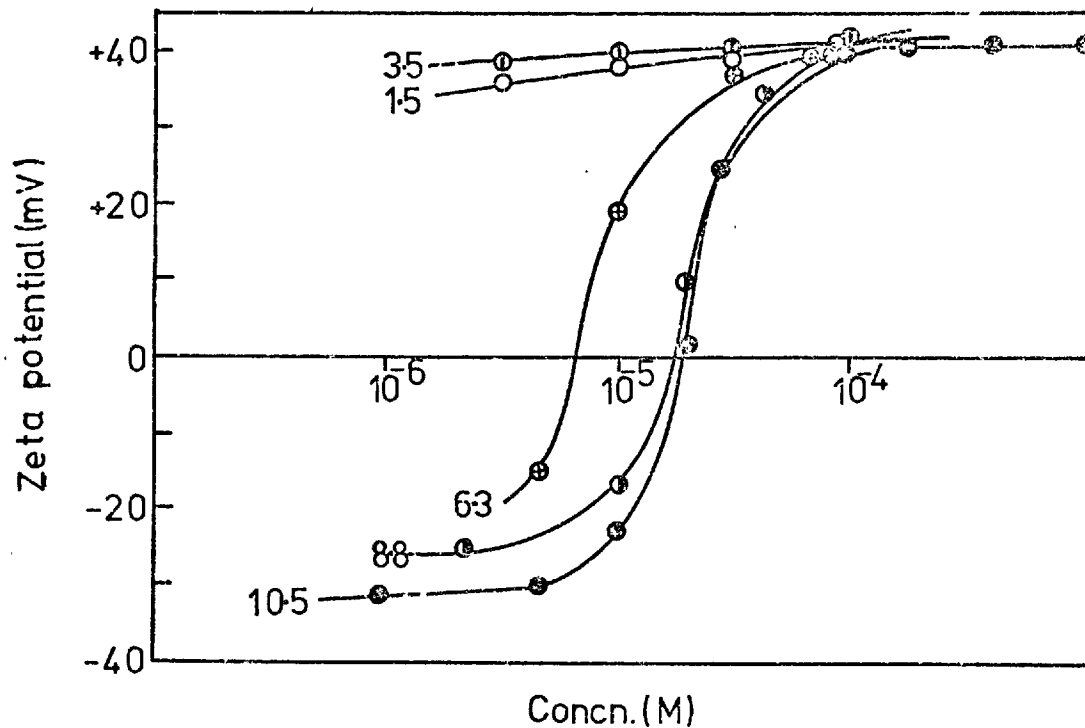


Fig. 4. 8. Zeta-potential of rutile as a function of CTAB concentration at various pH values.

concentrations the zeta-potential was positive over all the pH range studied. The difference in zeta-potential between that obtained in the absence and presence of CTAB at low pH indicates that specific adsorption was also occurring in this region in addition to at alkaline pH values. These results are similar to those obtained by Doss (193) for dodecyl trimethylammonium chloride on alumina, although the zeta-potential versus pH curves obtained in that work were concomitant at pH values below the z.p.c.

The same data has been presented in Fig. 4.8 as a function of CTAB concentration at various pH values. The results, like those obtained with the alkyl sulphates, are consistent with adsorption of surfactant ions by Coulombic attraction, followed by hydrocarbon chain interactions at high adsorption densities. At pH values below the i.e.p., the positive ion primarily acts as a counter-ion in the electrical double layer. There is evidence, however, to suggest that there was specific interaction between the surfactant and the rutile surface at all pH values.

Doss (193) postulated that specific adsorption of the dodecyl trimethylammonium ion on alumina was driven by entropy changes as chemical affinity of the surfactant ion for the surface or desolvation of the polar group seemed unlikely. Specific adsorption of sodium ions by rutile has been noted by some authors (136). At alkaline pH values, where the pH was controlled by NaOH, adsorption of Na^+ ions followed by ion exchange with the trimethylammonium ion may be an alternative mechanism of adsorption.

The onset of hemimicelle formation can be determined from the curves as with the alkyl sulphates. For example, at pH 10.5 the first abrupt change in the slope of the zeta-potential against CTAB concentration curve occurred at about 7×10^{-6} M CTAB.

4.2 Adsorption studies

4.2.1 Adsorption of alkyl sulphates at the rutile/water interface

A series of tests were conducted to determine the variation of SOS adsorption density at the rutile/water interface with equilibrium SOS concentration at various pH values. The results are shown in Fig. 4.9. The curves have the sigmoidal shape that generally characterizes surfactant adsorption in oxide systems. As the pH was increased adsorption decreased rapidly. The results are presented logarithmically to show the details of the adsorption process at low adsorption densities; if presented in a rectilinear form, adsorption at high pH values tends to zero. The sigmoidal shape at pH values above the z.p.c. and the dependence of the saturation plateau on pH suggests that adsorption is occurring as clusters around ionized sites (194) which are positively charged. At a certain surfactant concentration, which increases as the number of positive sites decrease, condensation of the surfactant occurs in reversed orientation onto the hydrocarbon chains of the adsorbed ions.

The adsorption isotherms of SDS, STS, SHS and SOS on rutile at pH 3.1 ± 0.1 and 25°C are shown in Fig. 4.10. The curves follow Traube's rule (195) in that adsorption from solution increased markedly as the homologous series was ascended. This trend is a direct corollary of the results obtained in the electrokinetic studies.

Marked on the graph is the adsorption density required for a statistical, close-packed, vertically oriented monolayer based on a cross-sectional area of 25\AA^2 for an alkyl sulphate ion (196). Also indicated by cross-hatching is the range over which complete transfer of surfactant-coated rutile particles into various oil phases occurred (c.f. section 5.1 Extraction investigation).

All the isotherms are sigmoidal and are typical of a type S2 isotherm in Gile's classification system (197) for adsorption isotherms.

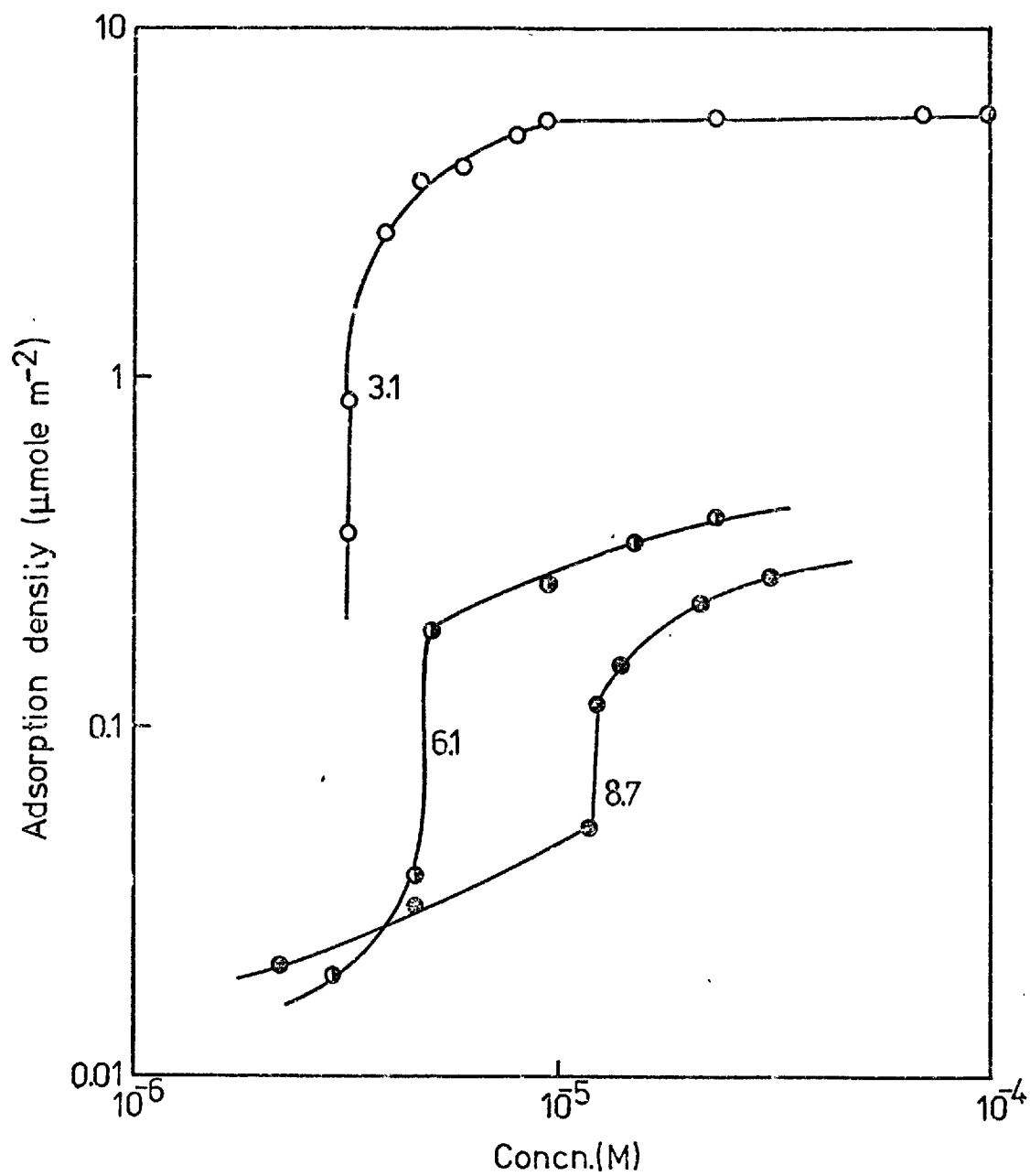


Fig. 4. 9. Adsorption isotherms of SOS on rutile at various pH values.

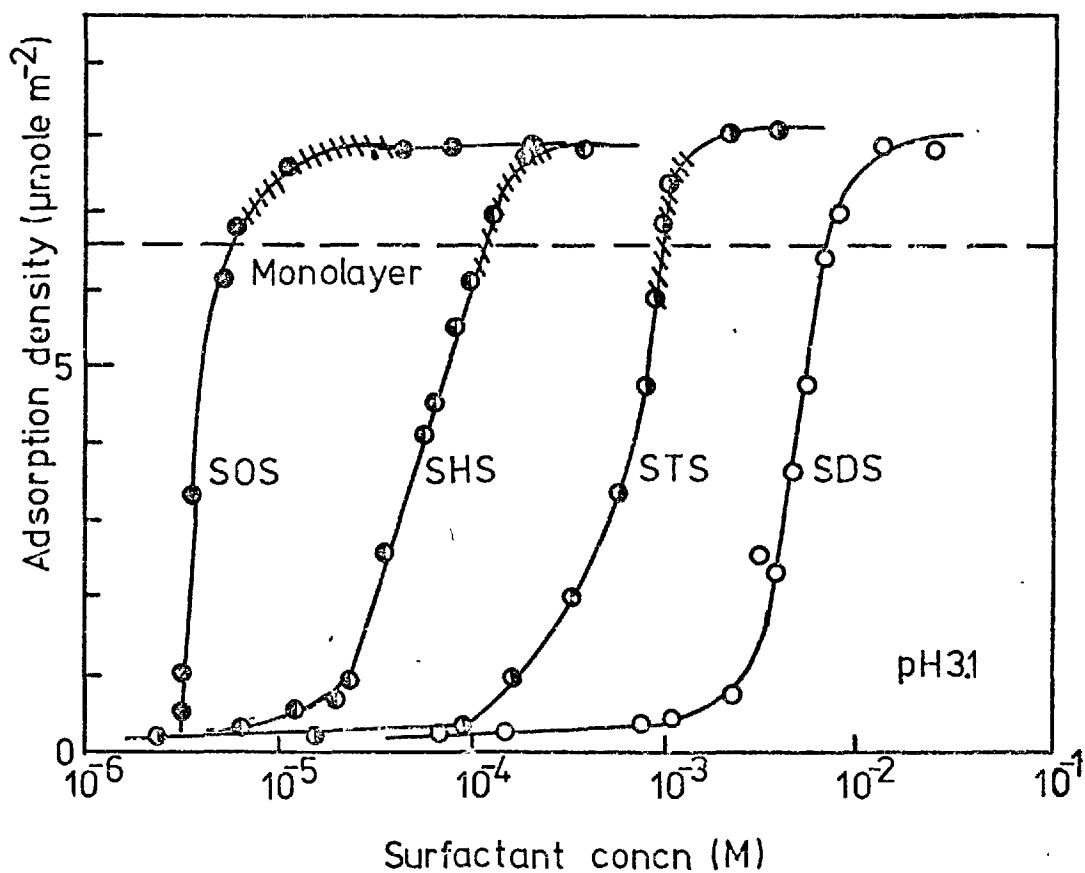


Fig. 4. 10. Adsorption isotherms of alkyl sulphates on rutile at pH 3.1.

This type of isotherm is indicative of adsorption of a monofunctional surfactant ion which has moderate intermolecular attraction with the adsorbate. As a result, the adsorbed molecules assume a vertical orientation. The S-shape also indicates that there is competition for surface sites from the solvent molecules. The isotherms may be discussed in terms of three regions, viz

I: an approximately linear region at low adsorption densities and surfactant concentrations, where adsorption does not increase significantly as concentration is increased;

II: a region following region I where adsorption density increased rapidly over a small concentration range of surfactant; and

III: a region where the isotherm levelled off as saturation was reached.

Adsorption in region I obeys an adsorption isotherm of the Freundlich type (198)

$$\log x = \log k + \frac{1}{n} \log c \dots \dots \dots (4)$$

where, x = moles of surfactant adsorbed,
 c = equilibrium aqueous concentration of surfactant,
and $\frac{1}{n}$ and k are constants.

Adsorption of alkyl sulphate ions in this region is primarily due to ion exchange with anions in the diffuse double layer. It has been suggested by Fuerstenau and other authors (139) (184) (199) that the inflexion point in the adsorption density-equilibrium surfactant concentration isotherm at the end of region I corresponds to the initiation of hemimicellization. Under certain circumstances this may be the case, but in this work and other studies (200), the point which corresponds to the onset of hemimicellization, and thus adsorption in the Stern plane, is at surfactant concentrations significantly below the beginning of region II. A comparison between the critical hemimicelle concentration (C_{HMC}) (obtained from electrokinetic data) and the beginning of

rapid adsorption is given in Table 4.2.

Table 4.2.

Critical hemimicelle concentration and the first inflexion point in the adsorption isotherms of alkyl sulphates on rutile at pH 3.1.

Chain length (carbon atoms)	C_{HMC} (M)	Inflexion point (M)
12	3×10^{-6}	2×10^{-3}
14	10^{-6}	10^{-4}
16	3×10^{-7}	2×10^{-5}
18	4×10^{-8}	3×10^{-6}

The C_{HMC} is dependent on the adsorption density of the surfactant at the solid/liquid interface (201) and consequently the potential at the solid/liquid interface (202). It is not a simple function of a bulk aqueous property of the surfactant e.g. $C_{HMC} \approx 1/100$ c.m.c. In those cases, therefore, where the C_{HMC} corresponds to the initiation of a rapid increase in adsorption, it is possible that equilibrium surfactant concentration required for the onset of hemimicellization is coincident with the concentration at which formation of a second surfactant layer occurs, and that increased adsorption of surfactant is a reflection of the second phenomenon. The results in this work indicate that whilst hemimicellization causes adsorption in the Stern layer and a corresponding change in the zeta-potential, it does not automatically lead to increased adsorption in the double layer as a whole.

Adsorption of surfactant ions in the Stern layer has been shown (203) from consideration of the Stern theory to be an equation of the Langmuir type (204)

$$n_s = \frac{K_1 c}{1 + K_2 c} \dots \dots \dots (5)$$

where, n_s = number of surfactant ions adsorbed in the Stern layer,
 c = concentration of surfactant ions,

$$K_1 = N_1 K_2,$$
$$K_2 = K_3 \exp (-\Delta\bar{G}_{\text{ads}} / KT),$$

N_1 = number of adsorption sites available per unit area,
and K_3 = constant.

It should be noted that the free energy of adsorption is dependent on the potential at the Stern plane and therefore K_1 and K_2 are not constants. Hejl and Skrivan (205) have used this equation in an attempt to show discrepancies between theoretically calculated values for the adsorption of surfactant ions on corundum and the experimental values obtained by Modi and Fuerstenau (206) (207). The authors only allow for the free energy contribution to adsorption of Coulombic attraction, however, and ignore specific adsorption contributions. Their conclusion that the electrostatic mechanism of hydrophobization of corundum by SDS is invalid must, therefore, be viewed with some doubt.

The mechanism of adsorption in region II where adsorption increased rapidly has been discussed briefly above. Fuerstenau and coworkers (139) (192) (201) have suggested, after extensive studies of the adsorption of alkyl sulphonates on alumina, that increased adsorption is a result of the onset of hemimicellization. In view of the low surfactant concentrations at which the zeta-potential was reversed in this study, this mechanism would appear unlikely. The steep rise in adsorption density is suggestive of a 'phase' change (200) such as a condensation phenomenon. This is consistent with the theory of Cases et al (144) (145) that the rapid increase in adsorption is attributable to reversely oriented surfactant ions adsorbing on the homogeneous surface presented to the aqueous phase by an initial first layer of surfactant. In view of later results indicating the presence of pre-micelles, e.g. dimers, in aqueous solutions of the surfactants used in this study (c.f. Chapter 6. Oil/water interface) the suggestion of Jaycock and co-workers (208) that increased adsorption could be due to adsorption of multiple surfactant units is of interest.

Adsorption continues through region II until the saturation adsorption density is reached. Saturation often coincides with the critical micelle concentration (209), but the most probable cause is the completion of a bimolecular adsorption layer (210) and the presentation of polar groups to the aqueous phase. Maximum adsorption corresponded to 1.2 close-packed vertically oriented monolayers which is indicative of the latter reason for saturation. There was no indication of a monolayer plateau, but this was probably not detected as the second layer began condensing on more active patches before the first layer was fully completed (211).

All the adsorption isotherms obtained in this investigation were reversible.

The mode of orientation of the surfactant ions at the solid/liquid interface has been the subject of discussion in many studies (183) (200) (208). Prior to neutralization of the charged surface sites the most probable orientation of the surfactant ion is angled. Vertical orientation is unlikely owing to the disruption of the hydrogen bonds present in the water (200) by the hydrocarbon chains of the surfactant. Similarly, horizontal orientation is improbable due to the presence of structured, ice-like water (212) bound to the surface by ion-dipole interaction and hydrogen-bonding. This latter orientation is possible, however, when the attractive forces are weakened, such as at z.p.c.

After neutralization of the surface sites, there are two further modes of orientation by which the surfactant ions can adsorb at the solid/water interface. The first involves adsorption due to dipolar attraction and hydrophobic bonding between the hydrocarbon chains resulting in the polar group being adsorbed to the solid surface. The second is the result of physical hydrocarbon chain interactions only and leads to reversed orientation of the surfactant with the polar group facing out into aqueous surfactant solution. Adsorption as a

result of either of these mechanisms is reflected in increased adsorption in region II of the isotherm. Whilst there is probably a distribution between these two possibilities, the extraction results (c.f. section 5.1) indicate that adsorption with reversed orientation probably predominates.

4.2.2 Adsorption of CTAB at the rutile/water interface.

The variation of adsorption density with equilibrium CTAB concentration at various pH values was investigated. The results are shown in Fig. 4.11. The results indicate that two mechanisms of adsorption are occurring in the system. At pH values above the z.p.c. (pH 5.3) the curves are sigmoidal and similar to those obtained at various pH values with SOS. The results are consistent with Coulombic attraction at low surfactant concentrations, followed by association of the hydrocarbon chains due to Van der Waals forces at higher adsorption densities.

At pH values below the z.p.c., where the distribution of negative adsorption sites is very low and Coulombic attraction is generally not the primary driving force of attraction, the adsorption isotherms indicate that significant adsorption has occurred. The curves correspond to adsorption isotherm type S1 in Giles's classification system (197). The mechanism of adsorption thus indicated is one similar to that in the case of type S2 isotherms with the exception that saturation is not attained. The curves at low surfactant concentrations ($< 10^{-4}$ M) are consistent with the results obtained at pH values above the z.p.c. in that there was a decrease in adsorption with decreasing pH. At a certain concentration, however, which was independent of pH, the adsorption increased rapidly with little change in the equilibrium surfactant concentration and showed little tendency to reach saturation. These results suggest that multimolecular layers are adsorbing on the rutile surface in a manner similar to precipitation of the surfactant.

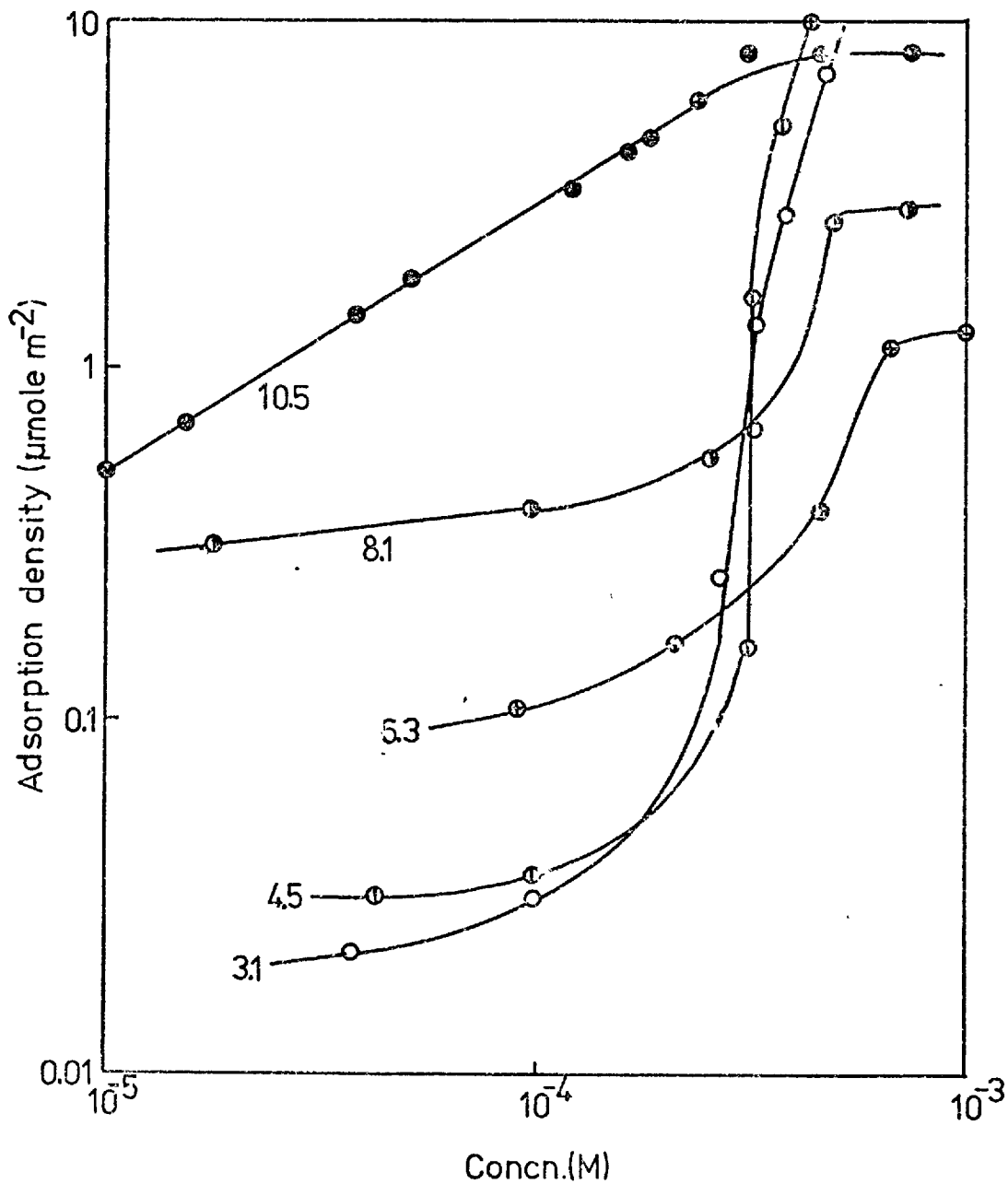


Fig. 4. 11. Adsorption isotherms of CTAB on rutile at various pH values.

It can be seen from Fig. 4.8 that the rutile zeta-potential at these pH values and surfactant concentrations was approximately constant, indicating that adsorption of a neutral molecule or ion pair was taking place.

The adsorption isotherm of CTAB on rutile at $\text{pH } 10.5 \pm 0.1$ is shown in rectilinear form in Fig. 4.12. Marked on the curve by cross-hatching is the region in which extraction into various oil phases occurred (c.f. 5.1 Extraction investigation). Also indicated is the adsorption density required for a statistical, close-packed, vertically oriented monolayer based on a cross-sectional area of 26\AA^2 for a trimethylammonium ion (213). The inflexion point marking the onset of the rapid increase in adsorption density occurred at about 10^{-5} M CTAB. This is very close to the value found for the critical hemimicelle concentration, 7×10^{-6} M CTAB. These results show that, in the system modified by CTAB, the equilibrium surfactant concentration required for the initiation of hemimicellization is coincident with that required for the onset of increased adsorption as a result of condensation upon the hydrocarbon sites provided by the first layer of adsorbed surfactant. Saturation in this system occurred at an adsorption density corresponding to 1.4 close-packed, vertically oriented monolayers. This probably corresponds to a bimolecular adsorption layer. Although the polar head group of the cetyltrimethylammonium ion has almost the same cross-sectional area as that of the alkyl sulphate ions, saturation was reached at a higher adsorption density in the case of the former surfactant. This suggests that bimolecular adsorption layer is more compact in the case of CTAB, which presumably reflects the nature of the charged head group i.e. the field intensity around the trimethylammonium ion is reduced by the presence of methyl groups (189), and, therefore, the repulsive forces between the head groups are decreased.

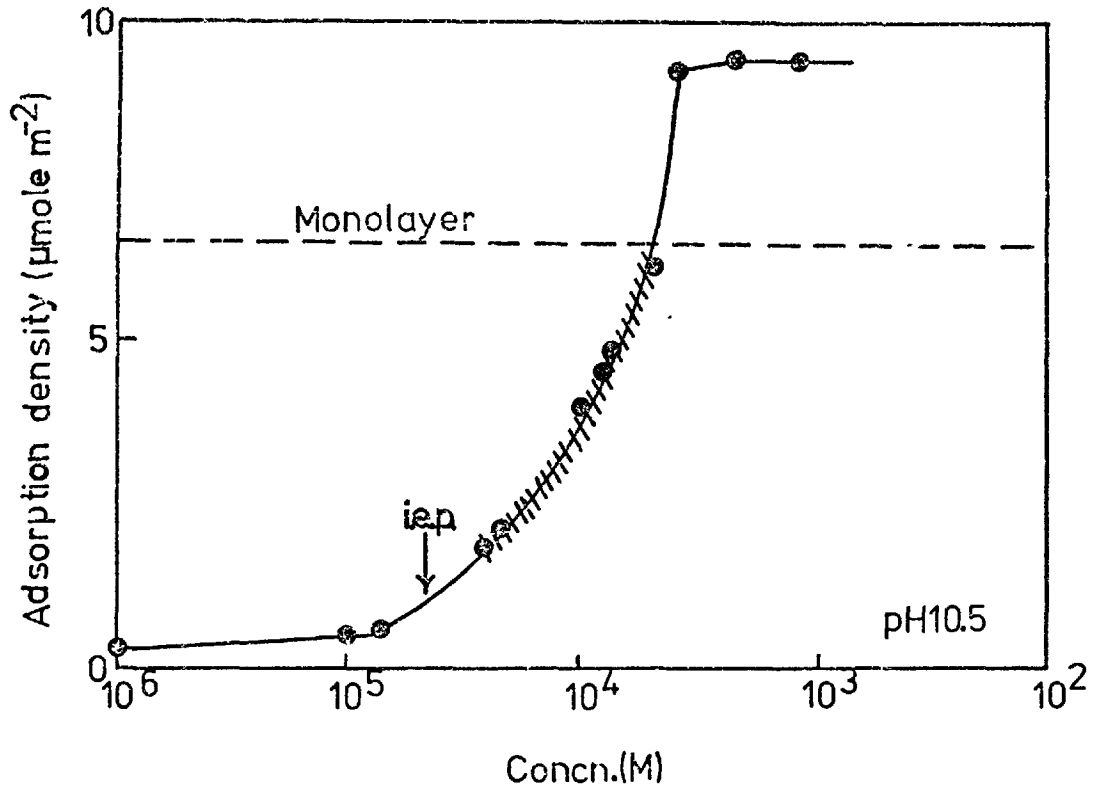


Fig. 4. 12. Adsorption isotherm of CTAB on rutile at pH 10.5.

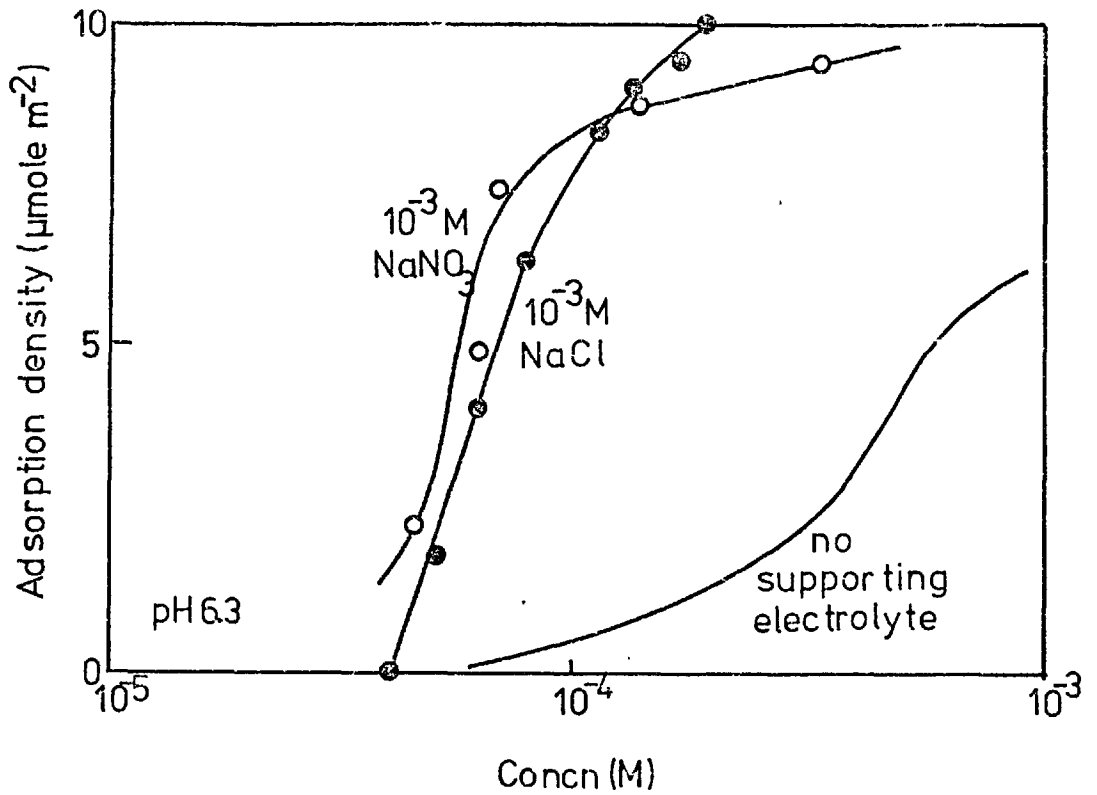


Fig. 4. 13. Adsorption isotherms of CTAB on rutile in the presence of supporting electrolyte at pH 6.3.

4.2.3 Effect of supporting electrolyte on adsorption of CTAB at the rutile/water interface

To determine whether or not the adsorption of CTAB at pH values below the z.p.c. was related to the presence of chloride ions from the HCl used to modify the pH, the effect of sodium chloride and sodium nitrate on adsorption at $\text{pH } 6.3 \pm 0.1$ was investigated. The results are shown in Fig. 4.13. The concentration of both salts was 1 mM. The curves are similar to those obtained at pH values below the z.p.c. in the presence of HCl, and they are characterized by an extremely rapid rise in adsorption density at a certain equilibrium concentration. In both cases there was no change in pH upon adsorption, therefore adsorption of the cationic surfactant by ion exchange with hydrogen ions on the surface (214) can be discounted.

A potentiometric titration was carried out to determine the chloride and bromide ion concentration in solution following adsorption under the conditions used above. The titration was carried out by titrating the equilibrium chloride/bromide solution against AgNO_3 and measuring the potential with a silver electrode. The results showed that following adsorption from a solution containing an initial CTAB concentration of 1 mM at pH 6.3 in the presence of 1 mM NaCl, the chloride ion concentration was unchanged, but the bromide ion concentration had been reduced to 8.5×10^{-4} M. This corresponds to a bromide ion adsorption density on the rutile surface of $1.86 \mu\text{mole m}^{-2}$. This value is comparable to the adsorption density of the cetyltrimethylammonium ions on the rutile surface under the same conditions, $5.54 \mu\text{mole m}^{-2}$. It was observed that CTAB solutions were stable in salt solutions far in excess of 1 mM. These results suggest, therefore, that CTAB is 'salting out' onto the rutile surface in the presence of chloride ions and it is this effect that is causing the large rise in adsorption reflected in the isotherms below the z.p.c.

5. SOLID/WATER/OIL SYSTEM

5.1 Extraction studies.

5.1.1 Systems modified by alkyl sulphates.

5.1.1.1 Effect of hydrocarbon chain length.

(a) System : rutile/water/n-heptane.

The response of rutile in the oil/water system modified by alkyl sulphates with 12, 14, 16 and 18 carbon atoms in the hydrocarbon chain was investigated. The initial surfactant concentration and pH were varied and their effect on the behaviour of the collector-coated rutile particles noted. The results obtained are shown in Figs. 5.1 - 5.4. The key to the symbols used in these and succeeding diagrams is given in Table 5.1.

Table 5.1

Key to response diagrams

Symbol	Description
○	negligible concentration at interface
⊙	partial concentration at interface
⊗	complete concentration at interface
⊙ (with dots around it)	partial extraction into organic phase*
⊗ (with dots around it)	total extraction into organic phase

* Note: inner circle still denotes extent of concentration at interface.

The alkyl sulphates exhibited a progression in their effect from SDS to SOS. The characteristics of this trend were,

(1) the area of complete concentration at the interface in the acid region of the pH range extended over a smaller initial surfactant concentration range with increasing chain length.

The upper pH value at which recovery started to decrease, however, remained constant at about pH 7.

(2) The pH value in the alkaline region at which recovery was reduced

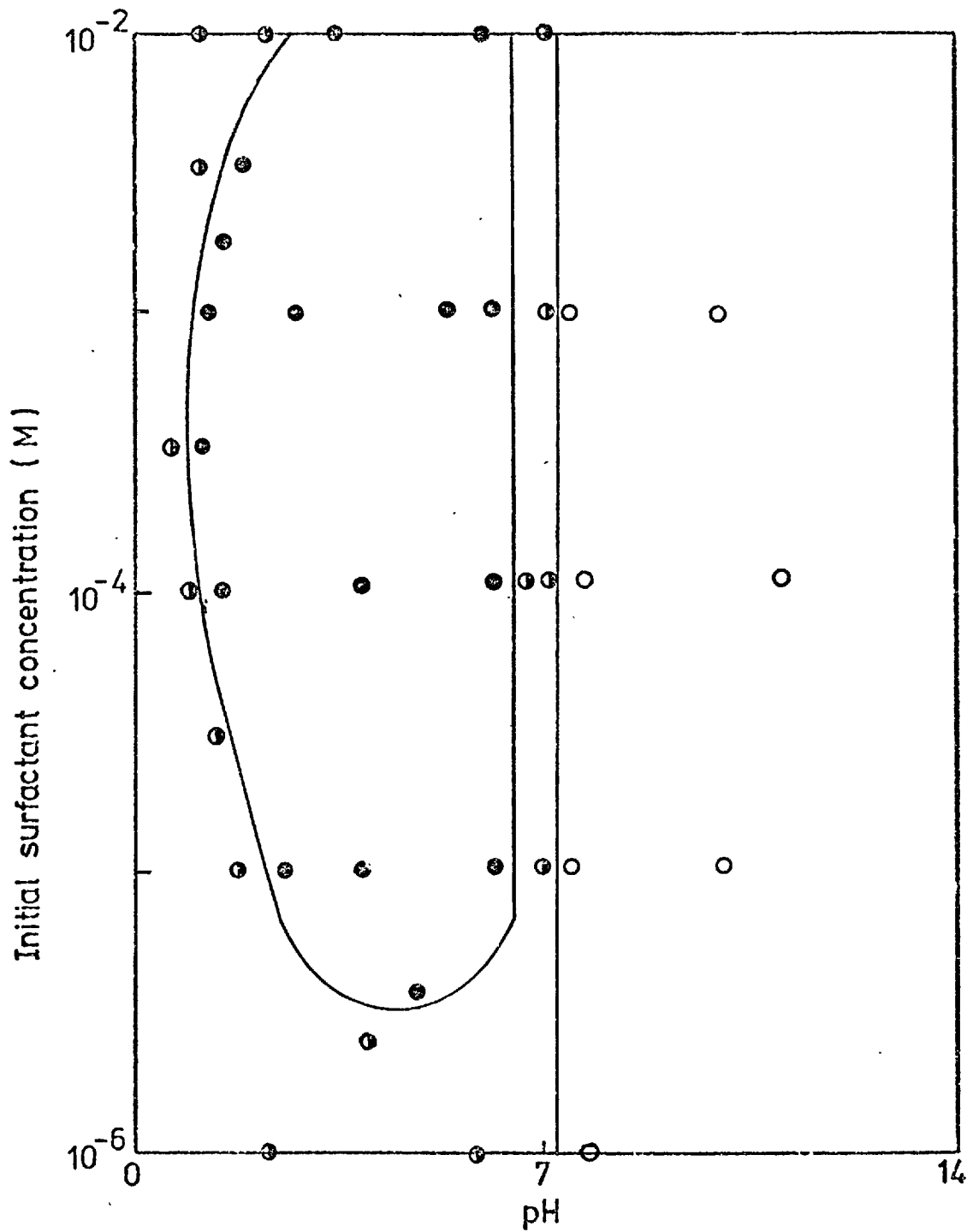


Fig. 5. 1. Response of system : rutile/water/n-heptane modified by SDS.

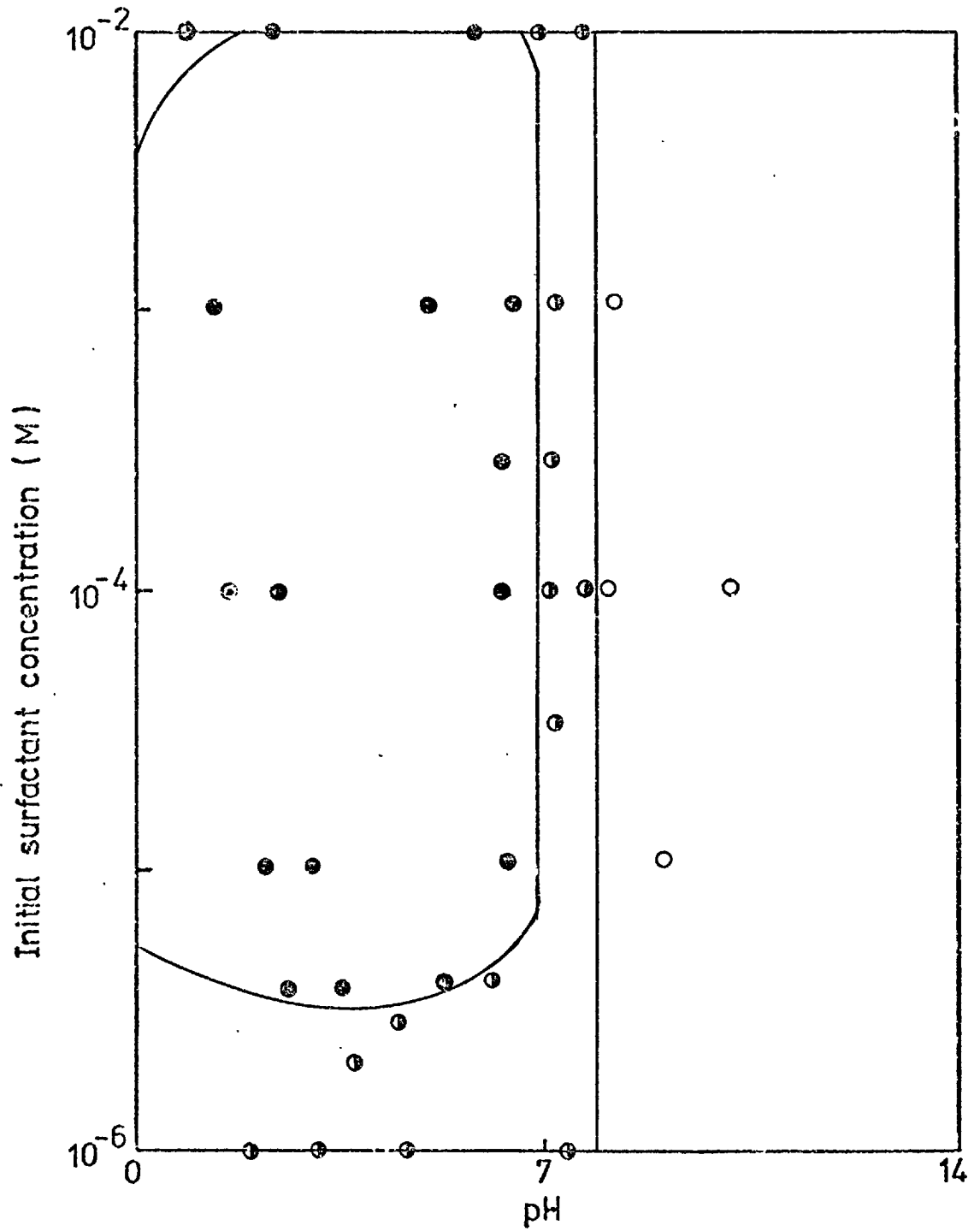


Fig. 5. 2. Response of system : rutile/water/n-heptane modified by STS.

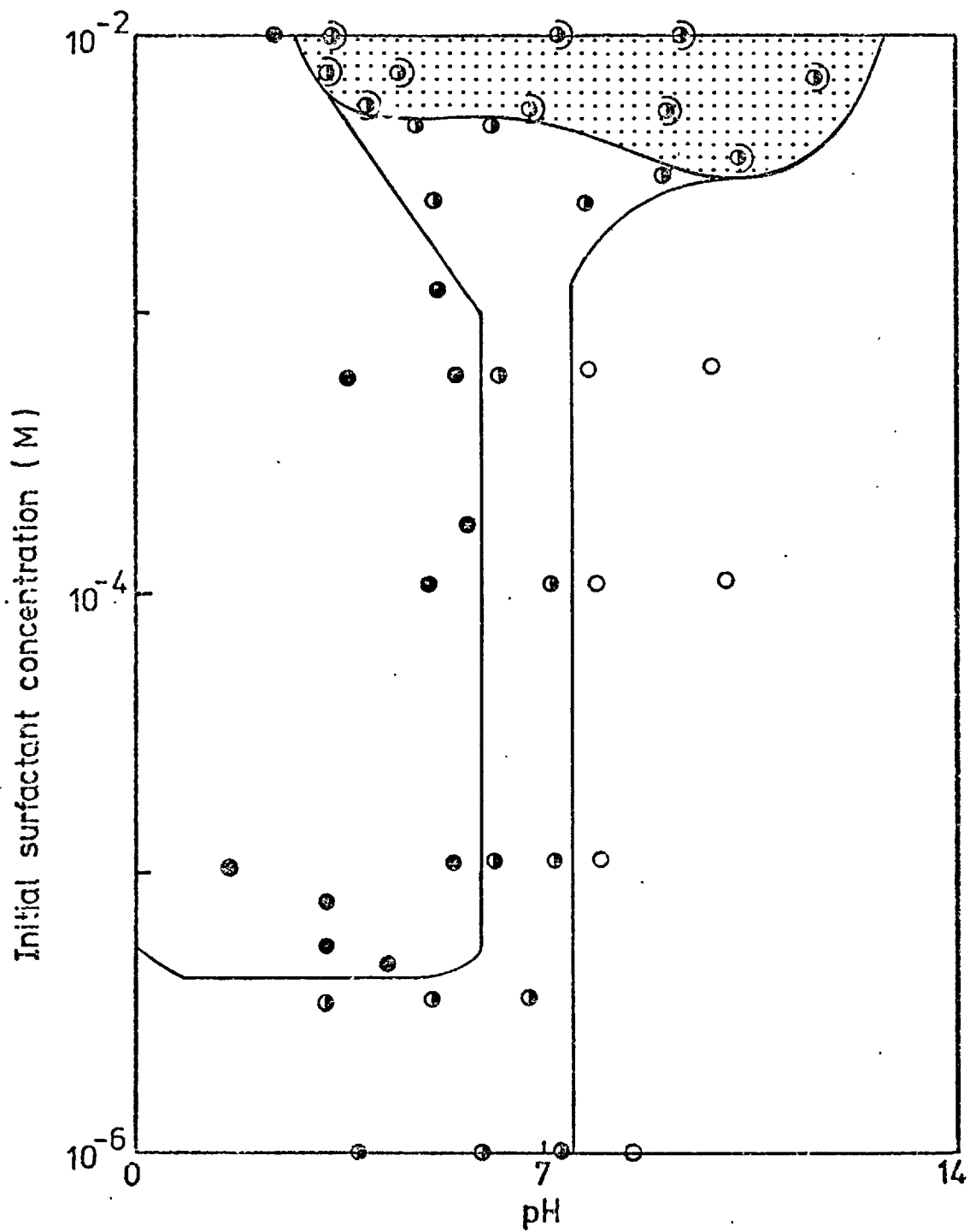


Fig. 5. 3. Response of system : rutile/water/n-heptane modified
by SHS.

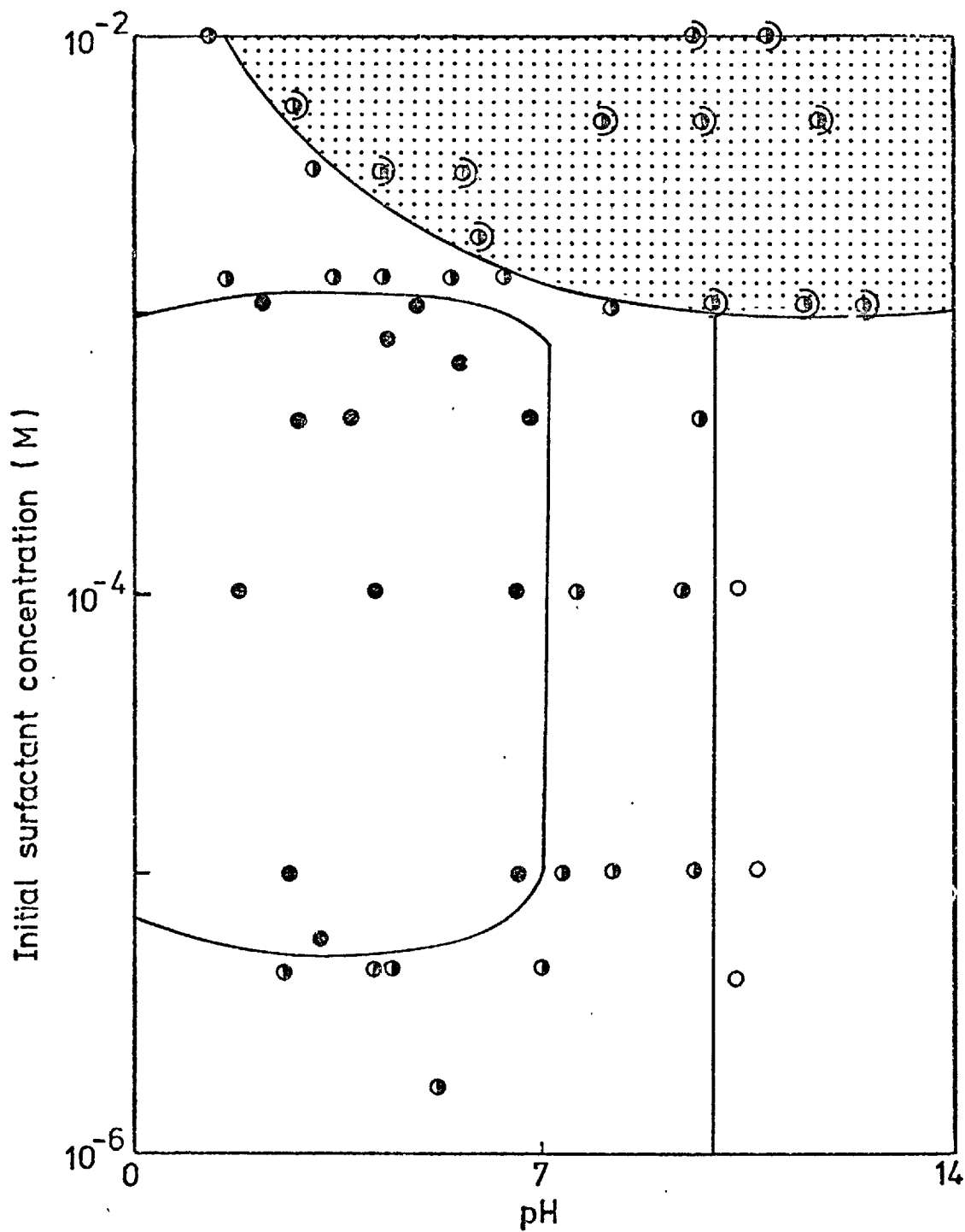


Fig. 5. 4. Response of system : rutile/water/n-heptane modified by SOS.

to zero increased with increasing chain length.

- (3) Total extraction of rutile did not occur in this system. At high surfactant concentrations in the systems modified by SHS and SOS, however, the rutile particles tended to transfer from the aqueous phase into the organic phase. Partial extraction in these systems was essentially independent of pH and occurred at decreasing initial surfactant concentration with increasing chain length.

In all extraction tests the rutile particles were dispersed in the aqueous phase at alkaline pH values and over all the pH range where surfactant was present in initial concentrations greater than 5 mM. Furthermore, in the acid region, the particles (especially those concentrated at the interface) were flocculated.

These results are consistent with the rutile particles becoming hydrophobic as a result of adsorption of alkyl sulphate ions by the mechanism outlined in Chapter 4. Alkyl sulphate ions adsorb onto the positively charged rutile particles, at pH values below the z.p.c., by Coulombic attraction followed by association of the hydrocarbon chains due to Van der Waals forces of attraction.

The effect of hydrocarbon chain length on the response of the system as initial surfactant concentration and pH was varied is shown by the differences in the position of the boundaries separating the areas of different response. The point at which complete concentration at the interface ceased at low initial surfactant concentration did not change with increasing chain length. Adsorption in this region is driven by the free energy changes arising as a result of Coulombic attraction, and hydrophobic association of the adsorbed species does not contribute to adsorption, i.e.

$$\Delta G_{ads} = ze\psi_s \dots \dots \dots (1)$$

Hydrocarbon chain length therefore has no effect on adsorption and consequently the minimum surfactant concentration required for complete

concentration of the rutile at the interface would also be expected not to vary greatly with chain length.

At the upper initial surfactant concentration required for complete concentration of the rutile at the oil/water interface the contribution of the hydrocarbon chain to adsorption is significant, viz,

$$\Delta G_{ads} = ze\psi_0 + n\phi \dots \dots \dots (2)$$

The cessation of complete concentration of the rutile at the interface may be attributable either to the attainment of the c.m.c. or to the formation of a reversed bilayer of alkyl sulphate on the rutile particles. In either case, the contribution of the $n\phi$ term would increase with increased chain length and the required surfactant concentration would decrease.

Similarly, the pH in the neutral pH region above which concentration at the interface ceased increased with increasing chain length. In this region, above the z.p.c., the net surface charge is negative and the primary mechanism of adsorption is the tendency of the hydrocarbon chains to be expelled from the aqueous phase, i.e. the contribution of the $n\phi$ term, which would increase as the homologous series is ascended.

The flocculation behaviour of the collector-coated rutile particles is a reflection of the extent of adsorption of the anionic surfactant on the oxide surface. At pH values where the surfactants adsorb on the surface, adsorption of the collector reduces the net surface charge and coagulation occurs. As adsorption continues, the charge on the surface increases until the repulsive forces result in the particles becoming dispersed. At alkaline pH values adsorption does not occur and the negatively-charged particles remain dispersed.

(b) System : rutile/water/benzene.

The response of the system rutile/water/benzene in the presence of alkyl sulphates with 12, 14, 16, and 18 carbon atoms in the hydro-

carbon chain, was determined as a function of initial surfactant concentration and pH. The results are shown in Figs. 5.5 - 5.8.

Total extraction occurred in this system when the number of carbon atoms in the hydrocarbon chain was equal to or exceeded 14 atoms. Extraction occurred in the acid region of the pH range when the initial surfactant concentration was between 0.5 mM and 1 mM. Little variation in the position of the extraction area was observed with the different surfactants. The corresponding area on the adsorption isotherms over which extraction took place is shown by the cross-hatching in Fig. 4.10 for each surfactant. In each case extraction occurred at adsorption densities between approximately monolayer coverage and the point at which saturation was reached.

Concentration of the particles at the oil/water interface occurred under similar conditions to that obtained with n-heptane. At high surfactant concentrations only partial extraction was obtained, which was confined to acid pH values and extraction decreased with increasing surfactant concentration.

Similar to the n-heptane system the rutile particles were dispersed in the aqueous phase at all pH values at high surfactant concentrations and at low concentrations in the alkaline region. Particles in the organic phase were dispersed.

4.1.1.2 Effect of organic phase.

The differences observed between the systems with n-heptane and benzene as the organic phase indicated that the nature of the oil was a critical factor in determining whether extraction took place or not. The effect of various organic liquids on rutile extraction was, therefore, investigated. The response of the systems involving cyclohexane, diethyl ether, isobutyl methyl ketone and n-dodecanol modified by SOS are shown in Figs. 5.9 - 5.12 respectively.

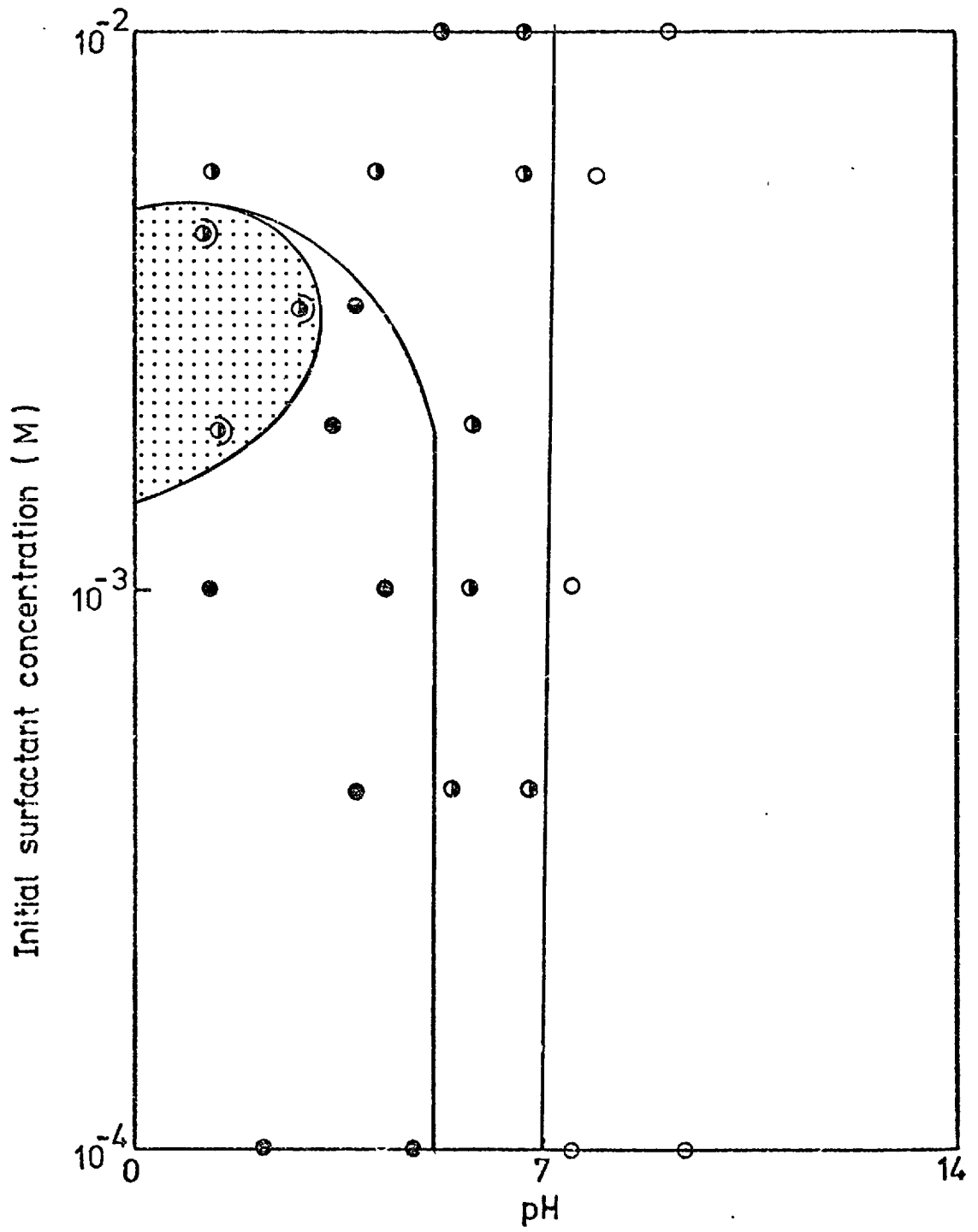


Fig. 5. 5. Response of system : rutile/water/benzene modified
by SDS.

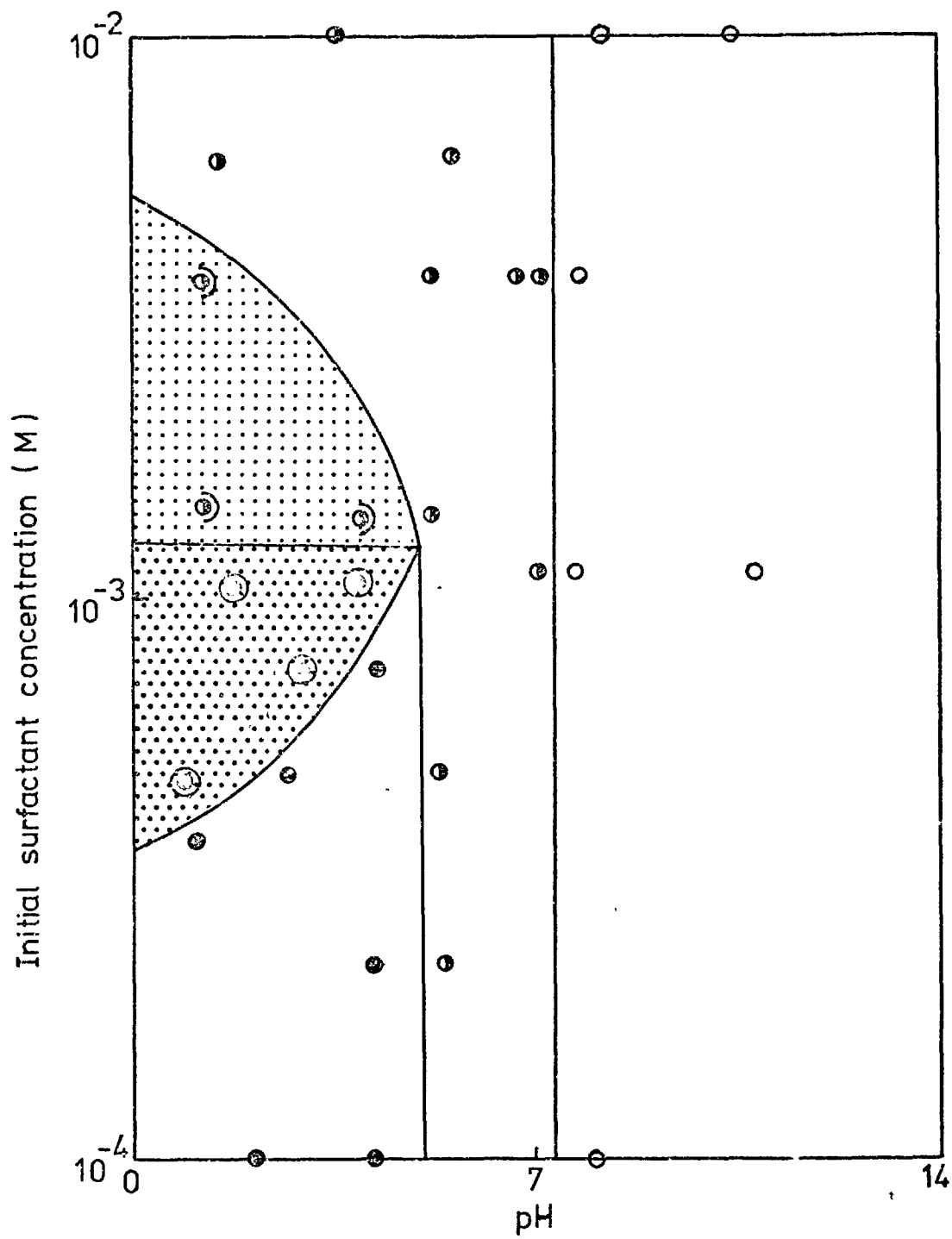


Fig. 5. 6. Response of system : rutile/water/benzene modified by STS.

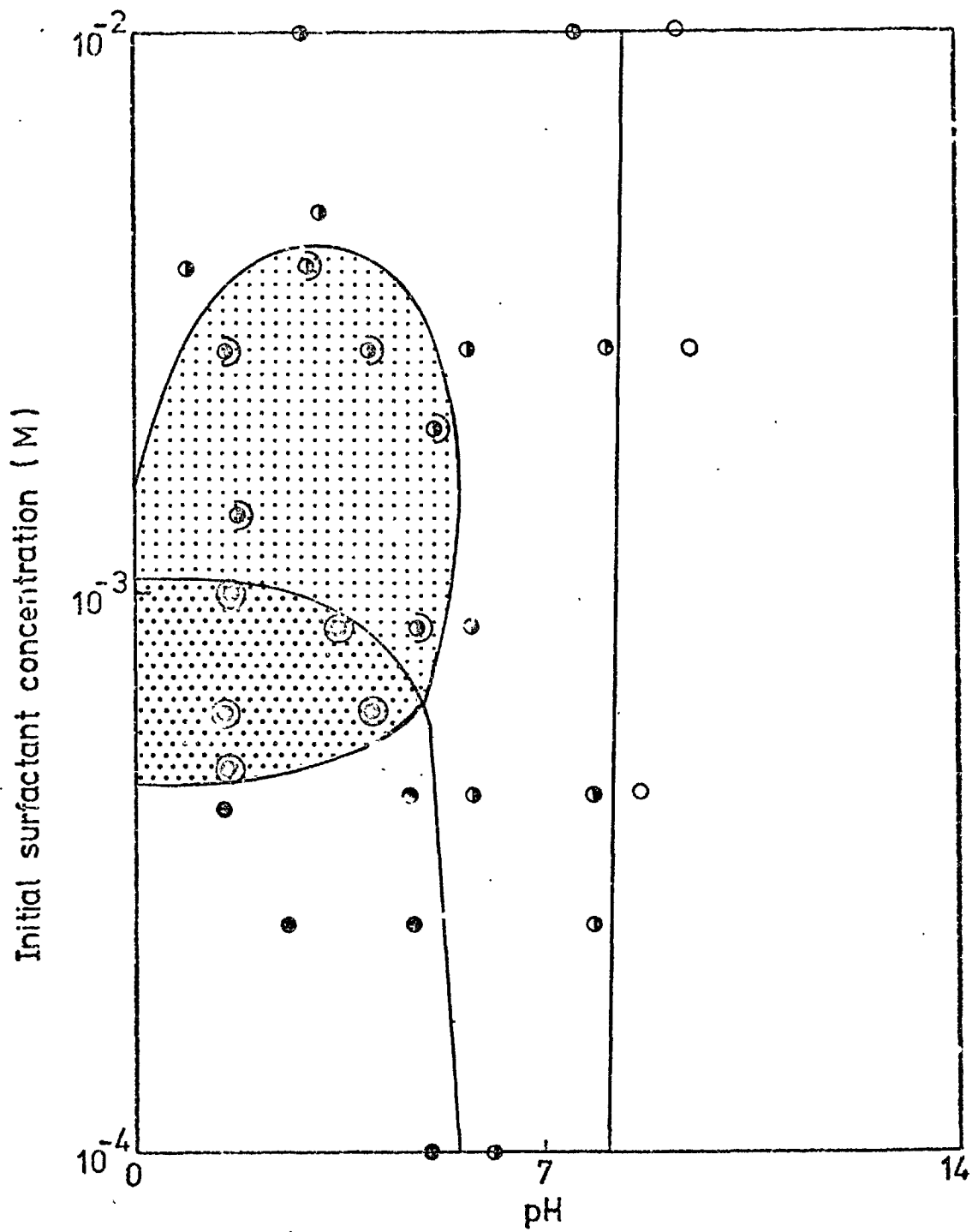


Fig. 5. 7. Response of system : rutile/water/benzene modified
by SHS.

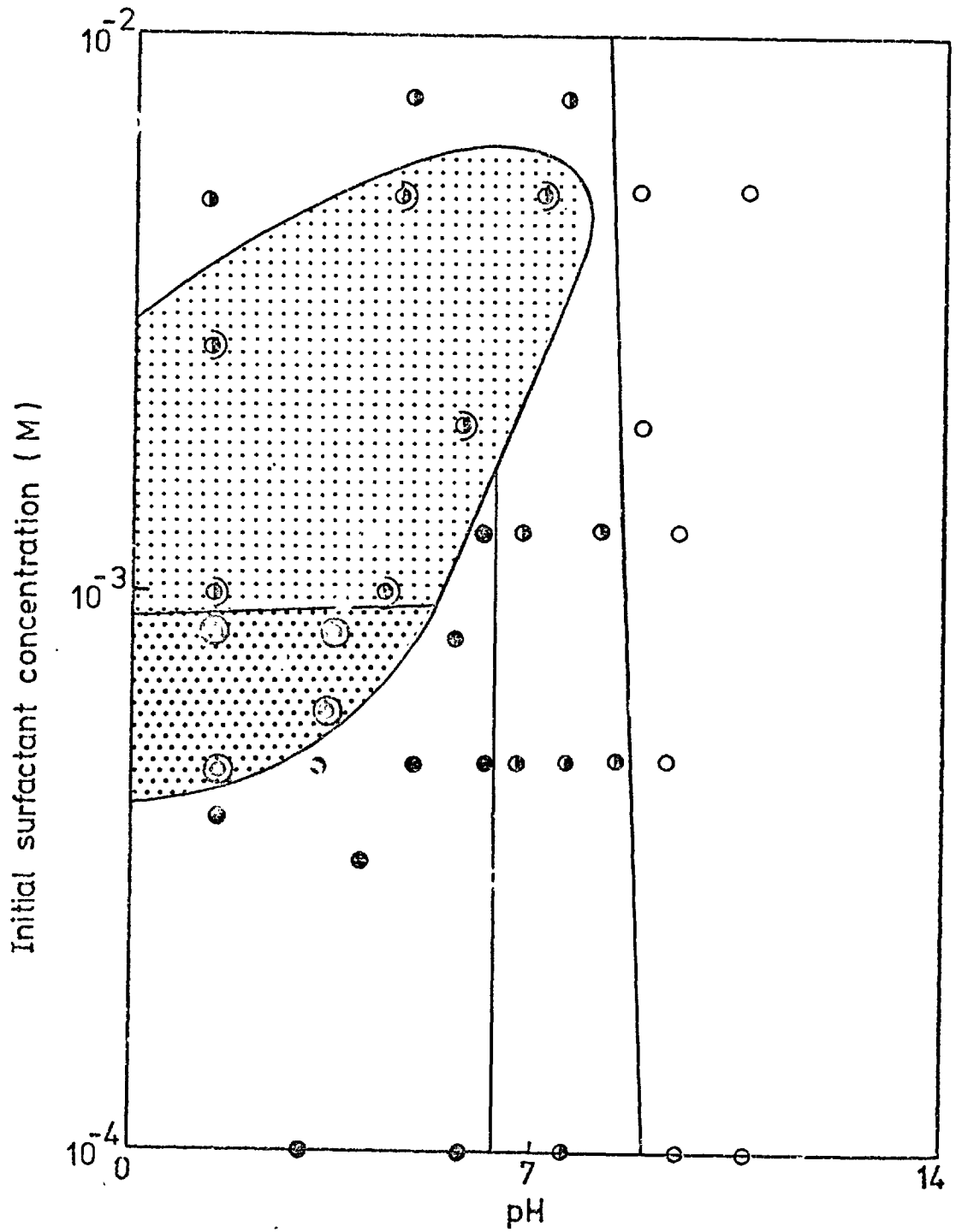


Fig. 5. 8. Response of system : rutile/water/benzene modified by SOS.

Total extraction of rutile into cyclohexane and diethyl ether occurred under similar conditions to that obtained with benzene (c.f. Fig. 5.8). Transfer of particles from the aqueous phase into n-dodecanol and isobutyl methyl ketone did not, however, occur to any significant extent.

In addition to the oils mentioned above, extraction tests were carried out on various other oils and these are summarized in Table 5.2 together with their effect on extraction. Changing the surfactant from SOS to STS did not change the classification of the oils.

Table 5.2

Classification of oil phases according to their effect on extraction in the system, rutile/water/oil modified by alkyl sulphates.

Extraction	No extraction
cyclohexane	n-hexadecane
toluene	n-heptane
benzene	n-hexane
dekalin	iso-octane
diethyl ether	1-octene
di-iso-propyl ether	1-hexene
	isobutyl methyl ketone
	n-dodecanol
	ethyl acetate
	n-butanol

The table shows that extraction does not occur into the straight-chain alkanes, alkenes or ketone. The oils with a cyclic structure and the ethers, however, do permit extraction.

A complete discussion of the probable reasons for the classification of oils into these two groups will be presented later (c.f. Chapter 7. General discussion).

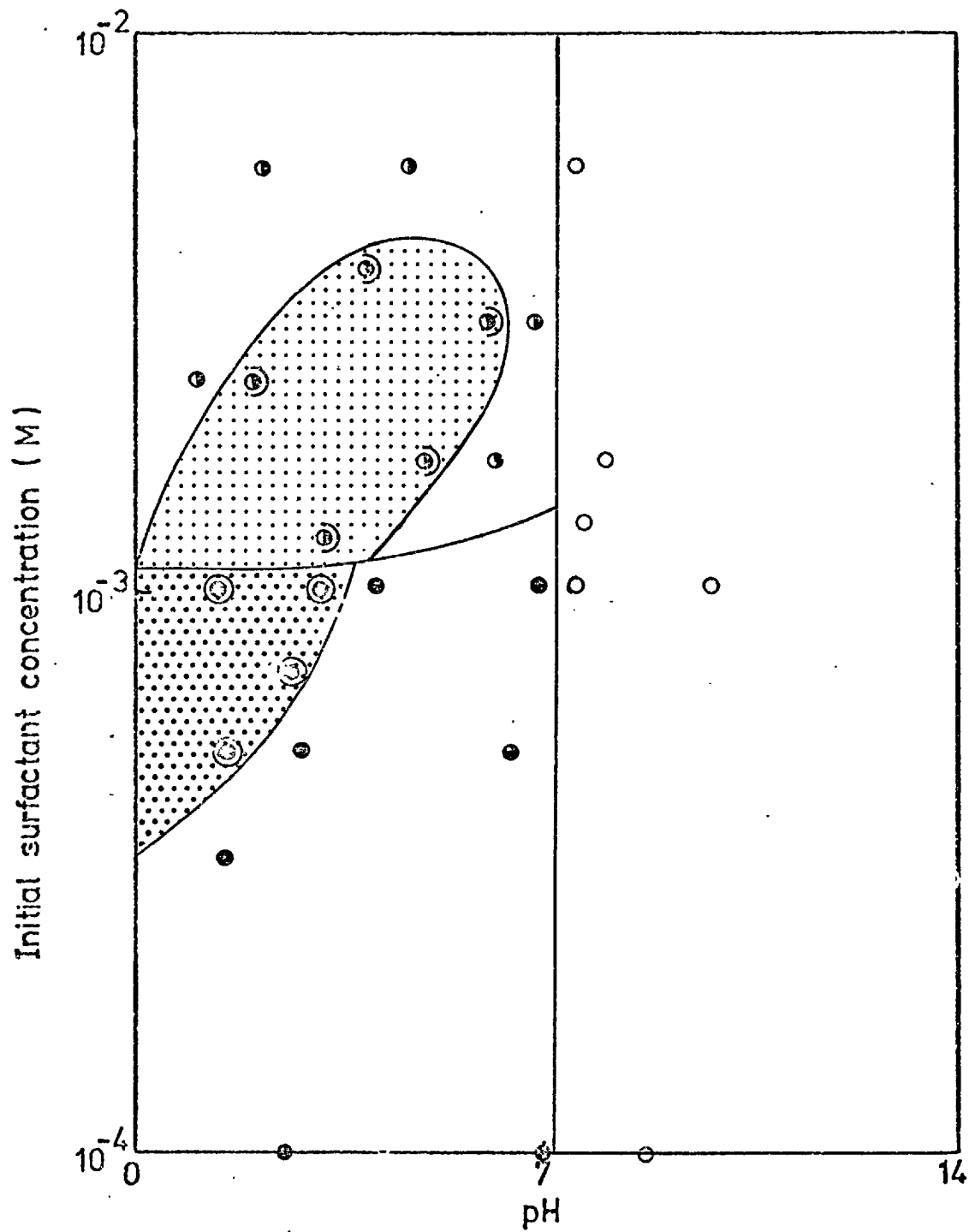


Fig. 5. 9. Response of system : rutile/water/cyclohexane
modified by SOS.

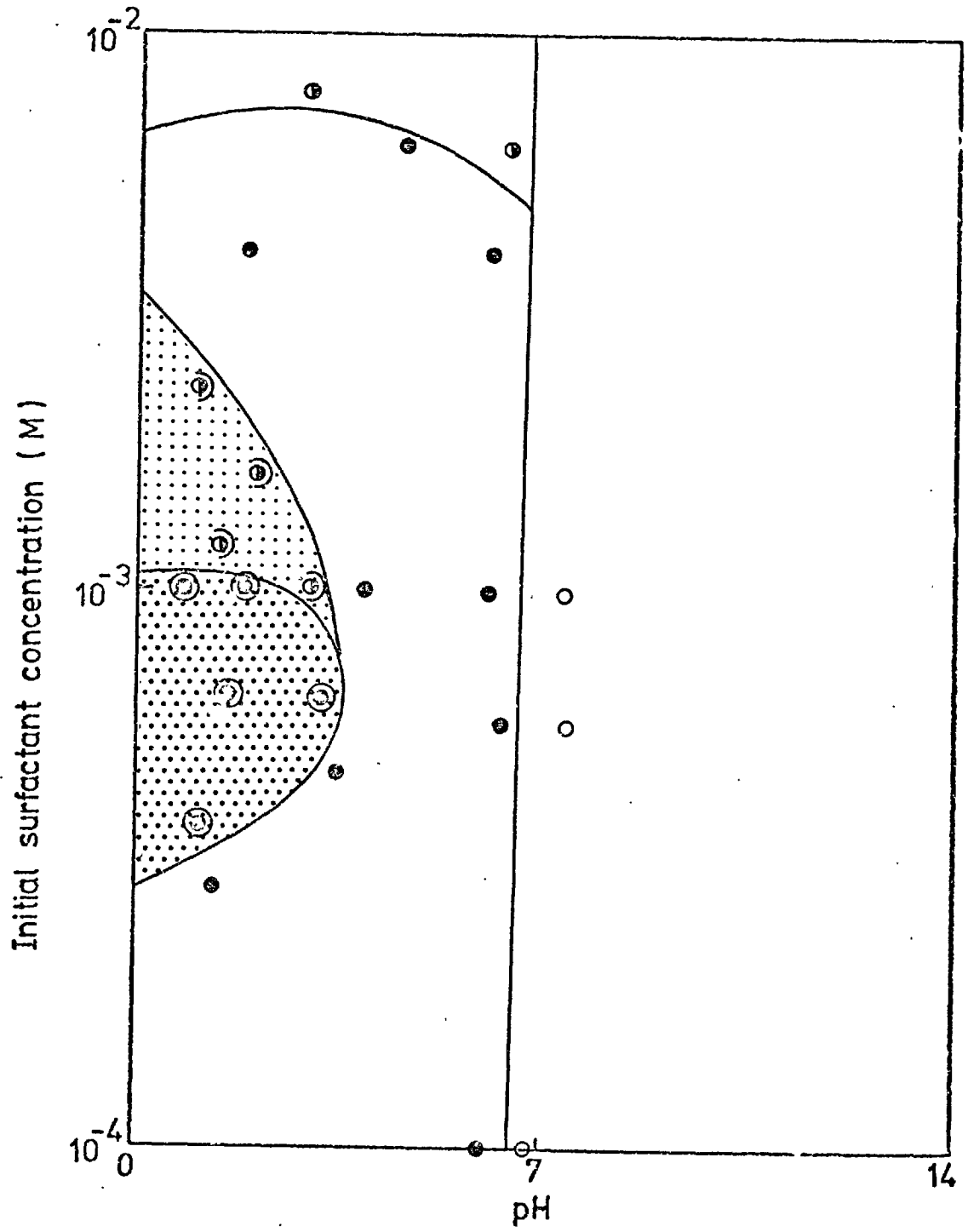


Fig. 5. 10. Response of system : rutile/water/diethyl ether
modified by SOS.

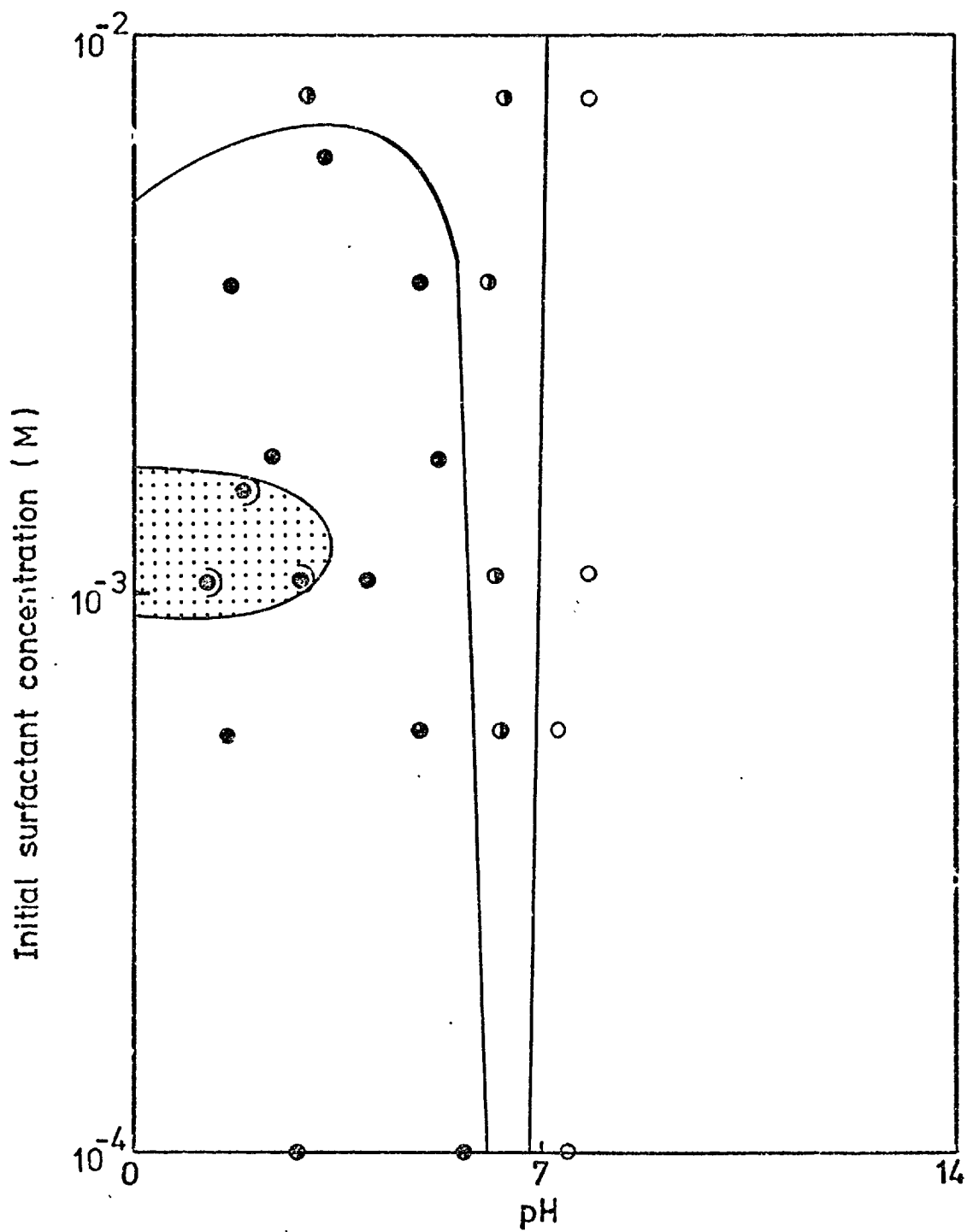


Fig. 5. 11. Response of system : rutile/water/isobutyl methyl ketone modified by SCS.

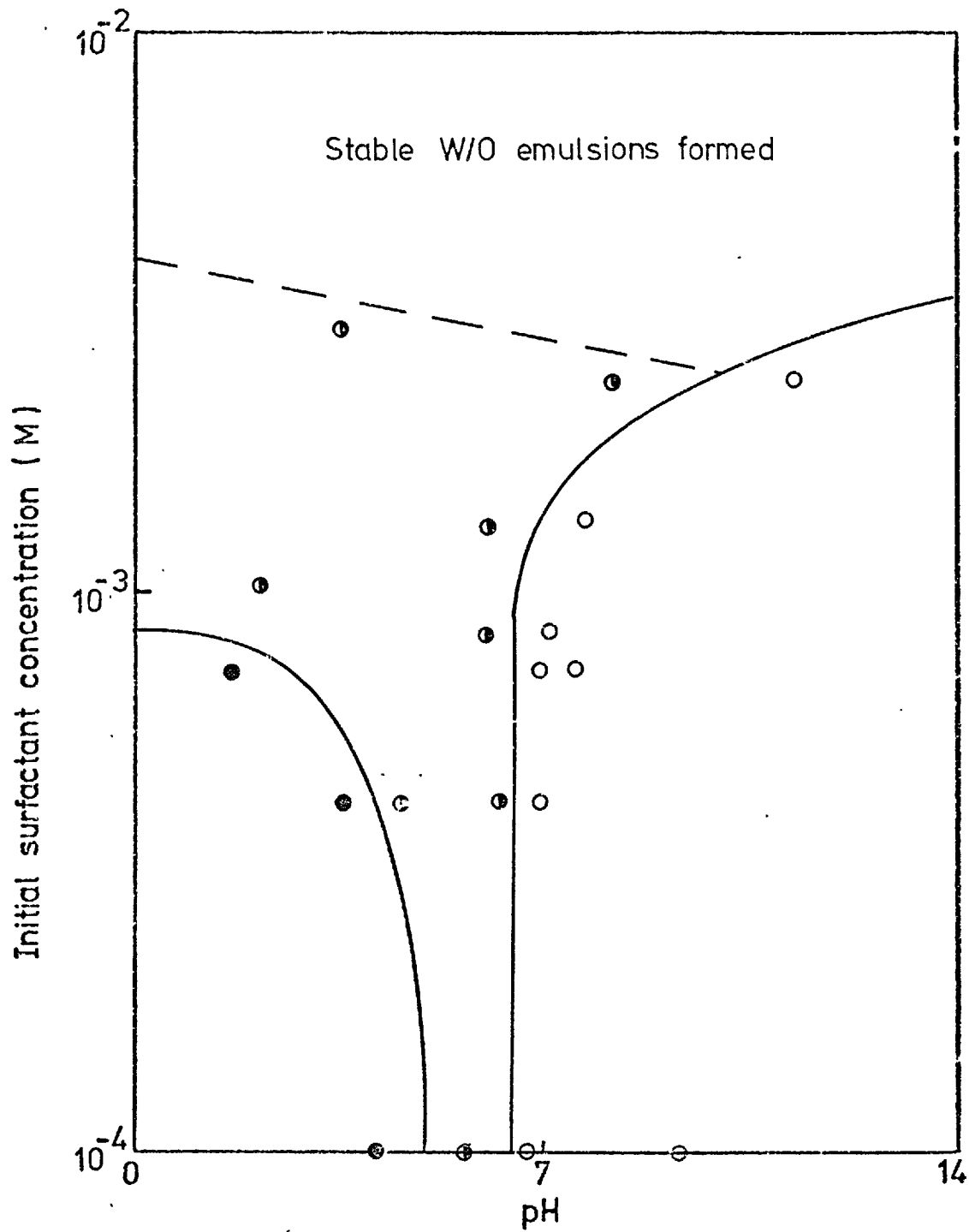


Fig. 5. 12. Response of system : rutile/water/n-dodecanol
modified by SOS.

5.1.1.3 Effect of additives.

Introduction of a neutral molecule, such as an alcohol, into conventional flotation systems has been shown (215) to increase the effective hydrophobicity of the mineral surface because of the co-adsorption of the molecule with the collector. Tests were conducted to determine whether or not an analogous result was obtained when an alcohol was added to a two-liquid-solid system. An organic phase consisting of between 10^{-3} M and 10^{-1} M n-hexadecanol in hexane was used in the system modified by SOS. The results showed that the alcohol increased the area over which concentration at the interface occurred, but it did not promote extraction.

5.1.1.4 Effect of agitation intensity.

Similar to air flotation systems, there will be an energy barrier (216) between the carrier phase (oil) and the solid particle which will have to be overcome before adhesion results. Extraction could, therefore, be dependent on the relative momentum of the particles and oil drops, and hence the agitation rate. To determine if this was the case or not a study was made of the effect of agitation on extraction. The tests were conducted in a 200 ml separating funnel equipped with baffles and agitation was provided by a variable constant speed stirrer. Speeds between 1000 and 3000 r.p.m. were used but no extraction of rutile into n-heptane in the presence of SOS was observed. It is therefore concluded that provided the agitation is above a certain minimum value, agitation has no effect on extraction.

5.1.1.5 Effect of phase volume.

Tests were carried out to determine the effect of organic phase volume on extraction of rutile into n-heptane with SOS. The results showed that qualitatively no significant effect occurred within the

range of phase volumes investigated, i.e. n-heptane/total volume : 9.1 to 69.2 %. With the exception of n-dodecanol in the presence of high concentrations of SOS, inversion of an O/W emulsion to a W/O emulsion was not observed.

5.1.1.6 Reversibility of extraction.

To assess whether mass transfer of mineral particles between the aqueous and organic phase was reversible or not, an extraction test was carried out under conditions where total extraction took place and the mineral-laden oil phase separated readily from the remaining aqueous phase. The organic phase was then agitated with distilled water for 1 hour and during this time the particles transferred from the interior of the organic phase to the interface. Further agitation with fresh distilled water resulted in the rutile becoming dispersed in the aqueous phase. It is, therefore, concluded that the mass transfer of rutile particles across the oil/water interface in the presence of long-chain alkyl sulphates is reversible.

5.1.2 Systems modified by CTAB.

The effect of CTAB on the extraction of rutile into various organic phases was determined. The results obtained with n-heptane and benzene are shown in Figs. 5.13 - 5.14 respectively. In both cases complete concentration at the interface occurred over all the pH range at initial surfactant concentrations below about 1 mM. Total extraction took place in the system rutile/water/benzene between initial CTAB concentrations of 5×10^{-5} M and 5×10^{-4} M and above pH 7.5 - 8.0. The area that this corresponds to on the adsorption isotherm at pH 10.5 is shown in Fig. 4.12 by the region of cross-hatching. Extraction occurred from an adsorption density which corresponded approximately to that required to neutralize the surface charge

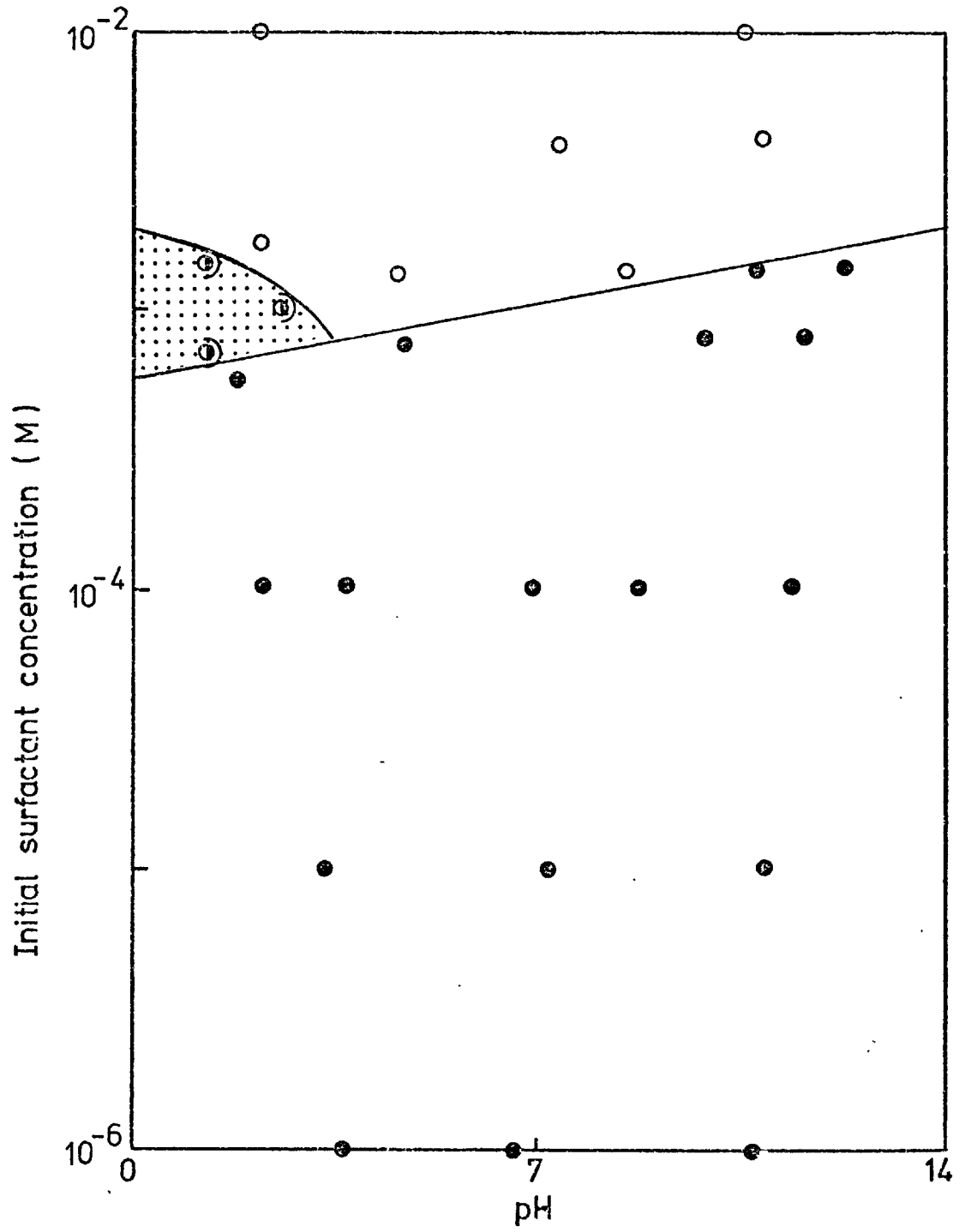


Fig. 5. 13. Response of system : rutile/water/n-heptane
modified by CTAB.

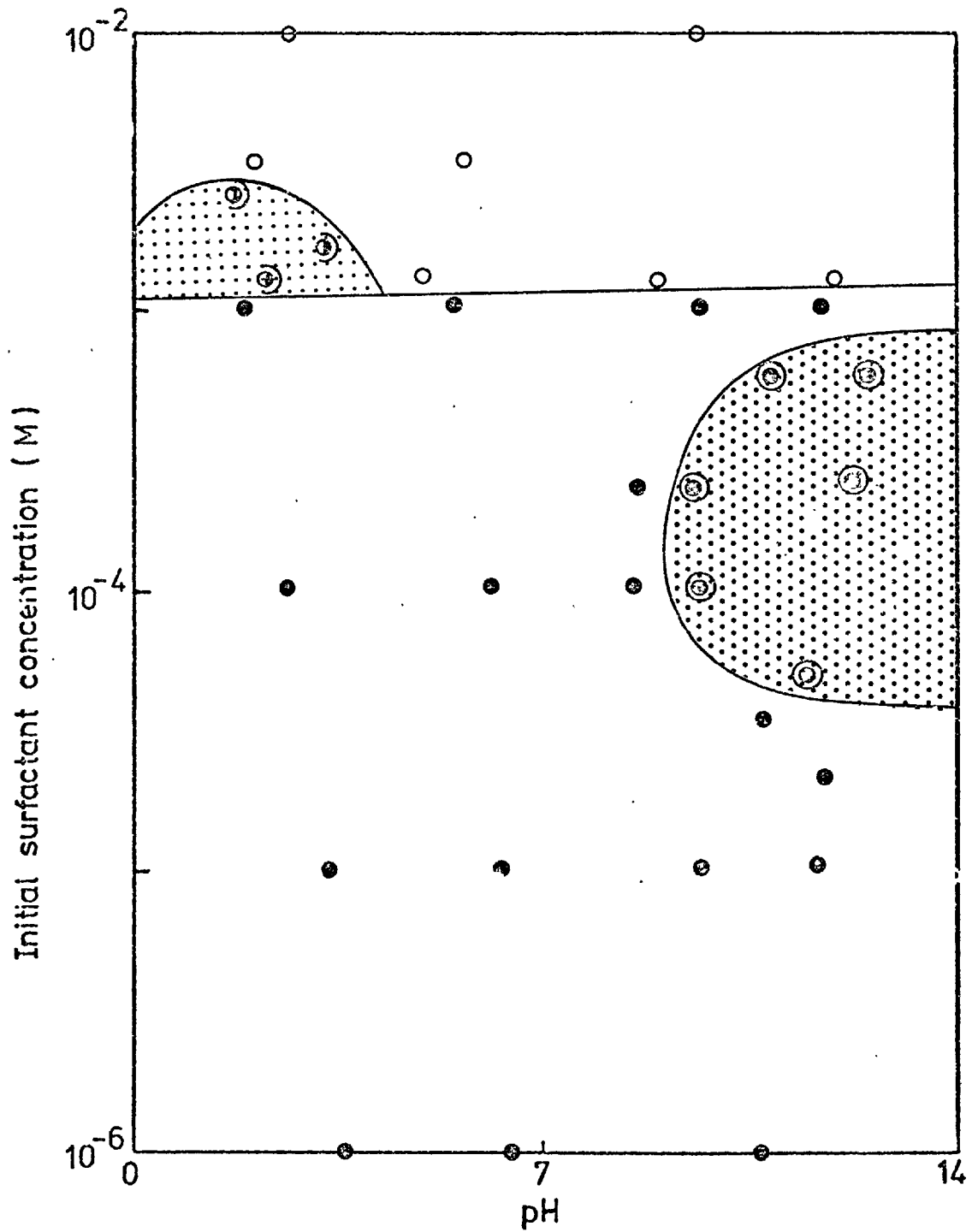


Fig. 5. 14. Response of system : rutile/water/benzene modified
by CTAB.

(i.e. 30% monolayer coverage), up to monolayer coverage (statistical, close-packed, vertically-oriented monolayer). Extraction ceased upon formation of a bilayer. Total extraction of rutile into n-heptane was not obtained under the conditions used.

Partial extraction of collector-coated rutile particles occurred into both oils in the acid region at CTAB concentrations between 1 mM and 2 mM. These results are consistent with the observed 'salting-out' effect of CTAB on rutile in the presence of chloride ions (c.f. 4.2.3 Effect of supporting electrolyte on adsorption of CTAB at the rutile/water interface).

Similar studies were carried out with different oils and the response of the rutile particles in each case is given in Table 5.3. Contrary to systems modified by the alkyl sulphates, extraction occurred into all oils with an interfacial tension against pure water of less than 49.6 mN m^{-1} .

Table 5.3

Classification of oil phases according to their effect on extraction in the system, rutile/water/oil modified by CTAB.

Extraction	No extraction
cyclohexane	n-hexadecane
toluene	n-heptane
benzene	n-hexane
1-hexene	iso-octane
dekalin	
isobutyl methyl ketone	
n-butanol	
ethyl acetate	

5.2 Contact angle measurements

5.2.1 Effect of alkyl sulphate concentration on the contact angle

The contact angle between rutile, benzene and surfactant solution

was measured as a function of alkyl sulphate concentration at pH 3.1 \pm 0.1 and 25°C. The receding contact angles (or sessile contact angles in the case of angles greater than 125°) are shown in Fig. 5.15 for the alkyl sulphates used. The advancing angles for SDS and STS are also shown. In the absence of surfactant both the receding and advancing angles were zero. The curves are typical in the case of SDS and STS (and possibly SHS) and show that the contact angle increased with increasing surfactant concentration, until a maximum was reached at a concentration that corresponds to monolayer coverage (indicated by an arrow). At higher surfactant concentrations the contact angle decreased sharply. The decrease in contact angles at high surfactant concentrations is a common phenomenon in solid/water/air systems (8) (70) and is due to the formation of a hydrophilic reversed bilayer. It has been suggested (70) that in the solid/water/oil system, the oil solubilizes the bilayer and, therefore, contact is maintained, although in these cases a considerable induction period is often a prerequisite for contact (217). The results of this and other studies (140) indicate that this conclusion is not correct.

Measurement of the 'receding' angles of the sessile drops for STS and SHS showed that they tended to 180°. 'Receding' contact angles measured on sessile drops in the system modified by SDS resulted in a maximum contact angle of 157°.

Hysteresis of the contact angles at low surfactant concentrations, where the contact angle is not changing significantly with increasing surfactant concentration, was about 5°. In the region where the contact angle was increasing rapidly, hysteresis was 10° - 20°. Contact angle hysteresis can be attributed to two causes. Surface roughness has a significant effect on hysteresis and has been theoretically investigated by Huh and Mason (218). Although the local contact angle may be given by Young's equation (219), sub-microscopic surface

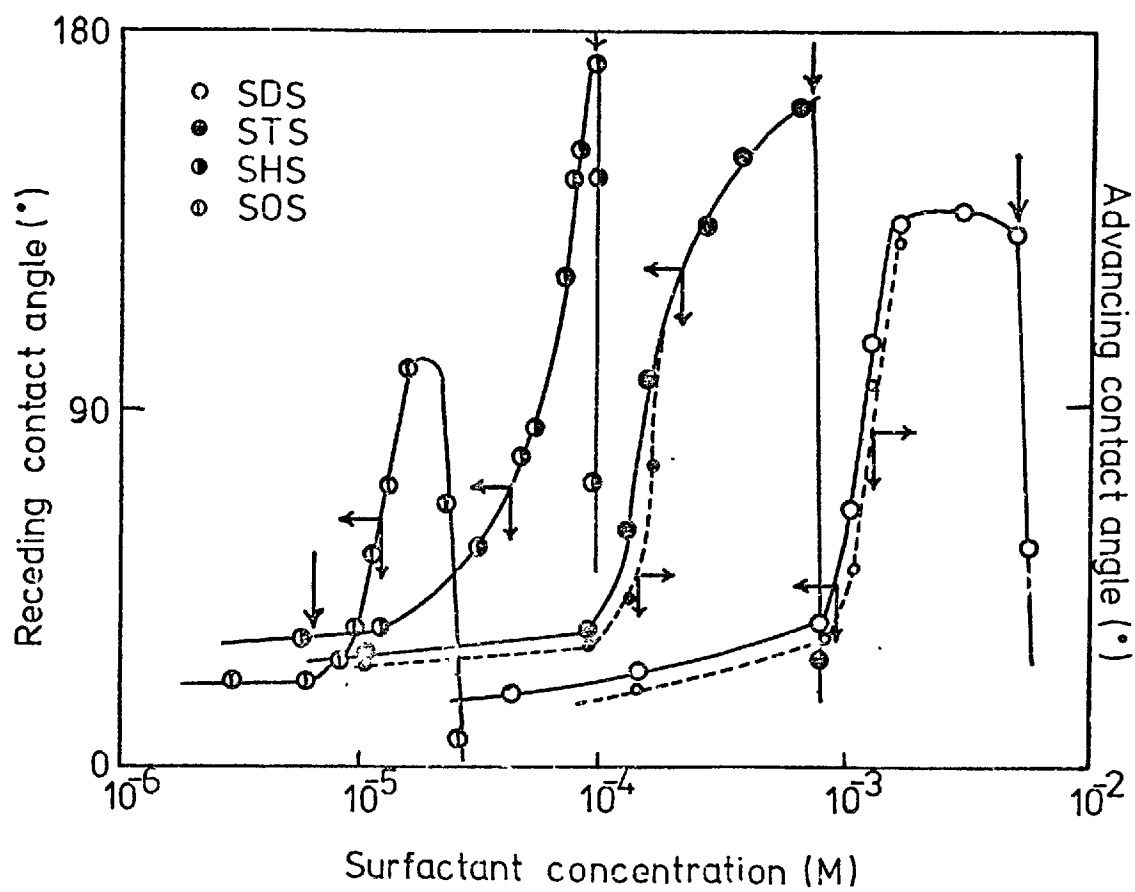


Fig. 5. 15. Effect of alkyl sulphate concentration on contact angles of benzene on rutile at pH 3.1.

roughness produces an apparent contact angle which is different from both the advancing and the receding contact angles. Wenzel (220) related the apparent and equilibrium contact angles by the expression

$$\cos \theta_{\text{apparent}} = r \cos \theta_{\text{equilibrium}} \dots \dots \dots (3)$$

where, r is the ratio of real to apparent surface area and is a qualitative measure of roughness. An alternative cause of hysteresis is that the solid/air interface is different after the recession of a liquid than the same interface prior to wetting (221). It has been suggested that rearrangement of the adsorbed species occurs upon displacement of an air bubble, and as this is not a spontaneous process, the advancing and receding angles are different. A similar mechanism has been proposed for hysteresis at the solid/water/oil interface (222) (223).

The curve for SOS (Fig. 5.15) does not reach high contact angle values, and is displaced to higher surfactant concentrations with respect to monolayer coverage than the shorter chained alkyl sulphates. The contact angles were not affected by raising the temperature nor by replacing the sodium ion in the surfactant molecule by a more hydrated cation such as lithium. If, however, the surfactant solution at equilibrium with the rutile surface was replaced by distilled water, the contact angle became 180° (over a period of several hours), before finally becoming zero when all the surfactant had diffused from the surface. These observations suggest that the reduced contact angles in the system modified by SOS are the result of a significant 'armouring' of the surface of the oil drop by the long-chain alkyl sulphate and reversed orientation of the surfactant ions on the solid surface.

Armouring has been suggested as the reason for cessation of flotation at high collector concentrations (224) (225). Grebnev and coworkers (226) investigated the relationship between the hydrocarbon

chain length of alkyl sulphates and their flotation properties with hematite and barite. They found that with collectors of up to 14 carbon atoms in the hydrocarbon chain, flotation efficiency increased with increasing chain length. In the case of surfactant with hydrocarbon chains greater than 14 carbon atoms flotation efficiency decreased. The authors attributed these results to the low rate of decomposition of micelles and the increased surface activity upon increasing chain length. This latter property was said to produce armouring of the air bubbles. The efficiency of flotation with the longer chain surfactants improved on dilution of the pulp or removal of excess collector prior to flotation. It is probable that, in the present investigation under dynamic conditions, the armouring effect at the oil/water interface is eliminated. Analogous behaviour has been reported as an explanation of the apparent non-contact between static air bubbles and particle surfaces under conditions where good recovery is known to occur in froth flotation (227).

The results of contact angle measurements are compared with those of adsorption measurements at the solid/water interface in Fig. 5.16.

According to Smolders (7) if $d\theta/d \ln C$ is positive

$\Gamma_{so} > \Gamma_{sw} + \Gamma_{ow} \cos \theta$. A given adsorption density will therefore be reached at the rutile/oil interface at an equilibrium surfactant concentration lower than that required to give the same adsorption density at the rutile/water interface. The effect of this will be to displace the curve correlating the contact angle with the logarithm of surfactant concentration to lower equilibrium concentrations than the adsorption isotherms acquired at the rutile/water interface. The curves shown in Fig. 5.16 are consistent with this interpretation.

The exact relationship between the contact angle and adsorption density is uncertain. Gaudin and Morrow (228) found no direct relationship between contact angle and adsorption density of dodecyl-

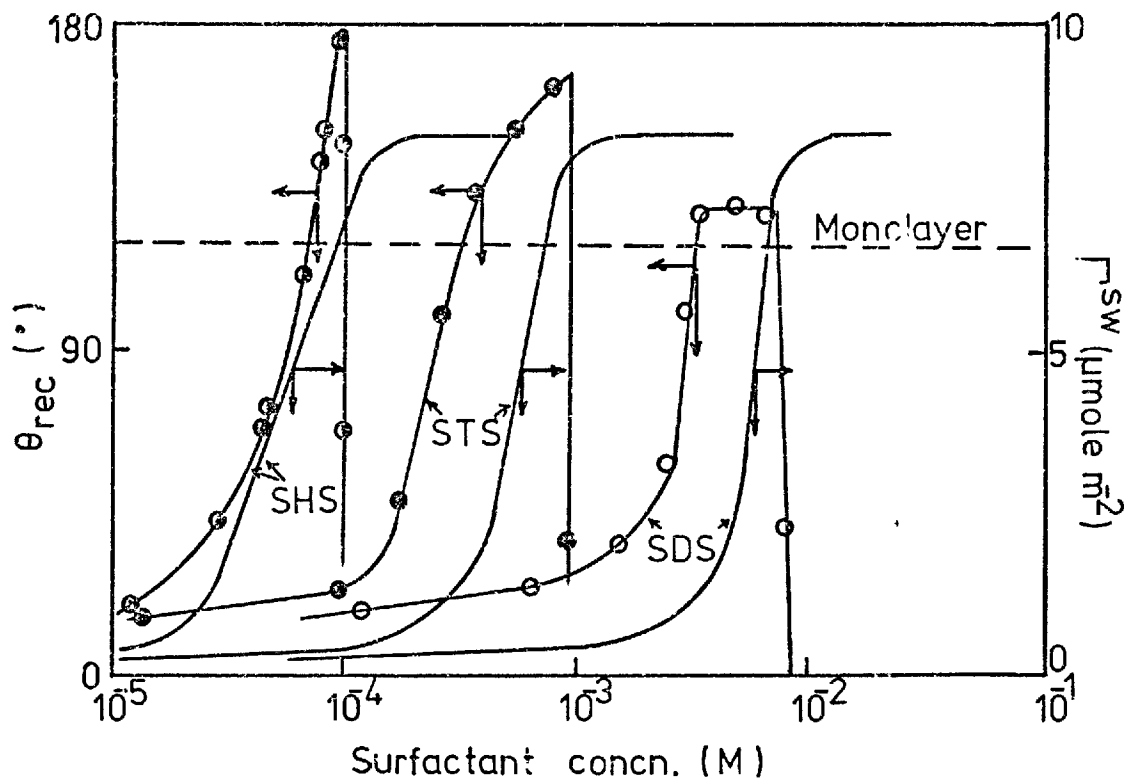


Fig. 5. 16. Comparison of contact angles of benzene on rutile and adsorption densities at the solid/water interface for SDS, STS and SHS at pH 3.1.

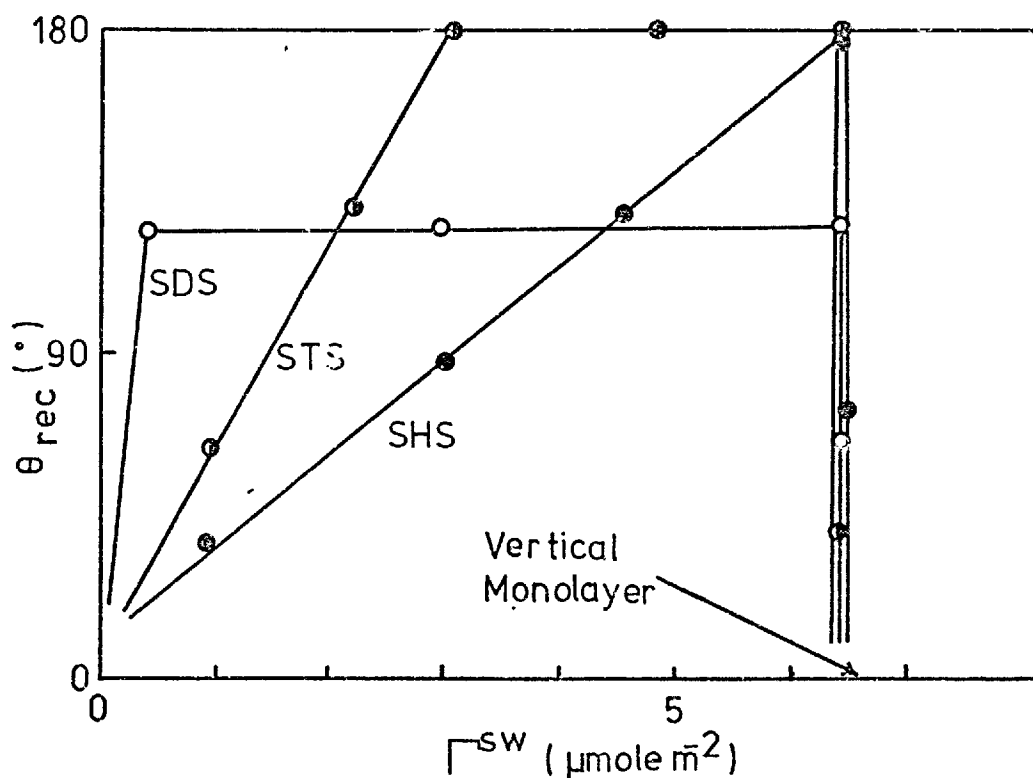


Fig. 5. 17. Contact angles of benzene on rutile at pH 3.1 as a function of alkyl sulphate adsorption density.

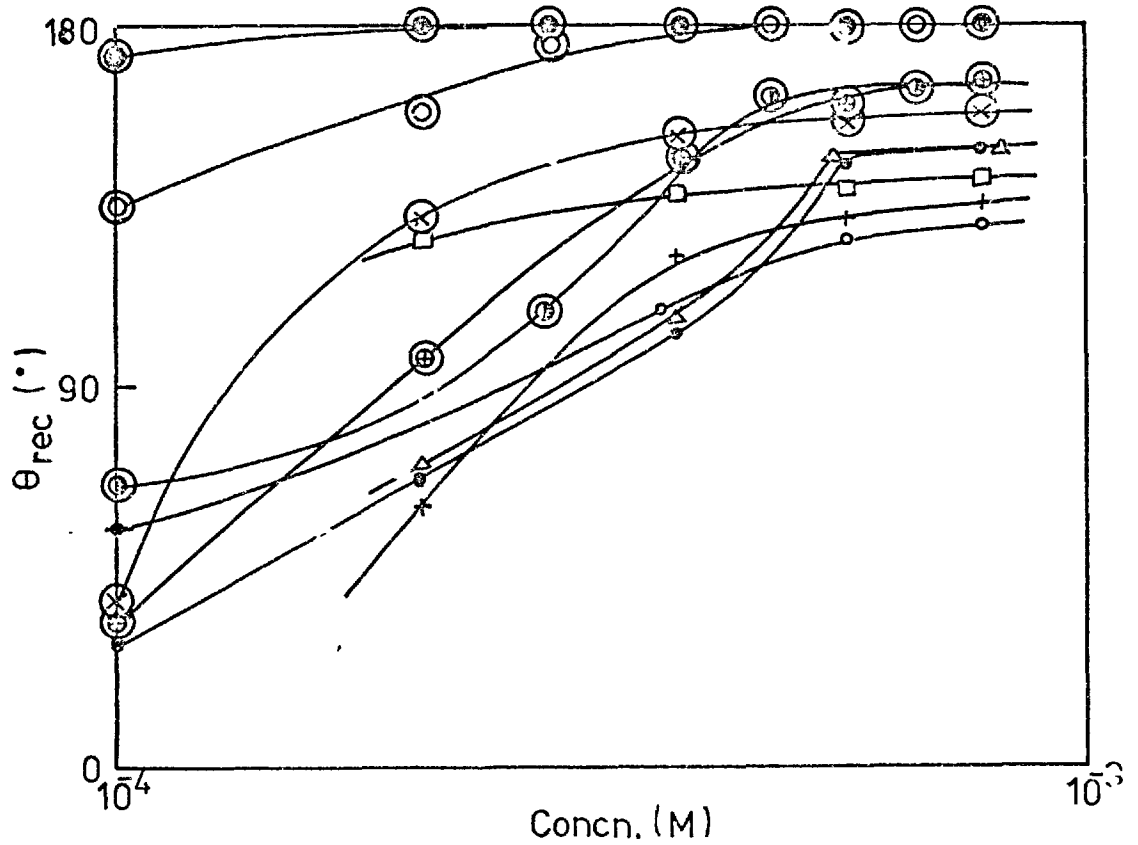
ammonium acetate on hematite. Other authors (229) (230) have suggested a linear relationship between adsorption density and contact angle or adsorption density and $\cos \theta$. In Fig. 5.17 the contact angles for SDS, STS and SWS are presented as a function of surfactant adsorption density. The contact angle in each case increased linearly with adsorption density until a maximum was reached. The contact angle then remained constant until the adsorption density corresponding to monolayer coverage was reached, when the contact angle decreased rapidly. The slope of the initial linear part of the curves increased with decreasing chain length. This suggests that as the chain length was increased there was a greater tendency for the surfactant to adsorb reversely oriented prior to monolayer coverage. Consequently the spreading of the oil drop was resisted because of presentation of polar groups to the oil phase.

Contact angles may also indicate a change in orientation of the adsorbed surfactant species even when the adsorption density does not change (231) (232). No significant differences between the two sets of data were observed in this study, which indicates that no abrupt change in the mode of orientation of the adsorbed surfactant occurred.

5.2.2 Effect of oil phase on the contact angles in systems modified by alkyl sulphates.

The contact angles of various oils on rutile at pH 3.1 are presented in Fig. 5.18 as a function of aqueous STS concentration in the range 10^{-4} M to 10^{-3} M STS. Those oils into which extraction occurred produced 'receding' contact angles in the extraction region approaching 180° . Oils with lower contact angles which did not tend to 180° (i.e. alkanes, alkenes and ketones) did not extract collector-coated rutile.

Fig. 5. 18. Effect of STS concentration on contact angles of various organic liquids on rutile at pH 3.1.



Key

Symbol	Oil	Symbol	Oil
⊙	diethyl ether	●	n-hexane
⊖	dekalin	▲	iso-octane
⊗	toluene	□	isobutyl methyl ketone
⊕	benzene	+	1-hexene
⊗	cyclohexane	○	n-heptane

5.2.3 Contact angles in systems modified by CTAB.

The contact angle between rutile, benzene and surfactant solution was measured as a function of CTAB concentration at pH 10.5 ± 0.1 and 25°C . The receding, advancing and sessile (for $\theta > 125^{\circ}$) contact angles are shown in Fig. 5.19. The curves are typical and similar to those obtained with the alkyl sulphates, and show that the contact angle increased with increasing surfactant concentration until a maximum was reached at a concentration that corresponded to a vertically oriented monolayer coverage. At higher concentrations the contact angle was reduced to zero. The 'receding' contact angles of the sessile drops in this system tended to 180° . Also shown in the figure is the adsorption isotherm of CTAB on rutile at pH 10.5. The curve is similar in slope to the contact angle curves and the data from both curves has been replotted in Fig. 5.20 in the form of receding contact angle against adsorption density of CTAB on rutile. The resulting graph is similar to those obtained for the alkyl sulphates, and show that the contact angle increased linearly with adsorption density until a maximum was reached. The contact angle then remained constant until the adsorption density corresponding to monolayer coverage was reached, when the contact angle decreased rapidly to zero.

The 'equilibrium' contact angles of the sessile drops of various oils on rutile in the presence of 10^{-4} M CTAB at pH 10.5 ± 0.1 are given in Table 5.4. The oils into which extraction occurred produced 'receding' contact angles which tended to 180° . Oils with lower contact angles which did not tend to 180° did not extract collector-coated rutile.

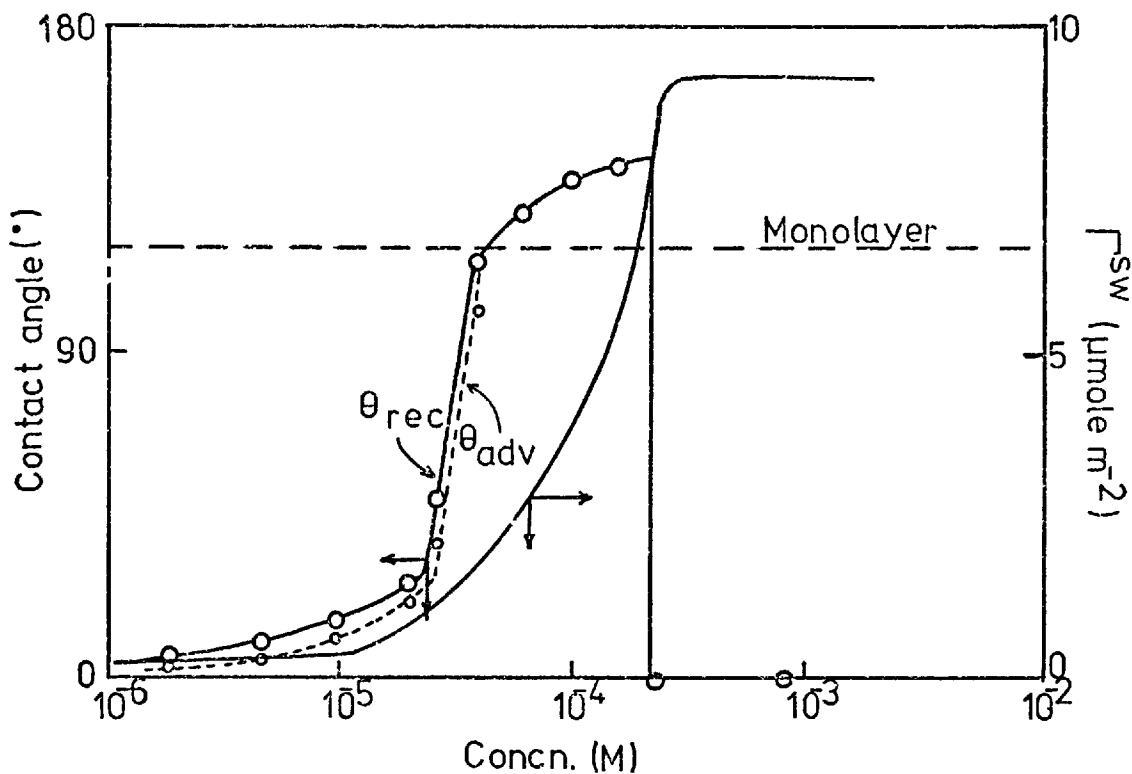


Fig. 5. 19. Comparison of contact angles of benzene on rutile and adsorption density of CTAB at the solid/water interface at pH 10.5.

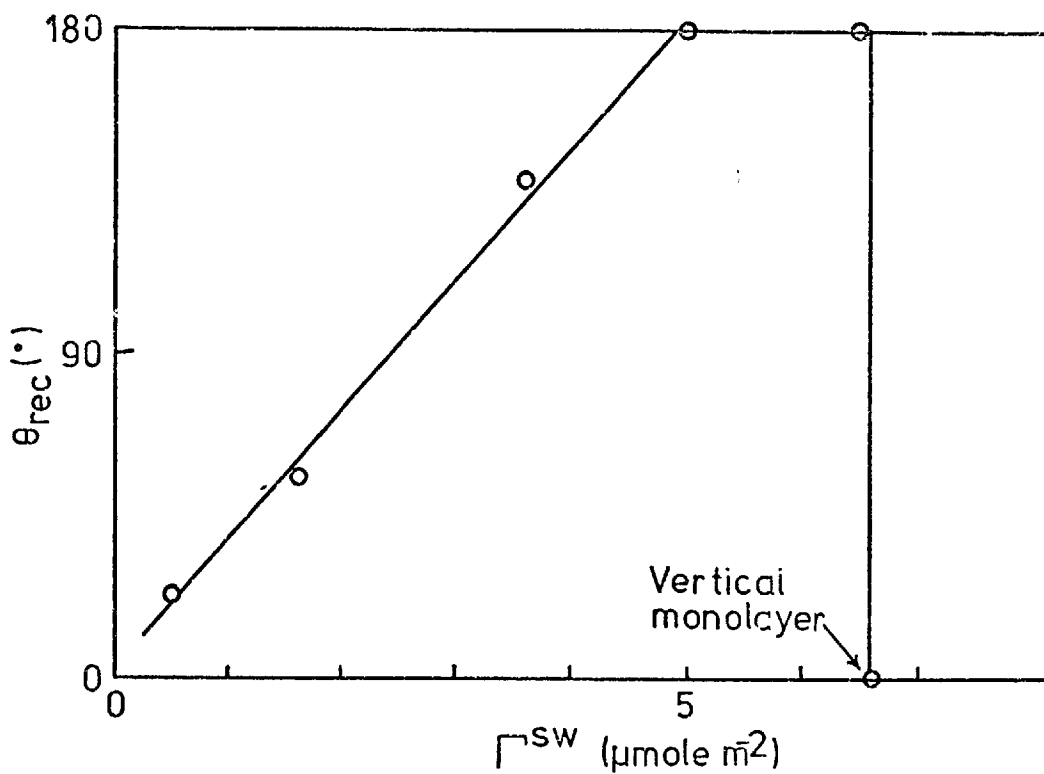


Fig. 5. 20. Contact angles of benzene on rutile at pH 10.5 as a function of CTAB adsorption density.

Table 5.4.

Sessile contact angles of various oils on rutile in the presence of 10^{-4} M CTAB at pH 10.5.

Oil	Sessile Contact angle (°)
n-heptane	96
n-hexane	94
iso-octane	102
cyclohexane	110
toluene	115
benzene	135
1-hexene	112
diethyl ether	180
isobutyl methyl ketone	180

6.

OIL/WATER INTERFACE

6.1 Interfacial tension measurements.

6.1.1 Effect of sodium alkyl sulphates on the benzene/water interfacial tension.

The effect of pH on the interfacial tension of the benzene/aqueous surfactant solution interface is shown in Fig. 6.1 for 10^{-5} M SOS at constant ionic strength ($I = 10^{-2}$ M). Above pH 3, variation in pH had little effect on the interfacial tension of the system. Similar observations have been made with SDS (233) and the decrease in interfacial tension at acid pH values has been attributed to hydrogen ion adsorption. As the interfacial tension did not change appreciably with variation in pH, all subsequent interfacial tension measurements were carried out at the natural pH of the surfactant solution.

The effect of the sodium alkyl sulphate concentration on the interfacial tension between benzene and water is shown in Fig. 6.2. The curves are typical in the case of SDS and STS, and show that the interfacial tension decreased with increasing surfactant concentration until the c.m.c. was reached (or the solubility limit, in the case of STS) when the interfacial tension became constant. Furthermore, at a given concentration the interfacial tension of the STS solution was lower than that of SDS. The curves for SOS and SHS, however, show that these surfactants did not have the expected effect of reducing the interfacial tension below that of STS. These results are not in agreement with those of Kling and Lange (160) who showed that for a homologous series of alkyl sulphates, the interfacial tension between n-heptane and water decreased with an increase in chain length. Their work was, however, carried out at elevated temperatures where the longer chain alkyl sulphates were appreciably soluble, whereas the results in this study were obtained at 25°C.

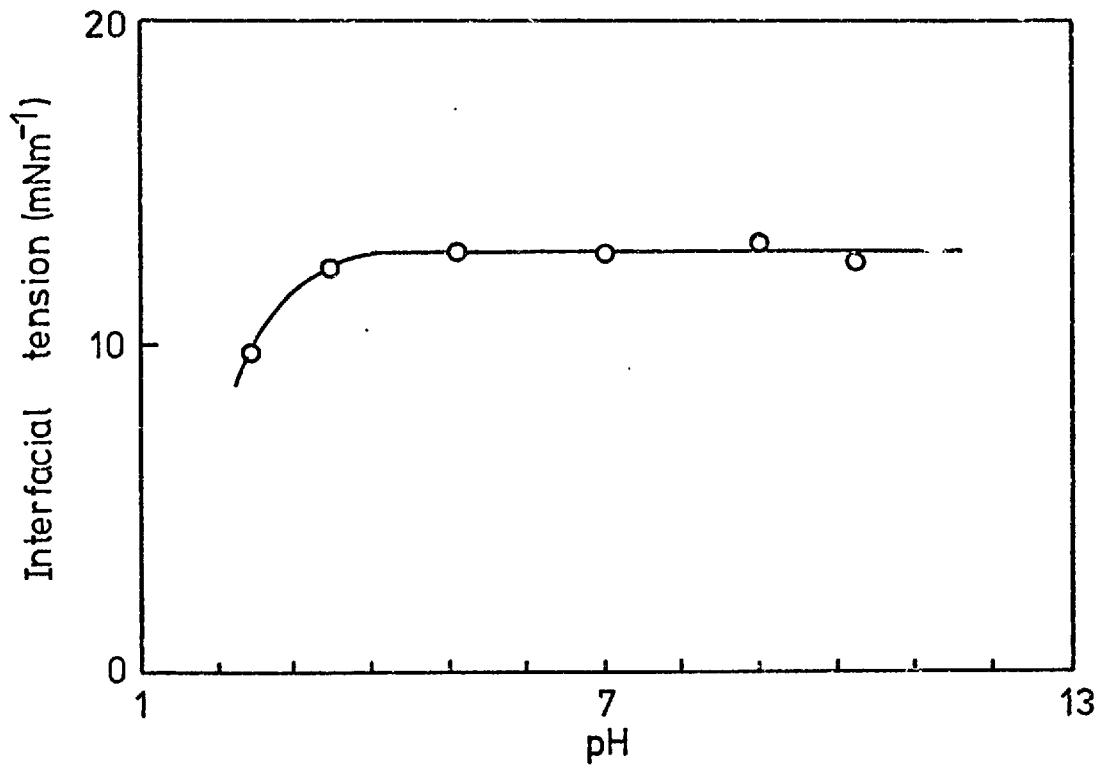


Fig. 6. 1. Effect of pH on the interfacial tension of the benzene/alkyl sulphate solution interface.

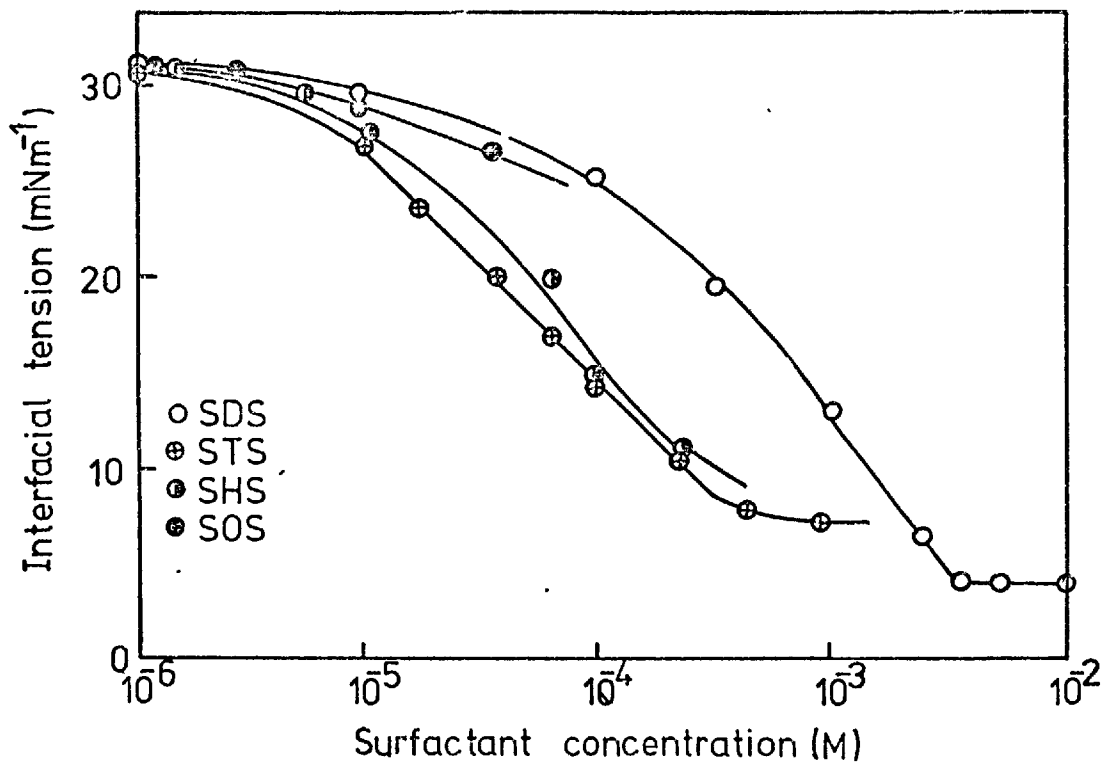
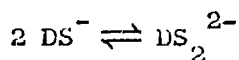


Fig. 6. 2. Interfacial tension between benzene and water as a function of sodium alkyl sulphate concentration.

The anomalous behaviour of SOS was not attributable to an increase in alkyl sulphate solubility in the benzene phase with an increase in chain length. This was shown by equilibrating SOS crystals with benzene for 24 h. No sodium was detected in the organic phase and the interfacial tension of the benzene with water was 30.1 mN m^{-1} which is in excellent agreement with that obtained for pure water and benzene (see Table 3.2). A similar interfacial tension was also obtained with benzene that had been equilibrated with an SOS solution and then separated from it. It is, therefore, concluded that SOS is not soluble in benzene.

Recently, substantial evidence has been presented indicating that surfactant solutions below their c.m.c. are not completely dissociated and that pre-micellar aggregates occur. The evidence has been reviewed by Muckerjee (234). The presence of pre-micellar association, e.g. dimerization, means that the monomer concentration can no longer be equated to the stoichiometric concentration. In the present study the anomalous behaviour of the longer chain alkyl sulphates might, therefore, be attributable to the increasing effect of dimerization with increasing chain length.

Much of the evidence for pre-micellar association has come from studies of the electrical conductance of SDS solutions, but the results are conflicting. Muckerjee et al (235) found that in the concentration range 10^{-4} - 10^{-3} M SDS the conductance did not agree with the Fuoss-Onsager extended theory (236) which is expected to apply to dilute solutions. The results obtained suggested that the species in solution were more conducting than the monomer, although deviation from the Fuoss-Onsager theory was not significantly dependent on concentration. The authors considered that the explanation of the results was an equilibrium between monomeric dodecyl sulphate ions (DS^-) and their dimers, i.e.



An intertwined model of the dimer was proposed (235) which permitted the maximum contact possible between the hydrocarbon chains whilst minimising charge repulsion between the polar head groups. In contrast Parfitt and Smith (237) presented conductance data which was well accounted for by the Fuoss-Onsager theory, although the design of their conductance cell has been criticized (234).

Investigations with other techniques have still not completely resolved the conflict, although on balance the evidence does support the presence of dimers. A potentiometric study of an SDS system by van Voorst Vader (238) indicated that dimerization was negligible. The use of an electrochemical cell involving a liquid junction in this work has, however, been criticized (234). An e.m.f. study using a sodium ion-sensitive glass electrode (239) has shown that sodium decyl sulphate behaves similarly to sodium chloride, but that SDS and STS exhibit marked deviations consistent with the formation of dimers. In this, as in the previous work, the use of liquid junctions introduces uncertainty in the interpretation of the results. A magnetic float technique was employed by Franks and Smith (240) to carry out density measurements on SDS solutions in the submicellar concentration range. The derived partial molar volumes deviated from the Debye-Hückel limiting law even at very low concentrations. Gillap and coworkers investigated the thermodynamics of adsorption of sodium decyl sulphate and sodium dodecyl sulphate at the air/water (241) and oil/water (242) interface. In the case of the air/water interface they calculated the standard thermodynamic functions for adsorption of the surfactants at the interface, and the results showed that although entropy changes were the main driving force for the adsorption process, the standard entropy of adsorption was the same for both chain lengths. The authors suggested that the adsorption of SDS did not reflect a bulk monomer - adsorbed monomer equilibrium and that dimers were present in solution.

A large increase in the standard entropy of adsorption with increasing chain length was, however, observed at the oil/water interface (242). The suggested explanation was that whilst monomers and dimers are present in bulk solution and both species are adsorbed at the air/water interface, the monomer is exclusively adsorbed at the oil/water interface. The increase in entropy may, therefore, be interpreted in terms of dissociation of the dimer and adsorption at the interface.

In the presence of benzene it was observed that the c.m.c. of SDS was reduced. This phenomenon has been reported by other authors (157) who considered it to be due to solubilization of the organic liquid in the SDS micelle in the aqueous phase. To determine whether this effect occurs in the bulk aqueous phase or predominantly at the oil/water interface, conductivity measurements were conducted on SDS solutions at different concentrations, in the presence and absence of benzene. The results are shown in Fig. 6.3. It can be seen that benzene lowered the conductivity of the solutions but had only a small effect on the apparent c.m.c. This difference suggests that the observed lowering of the c.m.c. in the interfacial tension measurements is attributable to premature micellization of SDS at the benzene/water interface.

The effect of temperature on the benzene/surfactant solution interfacial tension was determined for the four alkyl sulphates used. The interfacial tension of 10^{-5} M solutions of the alkyl sulphates at different temperatures are presented in Fig. 6.4, as a function of chain length. At 25°C the interfacial tension decreased with increasing chain length to a minimum at STS and then increased again. Increasing the temperature to 50°C moved the position of the minimum to between SHS and SOS. At still higher temperatures (i.e. 70°C) no minimum was obtained at all. Under these conditions the results were consistent with those of Kling and Lange (160). These results indicate that the longer chain length surfactants only behave 'normally' when the

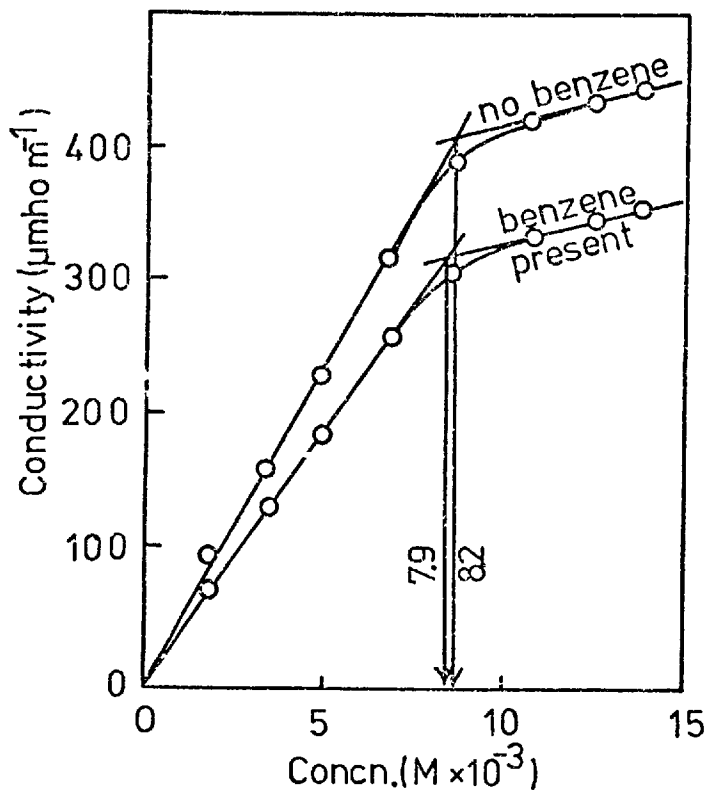


Fig. 6. 3. Conductivity of SDS solutions in the presence and absence of benzene.

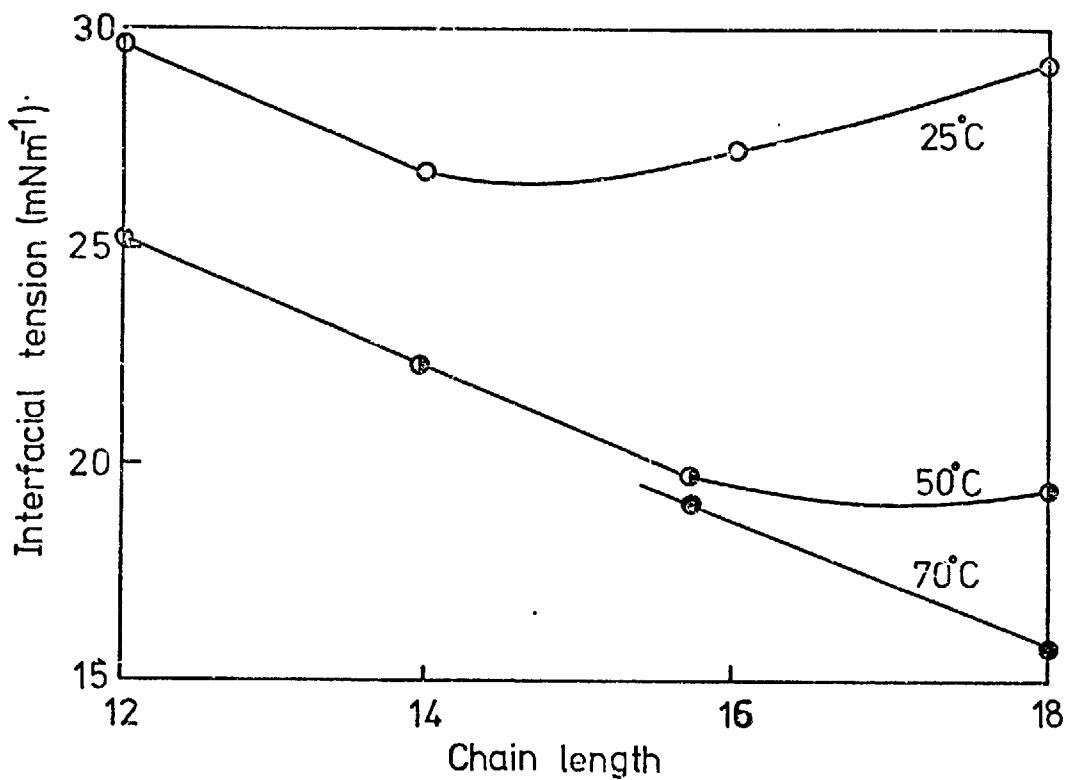


Fig. 6. 4. Interfacial tension between benzene and water as a function of sodium alkyl sulphate chain length at various temperatures.

temperature is raised so that the solubility is well above the Krafft points. This behaviour is indicative of the presence of dimers, which at high temperatures would more readily dissociate into the monomeric form. At elevated temperatures, therefore, the stoichiometric concentration would correspond to the monomeric concentration and the interfacial tension - surfactant concentration curves would be as predicted from Traube's rule.

6.1.2 Effect of sodium alkyl sulphates on the air/water surface tension.

To determine whether or not the longer chain alkyl sulphates also exhibited anomalous behaviour at the air/water interface, the surface tension of the alkyl sulphate solutions was determined as a function of surfactant concentration. The results shown in Fig. 6.5 are typical in the case of SDS and STS and similar to those obtained at the oil/water interface. The values of the c.m.c. for STS and SDS found by this method were 1.5×10^{-3} M and 8.0×10^{-3} M respectively, and are in good agreement with previously reported values (160). SHS and SOS, however, did not behave as expected, indicating that the anomalous behaviour is not confined to the presence of an oil/water interface. These results may be interpreted in a similar manner to those obtained at the oil/water interface i.e. the increase in dimerization with increasing chain length results in the displacement of the interfacial/surface tension - surfactant concentration curves to higher surfactant concentrations because of the decrease in monomer concentration.

6.1.3 Effect of potassium and lithium alkyl sulphates on the benzene/water interfacial tension.

The nature of the cation does not affect the surface activity of a surfactant (243), but it does affect the value of the interfacial tension (244). Potassium salts have been observed to have the greatest

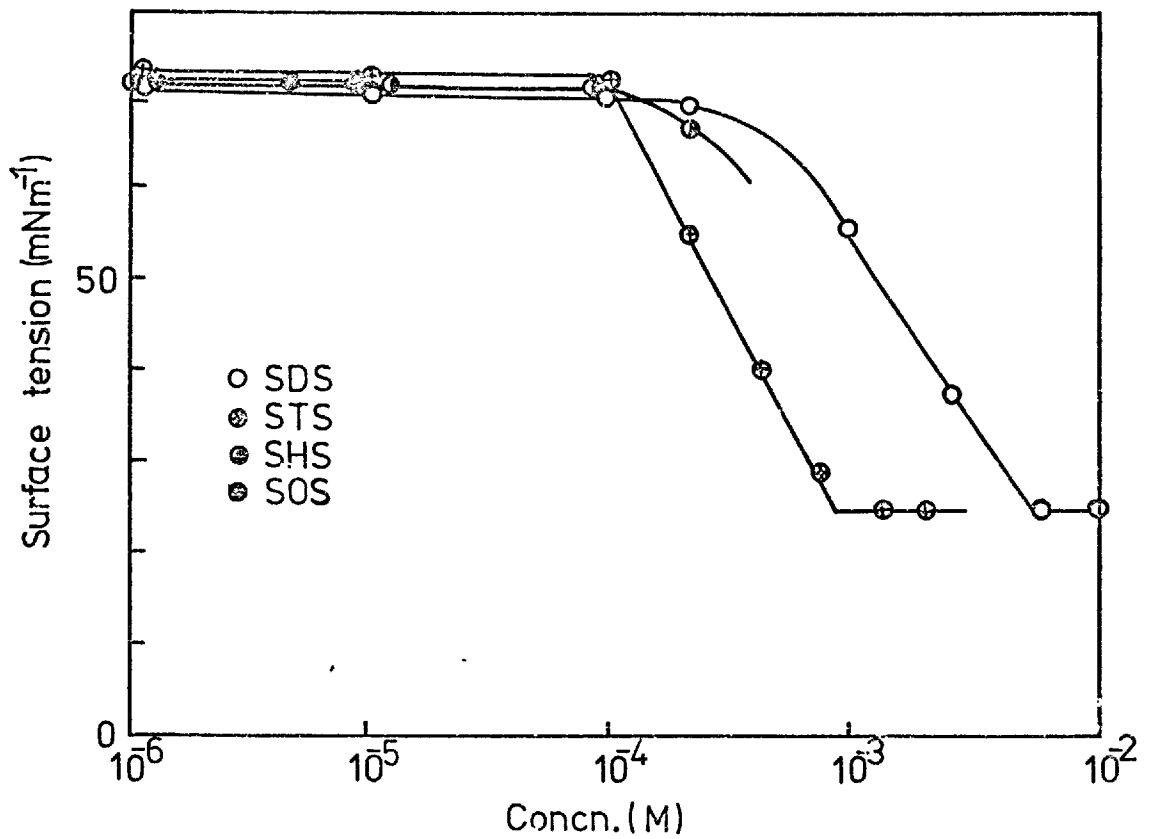


Fig. 6. 5. Surface tension of water as a function of sodium alkyl sulphate concentration.

effect with regard to lowering of interfacial tension (244), followed by sodium and lithium salts. This order is one of increasing polarization potential of the cation from potassium to lithium and, hence, increasingly large hydration sheaths. An increase in the size of the hydration sheath around the cation will reduce the number of counterions in the interfacial region and consequently the interfacial tension will be less affected.

The reverse of the above series has been found for the effect of the cation on the Krafft point of alkyl sulphates (245) i.e. the Krafft point for the potassium salt is greater than that for the sodium salt, whilst lithium has the greatest effect with regard to reducing the Krafft point. The effect on the Krafft point is due to a similar reason as that described above, i.e. a heavily hydrated cation will not be in such close proximity to the surfactant anion as one that is less hydrated. The net result is that repulsion between the surfactant anions is greater in the former case, and the solubility of the surfactant is greater. Similar reasoning can be made with respect to the formation of dimers. Lower concentrations of dimers would be expected in a solution of lithium salt because of the greater hydration of the lithium cation and a corresponding greater repulsive force between the anionic alkyl sulphate polar head groups. The reverse will be true for the potassium salt.

The effect of lithium and potassium alkyl sulphate concentration on the benzene/water interfacial tension is shown in Fig. 6.6. The curves are similar to those obtained for the sodium alkyl sulphates, except that in both cases the hexadecyl sulphate salt behaved as expected. Lithium octadecyl sulphate did not, however, produce the expected decrease in interfacial tension. Potassium octadecyl sulphate was insoluble over the concentration range investigated.

The same data is presented in Fig. 6.7 to show the effect of the

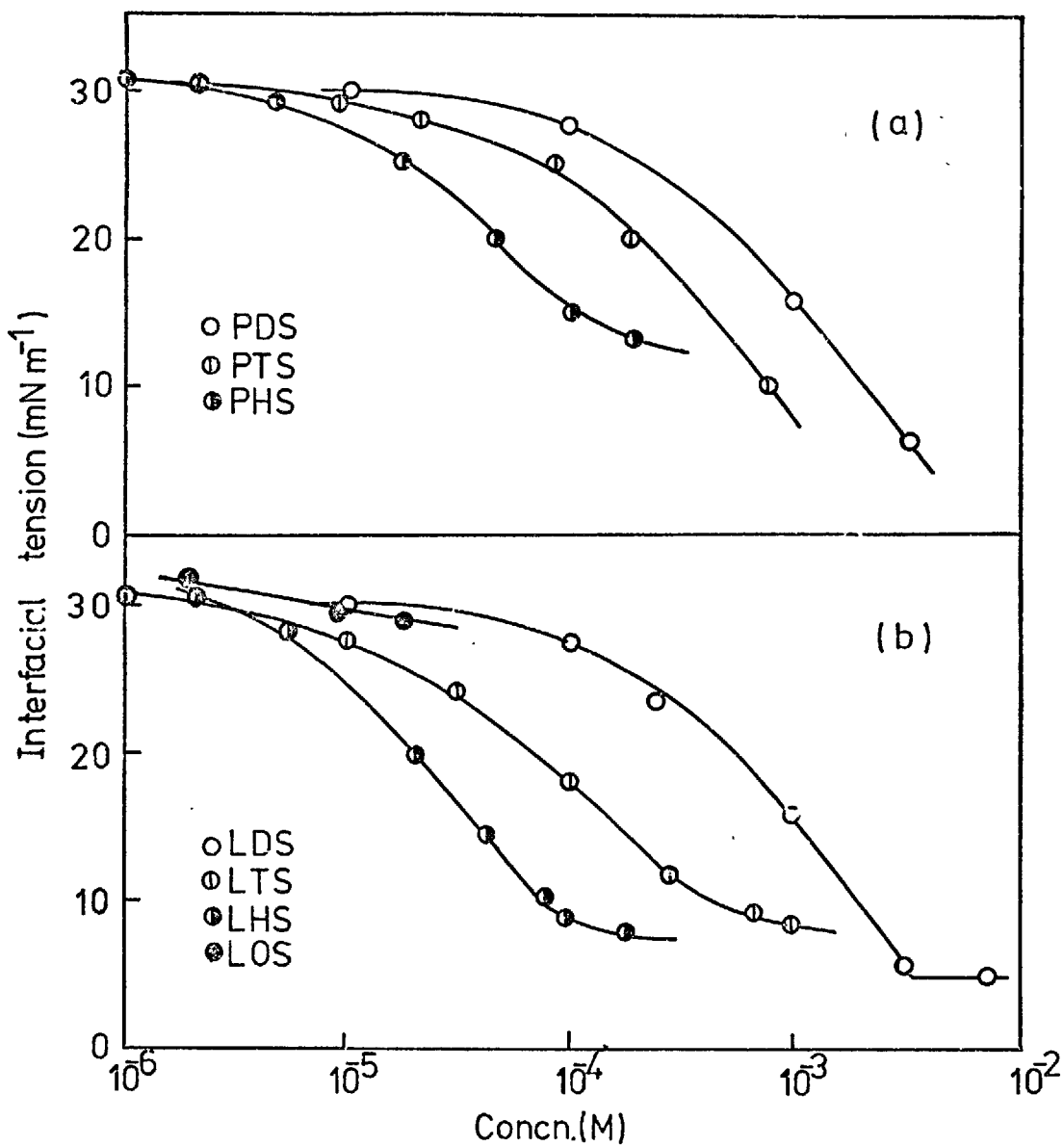


Fig. 6. 6. Interfacial tension between benzene and water as a function of (a) potassium alkyl sulphate concentration and (b) lithium alkyl sulphate concentration.

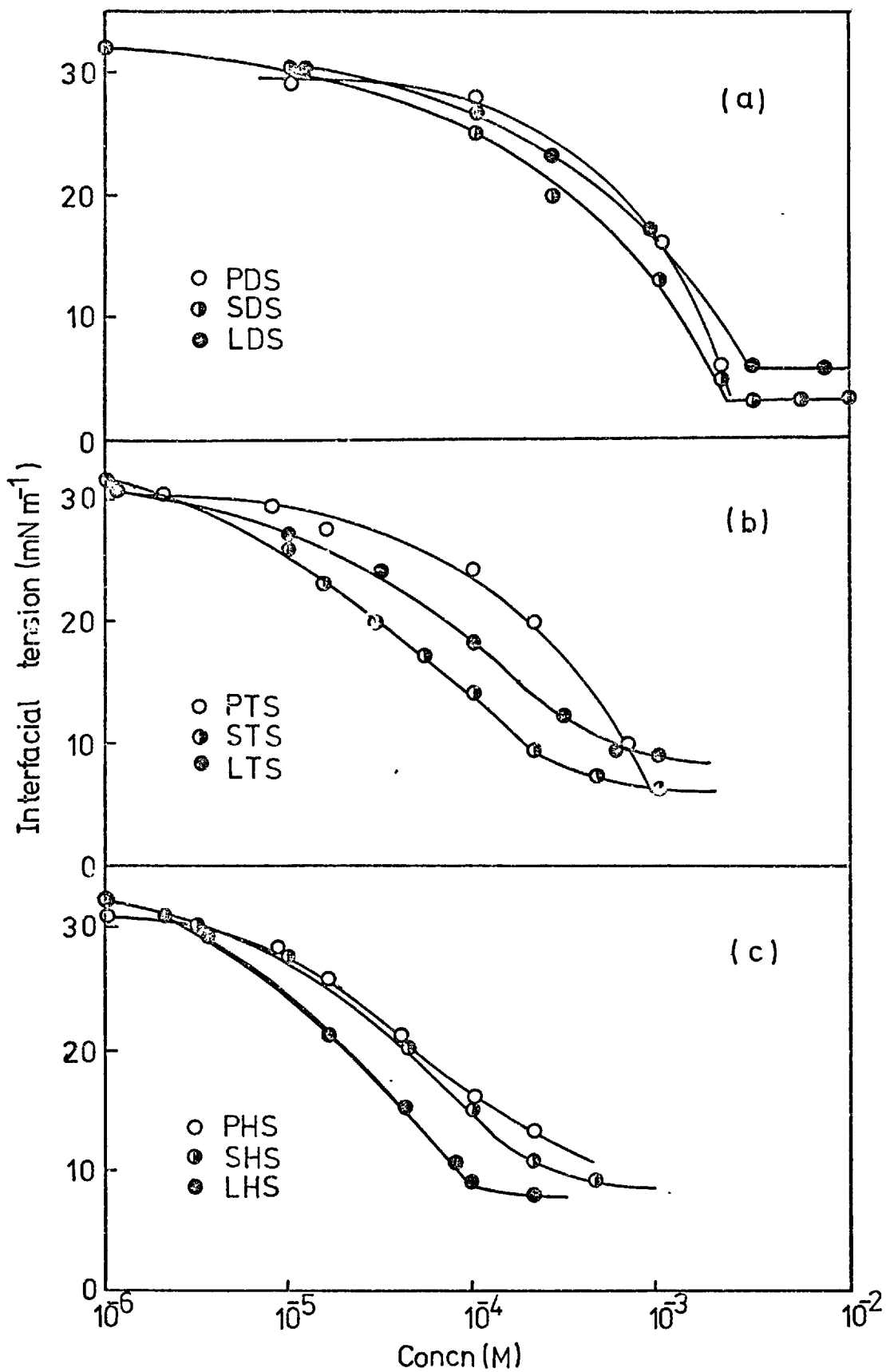


Fig. 6. 7. Interfacial tension between benzene and water as a function of surfactant concentration for (a) dodecyl, (b) tetradecyl and (c) hexadecyl sulphate salts.

cation on the interfacial tension for each surfactant chain length. In the case of the C_{12} and C_{14} surfactants, the sodium ion had the greatest effect with regard to lowering of interfacial tension, followed by the lithium and potassium ions. The sodium and lithium ions are in the same order as in the series above (744). The potassium ion, however, had less effect than expected by the reasoning presented. This result is consistent with the dimerization hypothesis, i.e. in the case of the sodium and lithium ions the concentration of dimers in solution is low and the surfactants behave normally, whereas the increased dimerization as a result of substituting the potassium ion in the molecule results in the interfacial tension - concentration being displaced towards higher concentrations, 'swamping' out the effect due to the decreased hydration of the cation. The displacement of the interfacial tension - concentration curve as a result of dimerization increased with increasing chain length. The series formed by the effect of the cation on the interfacial tension in the case of the hexadecyl sulphate is that the lithium ion produced the greatest lowering of interfacial tension, followed by the sodium and potassium ions which had approximately the same effect. These results are indicative of the formation of dimers in the solutions of the potassium and sodium salts, thus causing displacement of both the curves. In all the above cases, dimers will probably be formed in solutions of the lithium salts, but the extent of dimerization will be small. The cation did not affect the interfacial tension between benzene and water in the presence of octadecyl sulphate. This result suggests that dimerization occurred extensively in all the salts of the C_{18} surfactant.

6.1.4 Interfacial tension between various oils and water in systems modified by alkyl sulphates.

The interfacial tension between various oils and water were

determined for two alkyl sulphate concentrations; 6×10^{-4} M STS and 6×10^{-6} M SOS. The results are shown in Table 6.1. Under these conditions of equilibrium surfactant concentration, extraction of collector-coated rutile particles occurred into some of the oils at pH 3.1. The response of the rutile particles in the system under the given conditions is indicated in the table for each oil phase. It was found that there was no obvious correlation between extraction and the interfacial tension of the relevant oil/water system.

Table 6.1.

Interfacial tension between various oils and alkyl sulphate solutions, and, the response of rutile particles in each system

Oil	$\gamma_{(STS)}$ (mNm ⁻¹)	$\gamma_{(SOS)}$ (mNm ⁻¹)	Response of rutile particles
n-heptane	23.6	45.5	No extraction
n-hexane	23.3	43.5	No extraction
iso-octane	20.9	42.0	No extraction
cyclohexane	13.9	39.5	Extraction
toluene	8.9	33.0	Extraction
benzene	7.5	30.0	Extraction
1-hexene	8.1	27.5	No extraction
diethyl ether	4.5	8.5	Extraction
isobutyl methyl ketone	6.9	8.5	No extraction

6.1.5 Effect of CTAB on the oil/water interfacial tension.

Interfacial tension measurements were carried out to determine the effect of pH on the interfacial tension between benzene and CTAB solution. The results indicated that pH had no effect on the interfacial tension of the system. All subsequent measurements were carried out at the natural pH of the surfactant solution.

The effect of concentration of CTAB on the interfacial tension between benzene and water is shown in Fig. 6.8. The curve shows that the interfacial tension decreased with increasing CTAB concentration

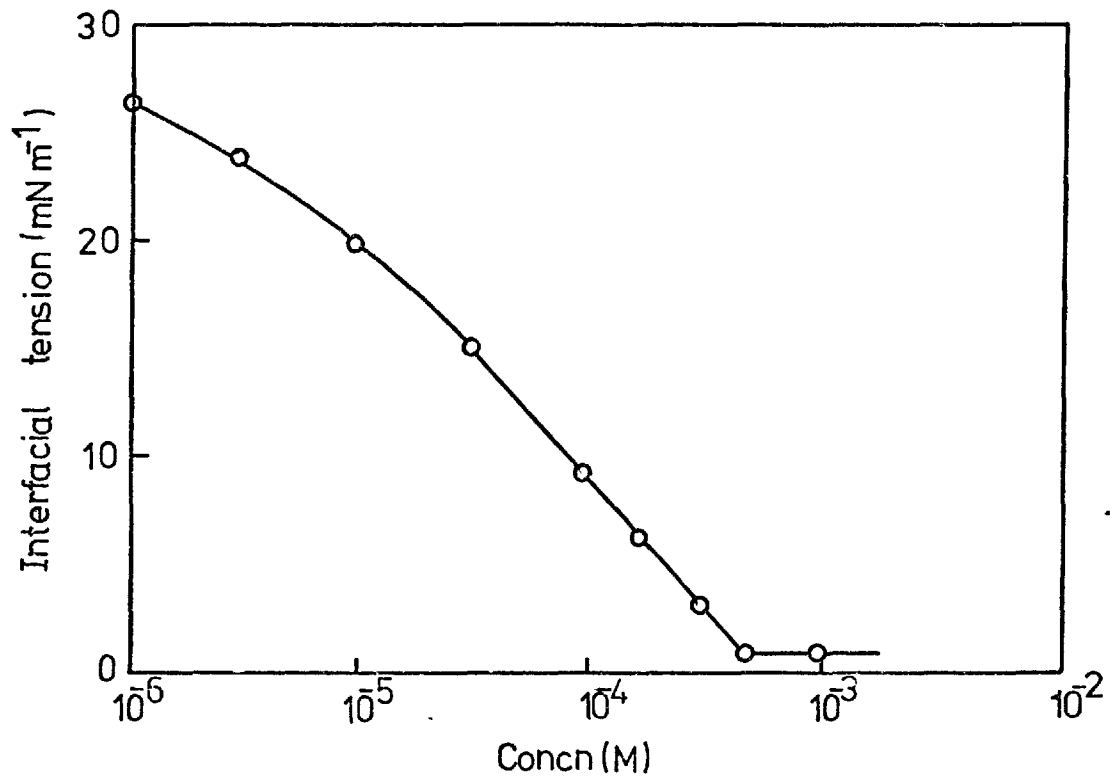


Fig. 6. 8. Interfacial tension between benzene and water as a function of CTAB concentration.

until the c.m.c. was reached. As with SDS, the c.m.c. of CTAB was reduced in the presence of the organic phase. The c.m.c. in the presence of benzene was 5.8×10^{-4} M CTAB. Some authors (246) have suggested that dimerization occurs in aqueous solutions of CTAB. It seems likely, however, that dimers are formed only at low concentrations where electrostatic interactions are negligible (246), as is probably the case with the shorter chain alkyl sulphates.

The interfacial tension between various organic phases and 10^{-4} M CTAB solution was also determined. The results are shown in Table 6.2 along with the response of collector-coated rutile particles under these equilibrium conditions at pH 10.5. The results show that extraction occurred when the interfacial tension between the oil and CTAB solution was less than the critical value of 17.5 mNm^{-1} .

Table 6.2.

Interfacial tension between various oils and CTAB solution, and, the response of rutile particles in each system

Oil	γ (mNm^{-1})	Response of rutile particles
n-heptane	18.8	No extraction
n-hexane	17.6	No extraction
iso-octane	22.6	No extraction
cyclohexane	17.4	Extraction
toluene	16.5	Extraction
benzene	10.5	Extraction
1-hexene	16.6	Extraction
diethyl ether	8.1	Extraction
isobutyl methyl ketone	8.8	Extraction

6.1.6 Adsorption at the oil/water interface

It has been shown from electrostatic and kinetic considerations (247) that Gibb's equation in the form

$$- d\gamma = RT\Gamma d\ln C \dots \dots \dots (1)$$

applies to adsorption of uni-univalent surfactants at the oil/water interface in the presence of excess inorganic electrolyte. In the absence of excess salt, allowance must be made for adsorption of the counter-ion which accompanies the long-chain surfactant ions at the oil/water interface (248). Thus, in the absence of electrolyte equation 1 becomes

$$- d\gamma = 2RT\Gamma d\ln C \dots \dots \dots (2)$$

This equation has been experimentally verified by Haydon and Phillips (249) for the petroleum ether/water interface in the presence of SDS and CTAB. The purity of the water in their investigation was found to be of critical importance, however, particularly in the case of the anionic surfactant. In the present study, in an effort to exclude surfactant ions from the water, the distilled water was passed through an activated carbon column prior to the final distillation stage. This resulted in the presence of trace inorganic ions leached from the carbon, giving an average conductivity of $4 \times 10^{-6} \text{ ohm}^{-1} \text{ cm}^{-1}$. Haydon and Phillips (249) suggested that such a value probably necessitated the application of equation 1. This equation was therefore used to calculate the surface excess as a function of surfactant concentration for the lithium alkyl sulphates up to C_{16} , SDS, STS and CTAB, i.e. those salts where dimerization was assumed to be negligible. The results obtained are shown in Table 6.3 along with the area occupied per surfactant ion at saturation.

Table 6.3.

Adsorption densities of surfactants at the benzene/water interface.

Concentration of surfactant (M)	Adsorption density ($\mu\text{mole m}^{-2}$)					
	SDS	STS	LDS	ITS	LHS	CTAB
2×10^{-6}	0.26	0.70	--	0.65	0.51	1.00
5×10^{-6}	0.41	1.10	--	0.91	1.10	1.23
10^{-5}	0.60	1.42	0.21	1.09	2.33	1.44
2×10^{-5}	0.79	1.89	0.33	1.33	2.66	1.75
5×10^{-5}	0.88	2.56	0.74	2.01	3.26	2.32
10^{-4}	1.23	2.56	1.00	2.26	3.26	2.32
2×10^{-4}	1.91	--	1.45	2.26	--	2.32
5×10^{-4}	2.28	--	2.26	--	--	2.32
10^{-3}	2.91	--	2.94	--	--	--
2×10^{-3}	2.91	--	2.94	--	--	--
Area/ion, \AA^2 (saturation)	37.1	64.9	56.5	73.5	50.9	71.6.

The adsorption of all surfactants at the benzene/water interface increased with increasing surfactant concentration until the adsorption density became constant over a concentration range from 25% of the c.m.c. to the c.m.c. This region of constant adsorption has been termed the 'saturation adsorption' region (250). The area/ion found for SDS is in good agreement with values found by other authors at various oil/water interfaces (157) (160) (184).

The value of the saturation adsorption density is determined by the nature of the hydrophilic group of the surfactant, and by the interaction of this group with other polar compounds present at the interface. The shape and size of the hydrocarbon chain has little effect on the saturation adsorption (250). The differences between the values obtained for the area/ion within an homologous series (for a

given cation) in this study, indicates that the assumption that dimerization is insignificant for the longer chain surfactants given in Table 6.3 is probably erroneous.

CHAPTER 7
GENERAL DISCUSSION

7.

GENERAL DISCUSSION

7.1 Displacement of water from a solid surface by an oil : Theoretical considerations.

A simple schematic model of the oil/water/solid system is shown in Fig. 7.1.

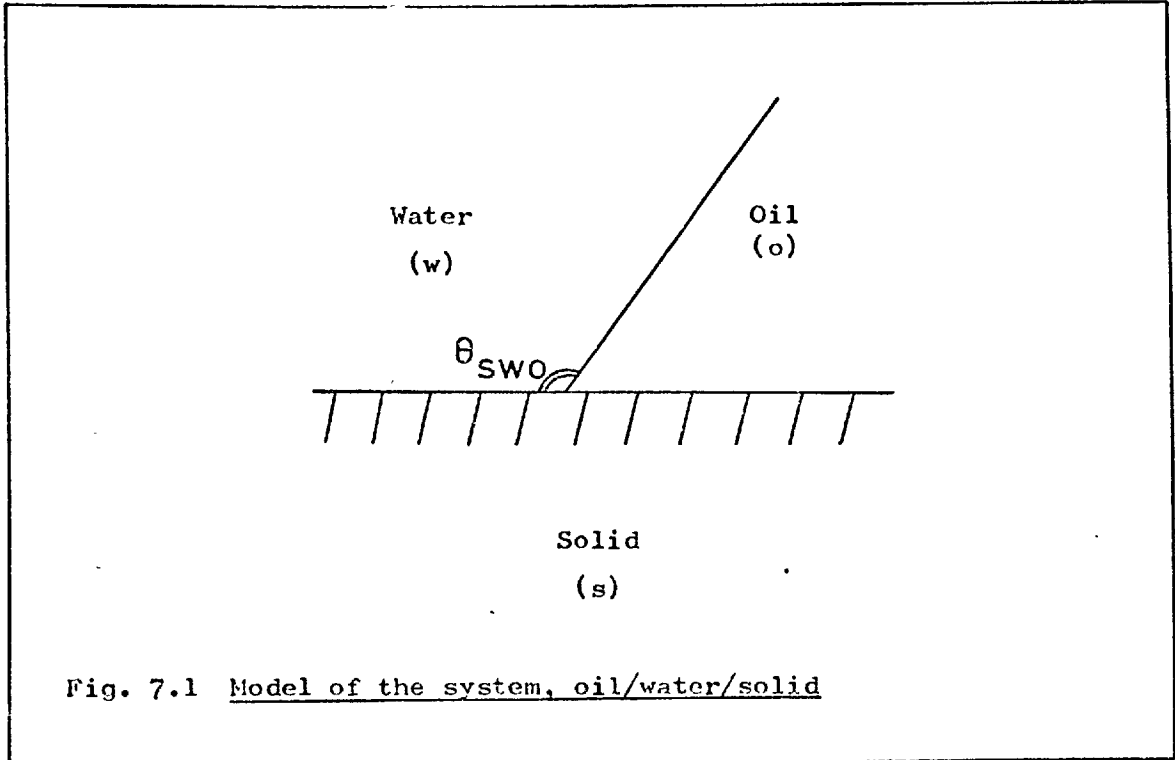


Fig. 7.1 Model of the system, oil/water/solid

At constant temperature and pressure, a small change in the surface free energy of the system is given by

$$dG = \frac{\partial G}{\partial A_{so}} \cdot dA_{so} + \frac{\partial G}{\partial A_{sw}} \cdot dA_{sw} + \frac{\partial G}{\partial A_{ow}} \cdot dA_{ow} \dots \dots \dots (1)$$

where A_{so} , A_{sw} and A_{ow} represent the areas of the respective interfaces,

$$= \gamma_{so} \cdot dA_{so} + \gamma_{sw} \cdot dA_{sw} + \gamma_{ow} \cdot dA_{ow} \dots \dots \dots (2)$$

When the oil spreads,

$$dA_{so} = dA_{ow} = - dA_{sw}$$

and equation 2 becomes

$$dG = \gamma_{so} \cdot dA_{so} - \gamma_{sw} \cdot dA_{so} + \gamma_{ow} \cdot dA_{so} \dots \dots \dots (3)$$

The spreading coefficient (251) of the oil phase on the solid, ($S_{o/s(w)}$)

which is defined as the free energy change for the process, is given by

$$S_{o/s(w)} = \gamma_{sw} - \gamma_{so} - \gamma_{ow} \dots \dots \dots (4)$$

When $S_{o/s(w)}$ is positive, spreading is spontaneous. It is interesting to note that equation 4, for conditions of spreading, is equivalent to the Von Reinders criterion for dispersion of the solid in the oil (69)

i.e.
$$\gamma_{sw} \geq \gamma_{so} + \gamma_{ow}$$

By combining equation 4 with the works of adhesion of water and oil on the solid i.e.,

$$W_{sw} = \gamma_w + \gamma_s - \gamma_{sw} \dots \dots \dots (5)$$

and,
$$W_{so} = \gamma_o + \gamma_s - \gamma_{so} \dots \dots \dots (6)$$

it can be shown that the spreading coefficient is given by the following equation

$$S_{o/s(w)} = (W_{so} - W_{sw}) - (\gamma_o - \gamma_w) - \gamma_{ow} \dots \dots \dots (7)$$

Equations 1 to 7 are equilibrium equations and apply when the phases are mutually saturated. The phases must, therefore, be at equilibrium with an adsorbed film of vapour at each of the interfaces. This is accounted for in the interfacial energy terms by inclusion of a film pressure, e.g.

$$\gamma_s = \gamma_{s^0} + \pi \dots \dots \dots (8)$$

where, γ_{s^0} is the interfacial energy of the solid in vacuo, and π is the equilibrium film pressure.

Lavelle (252) used the concept of a 'critical film pressure', π_c , to investigate spreading of various oils on chrome oxide in the presence of fatty acids. The spreading coefficients of both the oil and water are equal at the critical film pressure, therefore, by equating the two, he obtained the following expression

$$\pi_c = \gamma_{ow} \cdot \cos\theta_{sow} + (\gamma_w - \gamma_o) \dots \dots \dots (9)$$

Lavelle carried out interfacial contact angle studies and film balance measurements to establish the value of π_c and also found that spreading often corresponded to a contact angle of less than 180° . No satisfactory

explanation was given for this behaviour.

Bartell and coworkers (253) (254) introduced the parameter, adhesion tension, into the study of wetting phenomena. The adhesion tension (A_{SOW}) in a two-liquid/solid system (262) is defined as

$$A_{\text{SOW}} = \gamma_{\text{SW}} - \gamma_{\text{SO}} \dots \dots \dots (10)$$

$$= \gamma_{\text{OW}} \cdot \cos \theta_{\text{SOW}} \dots \dots \dots (11)$$

Comparison of equations 10 and 4 shows that when the adhesion tension exceeds the value of the oil/water interfacial tension spreading will occur. The adhesion tension is, therefore, a useful parameter for relating contact angle and spreading behaviour. It has been suggested (254) that the adhesion tension is the fundamental parameter that describes wetting.

Zisman and coworkers (255) investigated spreading of homologous series of organic liquids on low surface energy polymers. They observed that the cosine of the advancing contact angle was usually directly proportional to the interfacial tension of the pure liquids in such series. The authors showed that the empirical relationship took the form

$$\cos \theta_{\text{SLV}} = 1 - \beta (\gamma_{\text{L}} - \gamma_{\text{C}}) \dots \dots \dots (12)$$

Thus a plot of $\cos \theta_{\text{SLV}}$ against γ_{L} is a straight line which extrapolates to zero contact angle at γ_{C} . Zisman has called this value the critical surface tension and proposed that γ_{C} was characteristic of the solid. This parameter is a useful measure of wetting behaviour of organic liquids on such surfaces; liquids with surface tension less than γ_{C} spontaneously spread on the surface. γ_{C} is not, however, a fundamental property of the solid as it is dependent on the nature of homologous series of liquids. Girifalco and Good (256) have also noted that straight lines result if $\cos \theta$ is plotted against $1/\gamma_{\text{L}}$ or $1/(\gamma_{\text{L}})^{\frac{1}{2}}$, although different values for γ_{C} are obtained. No similar study has been carried out on high surface energy surfaces rendered oleophilic

by adsorbed surfactant films.

7.2 Adsorption at the rutile/water, water/oil and rutile/oil interfaces in relation to extraction of particles into the oil phase.

The mechanism of adsorption of the alkyl sulphates and CTAB at the rutile/water interface has been discussed in Chapter 4. The results presented are consistent with adsorption of long-chain surfactant ions by Coulombic attraction (the anionic surfactants adsorbing below the z.p.c., the cationic above) followed by association of the hydrocarbon chains through Van der Waals forces at higher adsorption densities. At a certain equilibrium surfactant concentration adsorption of the surfactant increased rapidly as a result of condensation of surfactant ions upon the homogeneous surface presented to the aqueous phase by the first layer of adsorbed surfactant.

Figs. 4.10 and 4.12 show the adsorption isotherms of the alkyl sulphates on rutile at pH 3.1 and CTAB on rutile at pH 10.5 respectively. Marked on the curves by cross-hatching are the equilibrium concentration ranges over which extraction of rutile particles into various oil phases occurred. Extraction did not occur in systems modified by SDS. This indicates that there is a critical chain length required to render the particles sufficiently oleophilic for extraction to occur.

Extraction occurred in systems modified by alkyl sulphates when the adsorption density of surfactant at the rutile/water interface was between monolayer coverage and saturation, the latter corresponding approximately to the solubility limit of the surfactant. Under these conditions the zeta-potential (Fig. 4.6) was between - 40 mV and - 50 mV. Extraction in systems modified by CTAB occurred between 30% of a monolayer and theoretical monolayer coverage. This corresponded to a potential at the slipping plane (Fig. 4.8) from approximately

0 mV to + 50 mV. Lavelle and Zettlemoyer (258) have shown that the number of hydroxyl sites on the rutile surface is equal to 10^{14} sites/cm². This corresponds to an area per site of 100 Å². The surface coverage of alkyl sulphate or CTAB required for neutralization of the surface, therefore, if all the sites are charged, is 25% of a monolayer. Neutralization of the negative charge at pH 10.5 by CTAB occurred at 30% of a monolayer indicating that the majority of the surface sites are charged. Neutralization of the positive charge at pH 3.1 by the alkyl sulphates occurred at approximately 1% of a monolayer which indicates that only a small proportion of the surface hydroxyls are charged at this pH. These results are consistent with the increasing number of neutral sites on the surface as the pH approaches the z.p.c.

Saturation adsorption was obtained at the oil/water interface in the surfactant concentration range where extraction occurred. The surface potential at the oil/water interface may be calculated from the Gouy equation for an ionized 1:1 electrolyte in the form (259)

$$\psi_o = \frac{2kT}{e} \cdot \sinh^{-1} \frac{134}{A \sqrt{n_o}} \dots \dots \dots (13)$$

where A is the area per electron charge in Å² and n_o is the electrolyte concentration in moles l⁻¹. The values of the surface potential are given in Table 7.1 for SDS, STS and CTAB at the upper equilibrium surfactant concentration at which extraction occurred, or, in the case of SDS, the c.m.c. in the presence of benzene.

Table 7.1 Surface potential at the benzene/water interface in the presence of SDS, STS and CTAB.

Surfactant	Concentration (M)	Area/ion (Å ²)	Surface potential (mV)
SDS	4 x 10 ⁻³	57.1	-220
STS	10 ⁻³	64.9	-248
CTAB	2.5 x 10 ⁻⁴	71.6	+279

The presence of a high surface charge at the oil/water interface with STS and CTAB does not appear to hinder extraction of the highly-charged rutile particles.

Extraction of rutile into an organic liquid occurred when the contact angle approached 180° (measured through the aqueous phase). The slight inconsistencies between the contact angle and adsorption density data at the rutile/water interface as a function of equilibrium surfactant concentration (Figs. 5.16 and 5.19) have been interpreted in terms of increased adsorption at the rutile/oil interface (section 5.2.1). Smolders (7) using Young's and Gibb's equations has derived an expression relating the adsorption densities at the three interfaces, solid/air, solid/water and air/water, with the contact angle and air/water interfacial tension. A similar treatment has been carried out by Lin and Metzger (260). For the solid/oil/water system the equation is

$$\Gamma_{so} = \Gamma_{sw} + \Gamma_{ow} \cos \theta + \frac{\gamma_{ow}}{RT} \sin \theta \cdot \frac{d\theta}{d \ln c} \dots \dots (14)$$

The terms on the right hand side of the equation can be determined from data already obtained, and; therefore, Γ_{so} can be evaluated. The results obtained in this investigation give adsorption densities at the rutile/oil interface corresponding to a thickness of about 40 surfactant monolayers in the extraction region for both the alkyl sulphates and CTAB. This is unlikely to be a true representation of

adsorption at the rutile/oil interface, so the validity of equation 14 to the solid/oil interface must be considered doubtful.

7.3 Work of adhesion of oil drops to the rutile surface.

The requirement for adherence of an oil drop to a solid surface is that there is a decrease in the surface energy upon adhesion. The work done per unit area by the system during adhesion of an oil drop to the solid surface is given by the Young-Dupré equation

$$W_{ad} = \gamma_{ow} (1 - \cos\theta) \dots \dots \dots (15)$$

The work of adhesion calculated from this equation is the theoretical maximum free energy available for adhesion and is not a measure of the free energy utilized (261). It does, however, give an indication of the conditions required for adherence of an oil drop to the rutile surface.

The results from the calculation of the works of adhesion of water and benzene to collector-coated rutile as a function of surfactant concentration are given in Tables 7.2 and 7.3 for STS at pH 3.1 and CTAB at pH 10.5 respectively. The work of adhesion of benzene to the rutile surface in the presence of both STS and CTAB increased with increasing surfactant concentration until a maximum was reached. The value of W_{so} then remained constant until a surfactant concentration corresponding to monolayer coverage was attained, when W_{so} fell rapidly. The rapid rise in W_{so} corresponds to the increase in contact angle over similar concentration ranges as shown in Figs. 5.15 and 5.19. In both systems W_{sw} decreased with increasing surfactant concentration and reached a minimum just prior to monolayer coverage.

Extraction in the system modified by CTAB occurred between approximately 4×10^{-5} M and 2×10^{-4} M CTAB when W_{so} was at its maximum value. Under these conditions W_{sw} was approaching its minimum value. In the system modified by STS extraction occurred between

Table 7.2 Work of adhesion of water and benzene on rutile as a function of STS concentration at pH 3.1.

STS concn. (M)	W_{sw} (mJm ⁻²)	W_{so} (mJm ⁻²)
10 ⁻⁵	50.1	2.9
10 ⁻⁴	25.5	2.5
1.5 x 10 ⁻⁴	18.0	6.0
2 x 10 ⁻⁴	9.1	12.9
4 x 10 ⁻⁴	2.6	14.6
6 x 10 ⁻⁴	1.0	13.8
8 x 10 ⁻⁴	0.2	14.2
10 ⁻³	10.5	3.5

Table 7.3 Work of adhesion of water and benzene on rutile as a function of CTAB concentration at pH 10.5.

CTAB concn. (M)	W_{sw} (mJm ⁻²)	W_{so} (mJm ⁻²)
10 ⁻⁶	55.6	0.4
10 ⁻⁵	41.7	1.3
3 x 10 ⁻⁵	27.4	6.8
5 x 10 ⁻⁵	9.9	18.9
8 x 10 ⁻⁵	4.5	18.9
10 ⁻⁴	3.0	17.8
2 x 10 ⁻⁴	13.0	0.0

9×10^{-4} M and 10^{-3} M STS where W_{so} was at a maximum and W_{sw} was at a minimum. These results indicate that the relationship between W_{so} and W_{sw} is a critical factor in determining under what conditions displacement of water by an oil phase takes place.

The work of adhesion of water and various oils on rutile in the presence of 6×10^{-4} M STS at pH 3.1 and 10^{-4} M CTAB at pH 10.5 were calculated using equation 15. The results are shown in Table 7.4. The table shows that the value of W_{so} does not appear to determine whether or not extraction occurs into a particular oil. The table does show, however, that the value of W_{sw} was lower in those systems where extraction occurred than in those where it did not. This again indicates that it is the relationship between W_{so} and W_{sw} , rather than the absolute value of W_{so} , that determines which oils displace water from the rutile surface.

7.4 Displacement of water from a rutile surface by an organic liquid.

The conditions required for displacement of water from a rutile surface by an organic liquid have been discussed above. The main criterion for spreading of the oil is that the contact angle (measured through the water phase) approaches 180° . This requirement is fulfilled by various oils under different conditions depending on the nature of the surfactant.

7.4.1 Systems modified by CTAB.

In systems modified by CTAB, spreading of an organic liquid occurred when

- (a) the adsorption density at the solid/water interface corresponded to between 30% of a statistical close-packed vertically oriented monolayer and theoretical monolayer coverage;
- (b) the zeta-potential was between approximately 0 mV and

Table 7.4

Work of adhesion of water and various oils on rutile in the

presence of (a) 6×10^{-4} M STS at pH 3.1 and (b) 10^{-4} M

CMAB at pH 10.5.

Oil	a			b		
	W_{sw} (mJm^{-2})	W_{so} (mJm^{-2})	Response of rutile particles	W_{sw} (mJm^{-2})	W_{so} (mJm^{-2})	Response of rutile particles
n-heptane	7.8	39.4	No extn.	16.8	20.7	No extn.
n-hexane	3.1	43.5	No extn.	16.4	18.8	No extn.
iso-octane	2.8	38.9	No extn.	17.9	27.2	No extn.
cyclohexane	0.5	27.3	Extn.	11.4	23.4	Extn.
toluene	0.1	17.5	Extn.	9.5	23.5	Extn.
benzene	0.5	14.5	Extn.	3.1	17.9	Extn.
1-hexene	3.4	22.9	No extn.	10.4	22.8	Extn.
diethyl ether	0.0	4.5	Extn.	0.0	16.2	Extn.
isobutyl methyl ketone	1.2	1.3	No extn.	0.0	17.6	Extn.

+ 50 mV;

(c) saturation adsorption was reached at the oil/water interface; and

(d) the organic liquid had an interfacial tension against pure water of less than 49.6 mNm^{-1} .

The charge on the rutile surface at the lowest surfactant concentration required for extraction was close to zero, and this corresponded to a surface coverage of 30% of a monolayer. Under these conditions not only was the surface oleophilic, but it was also hydrophobic.

The interfacial tension between two phases is given by (252)

$$\gamma_{12} = \gamma_{12}^{\text{dispersion}} + \gamma_{12}^{\text{polar}} + \gamma_{12}^{\text{hydrogen bonds}} + \gamma_{12}^{\text{bonds}} + \gamma_{12}^{\text{electrical double layer}} \dots \dots \dots (16)$$

where the terms on the right hand side of the equation represent the contributions due to various interactions across the interface. Where the surface charge is zero, the contribution due to dispersion forces will be the predominant factor. It may be assumed, therefore, that under these conditions γ_{sw} and γ_{so} are approximately constant and independent of the nature of the organic liquid. The criterion for dispersion of solid particles in an oil phase

$$\gamma_{sw} \geq \gamma_{so} + \gamma_{ow}$$

will, therefore, be fulfilled when the value of γ_{ow} is below a certain critical value. The results, in systems modified by CTAB, are consistent with this simple model of spreading.

As adsorption continues over the extraction region, although oleophilicity increases, the zeta-potential and, therefore, hydrophilicity (257) also increases. At a certain surfactant concentration the surface will have become sufficiently hydrophilic that the rutile surface will be preferentially wetted by water and extraction will cease. The formation of a close-packed reversely oriented bilayer with

polar groups facing into the liquid phase will increase this effect by preventing solubilization of the adsorbed surfactant layer by the oil phase.

7.4.2 Systems modified by alkyl sulphates.

In systems modified by the alkyl sulphates spreading of an organic liquid occurred when

- (a) the chain length of the surfactant exceeded 12 carbon atoms;
- (b) the adsorption density of the surfactant at the rutile/water interface was between that corresponding to a statistical close-packed vertically oriented monolayer and saturation (and/or the solubility limit of the surfactant);
- (c) the zeta-potential was between - 40 mV and - 50 mV; and
- (d) saturation adsorption was reached at the oil/water interface.

Again, water was only dispersed from the rutile surface by some oils, but in this case γ_{ow} did not appear to be the determining factor.

Glembotskii and coworkers (263) have shown that viscosity of the organic liquid is an important factor in determining the efficacy of non-polar oils in emulsion flotation processes. They concluded that the hydrophobic effect of the oil increased with an increase in its viscosity. The viscosities of some of the oils used in this investigation are shown in Table 7.5. The table shows that most of the oils have relatively low viscosities and that viscosity does not appear to be the factor controlling whether or not extraction occurs.

Table 7.5 Viscosities of various organic liquids at 25°C (165).

Oil	Viscosity (cp)	Response of rutile in system modified by alkyl sulphates.
n-heptane	0.41	No extn.
n-hexane	0.33	No extn.
cyclohexane	1.02	Extn.
benzene	0.65	Extn.
toluene	0.59	Extn.
diethyl ether	0.23	Extn.
n-butanol	2.95	No extn.
ethyl acetate	0.46	No extn.

The dipole moments of various organic liquids are shown in Table 7.6.

Table 7.6 Dipole moments of various organic liquids.

Oil	Dipole moment
n-heptane	0.0
n-hexane	0.0
iso-octane	0.0
cyclohexane	0.2
benzene	0.0
toluene	0.4
1-hexene	0.34
diethyl ether	1.15
n-butanol	1.66

Comparison of Tables 5.2 and 5.3, which classify the oil phase according to their effect on extraction in the systems modified by alkyl sulphates and CTAB respectively, shows that the non-polar oils behave similarly in both cases. In the absence of a dipole moment, therefore, the results may be explained by the presence of a critical interfacial tension below which the oils spread on the oleophilic rutile surface.

The polar nature of an organic liquid gives an indication of the interaction of

oil with water. Table 7.7 shows the solubility of water in various organic liquids.

Table 7.7 Solubility of water in various organic liquids at 25°C.

Oil	Solubility (Wt % H ₂ O)
n-heptane	0.015 ^a
n-hexane	0.013 ^a
cyclohexane	0.012 ^a
toluene	0.052 ^b
benzene	0.072 ^b
di-isopropyl ether	0.60 ^a
diethyl ether	1.26 ^b
isobutyl methyl ketone	3.84 ^c
ethyl acetate	19.55 ^a
n-butanol	3.2 ^a

a : ref. 265; b : ref. 266; c : ref. 267.

Neutralization of the surface charge in systems modified by alkyl sulphates occurred at low adsorption densities. Under these conditions, although the surface was hydrophobic, it was not sufficiently oleophilic for spreading to occur. The requirement for spreading was the formation of a close-packed vertically oriented monolayer. The high negative charge associated with this layer means that although the surface is oleophilic it is also hydrophilic. The presence of significant quantities of water in the organic liquid may lead to the formation of wetting films on the highly charged particles which would prevent spreading. Table 7.7 shows that those polar oils into which extraction did not occur had greater amounts of water dissolved in them than those oils into which extraction occurred. These results indicate that the presence of significant quantities of water in polar oils were the reason for the non-spreading of certain oils.

CHAPTER 8
CONCLUSIONS

8.

CONCLUSIONS

An investigation has been made of the interfacial conditions required for the extraction of TiO_2 (rutile) particles from an aqueous phase into various organic phases in the presence of sodium dodecyl, tetradecyl, hexadecyl and octadecyl sulphate, and cetyltrimethylammonium bromide. The techniques involved include contact angle, surfactant adsorption, zeta-potential and interfacial tension measurements and from the results the following conclusions have been made.

- 1) The zero point of charge (z.p.c.) and isoelectric point (i.e.p.) of rutile occur at pH 5.3 and 4.3 respectively. The difference is probably attributable to small amounts of anionic impurity remaining from the preparation process.
- 2) The adsorption of alkyl sulphates and CTAB at the rutile/water interface is consistent with that of Coulombic attraction followed by chain-chain interactions at high adsorption densities and/or after neutralization of the surface charge.
- 3) Increasing the alkyl sulphate chain length displaces the adsorption isotherms on rutile to lower equilibrium surfactant concentrations.
- 4) The onset of hydrocarbon chain interaction at the rutile/water interface is shown by a rapid change in zeta-potential and surfactant adsorption in the case of CTAB. With the alkyl sulphates, however, the change in zeta-potential and adsorption density are not coincident.
- 5) Maximum adsorption of alkyl sulphate and CTAB at the rutile/water interface at pH 3.1 and 10.5 corresponds to 1.2 and 1.4 statistical close-packed vertically oriented monolayers respectively. The results are consistent with the formation of a reversely oriented bilayer of different degrees of compactness.

- 6) CTAB 'salts out' on the rutile surface at low pH values in the presence of supporting electrolyte.
- 7) Extraction of rutile into benzene does not occur with SDS but it does with the higher homologues. With the longer chain alkyl sulphate extraction occurs with organic liquids that have a cyclic structure and the ethers, but not with alkanes, alkenes, ketones or alcohol-.
- 8) Extraction of rutile in the presence of alkyl sulphates occurs when the adsorption density of surfactant at the solid/water interface is between 1 and 1.2 vertically oriented monolayers, and the contact angle approaches 180° . At pH 3.1 this corresponds to a zeta-potential of between -40 and -50 mV.
- 9) With increasing alkyl sulphate chain length the contact angle versus concentration curve is displaced to lower equilibrium surfactant concentrations. Alkyl sulphates below C_{16} all gave maximum angles approaching 180° , but with C_{18} low angles were obtained. The latter is attributable to bilayer formation on the rutile surface and armouring of the oil drop.
- 10) In the presence of CTAB at pH 10.5 extraction of rutile occurs with those organic liquids with an interfacial tension against pure water of less than 49.6 mNm^{-1} , when the adsorption density at the solid/water interface is between 30% and 100% of a vertically oriented monolayer and with a receding contact angle of 180° . Under these conditions the zeta-potential is between 0 and +50 mV.
- 11) It is concluded that displacement of water from a rutile surface by an organic liquid occurs when the surface is sufficiently oleophilic to make the solid/oil/water contact angle 180° . In systems modified by CTAB this condition is fulfilled near the i.e.p., when the surface is hydrophobic, by oils which have an

interfacial tension which is less than a critical value. In systems modified by the alkyl sulphates, however, although the surface is hydrophobic at the i.e.p., it is not sufficiently oleophilic for spreading to occur. At higher adsorption densities, where the surface becomes oleophilic, the presence of a large surface charge also renders the surface hydrophilic. Under these conditions wetting of the surface by non-polar oils will still be determined by the value of the critical interfacial tension. With polar oils, the presence of significant quantities of water in the organic phase will result in the formation of aqueous wetting films on the highly charged particles which will prevent the spreading of the oil.

- 12) Interpretation of the interfacial tension data in the presence of alkyl sulphates is complicated by the tendency of the alkyl sulphate to dimerize as the chain length increases.

REFERENCES

REFERENCES

1. HAYNES, W., Obtaining metals from ores, English patent 488, 1860.
2. YOUNG, T.A., An essay on the cohesion of fluids, Trans. Roy. Soc., 95, 1805, 65 - 87.
3. DE BRUYN, P.L., OVERBEEK, J.Th.G., and SCHUHMAN, R., Flotation and the Gibbs adsorption equation, Min. Eng., 6, 1954, 519 - 523.
4. DE BRUYN, P.L., and AGAR, G.E., Surface chemistry of flotation, in 'Froth Flotation - 50th Anniversary Volume', ed. Fuerstenau, D.W., A.I.M.E., New York, 1962, 91 - 138.
5. GIBBS, J.W., 'The Collected Works of J.W. Gibbs', Longmans, Green and Co., New York, 1, 1931, p. 219.
6. GUGGENHEIM, E.A., The thermodynamics of interfaces in systems of several components, Trans. Far. Soc., 36 (1), 1940, 397 - 412.
7. SMOLDERS, C.A., Contact angles; wetting and de-wetting of mercury. II. Theory of wetting, Rec. Trav. Chim., 80, 1961, 650 - 658.
8. SMOLDERS, C.A., Contact angles; wetting and de-wetting of mercury. III. Contact angles on mercury, Rec. Trav. Chim., 80, 1961, 699 - 720.
9. SOMASUNDARAN, P., The relationship between adsorption at different interfaces and flotation behaviour, Trans. A.I.M.E., 241, 1968, 105 - 108.
10. KLASSEN, V.I., and MOKROUSOV, V.A., 'An Introduction to the Theory of Flotation', Butterworths, London, 1963.
11. SUTHERLAND, K.L., Physical chemistry of flotation. XI. Kinetics of the flotation process, J. Phys. Chem., 52, 1948, 394 - 425.
12. DERJAGUIN, B.V., and DUKHIN, S.S., Theory of flotation of small and medium sized particles, Trans. I.M.M., 70, 1961, 221 - 226.
13. DUKHIN, S.S., and DERJAGUIN, B.V., The secondary (diffusional) electrical double layer, Colloid J. USSR, 20, 1958, 663 - 665.
14. DUKHIN, S.S., The kinetics of the attachment of mineral particles to bubbles during flotation. III. Secondary electrical double layer in the vicinity of the moving bubble surface, Russ. J. Phys. Chem., 35, 1961, 611 - 616.
15. DERJAGUIN, B.V., DUKHIN, S.S., and LISICHENKO, V.A., The kinetics of the attachment of mineral particles to bubbles during flotation. I. The electric field of a moving bubble, Russ. J. Phys. Chem., 33, 1959, 389 - 393.
16. SAMYGIN, V.D., DERJAGUIN, B.V., and DUKHIN, S.S., Investigation of the Dorn effect on oil bubbles, Colloid J. USSR, 26, 1964, 424 - 431.

17. BLAKE, T.D., Current problems in the theory of froth flotation, Symposium on Bubbles and Foams, Nürnberg, Germany, Sept. 1971, V.D.I. Berichte, 182, 1972, 117 - 121.
18. BROWN, D.J., Particle trajectories, collision and attachment in froth flotation, Int. J. Air Pollution, 3, 1960, 35 - 43.
19. SVEN-NILSSON, I., Effect of contact time between mineral and air bubbles on flotation, Kolloid Z., 69, 1934, 230 - 232.
20. EVANS, L.F., Bubble-mineral attachment in flotation, Ind. Eng. Chem., 416, 2420 - 2424, 1954.
21. EIGELES, M.A., and VOLOVA, M.L., Kinetic investigation of effect of contact time, temperature and surface condition on the adhesion of bubbles to mineral surfaces, Proc. 5th. I.M.P.C., London, 1960, I.M.M., London, 271 - 284.
22. LASKOWSKI, J., and ISKRA, J., Role of capillary effects in bubble-particle collision in flotation, Trans. I.M.M., 79, 1970, C6 - C10.
23. LASKOWSKI, J., Particle-bubble attachment in flotation. Min. Sci. Eng., 6 (4), 1974, 223 - 235.
24. PHILIPPOFF, W., Some dynamic phenomena in flotation, Trans. A.I.M.E., 193, 1952, 386 - 390.
25. KIRCHBERG, H., and TOEPPER, E., The mineralization of air bubbles in flotation, Proc. 7th. I.M.P.C., New York, 1964, Gordon and Breach, New York, 1, 157 - 168.
26. SPEDDEN, H.R., and HANNAN, J.R., Attachment of mineral particles to air bubbles in flotation, Trans. A.I.M.E., 183, 1949, 208 - 213.
27. KITCHENER, J.A., Surface forces in thin liquid films, Endeavour, 22, 1963, 118 - 122.
28. RAO, S.R., Surface forces in flotation, Min. Sci. Eng., 6 (1), 1974, 45 - 53.
29. KITCHENER, J.A., Discussion of ref. 28, Min. Sci. Eng., 6 (4), 1974, 245 - 246.
30. COLLINS, D.N., and READ, A.D., The treatment of slimes, Min. Sci. Eng., 3, 1971, 19 - 31.
31. TRAHAR, W.J., and WARREN, L.J., The flotability of very fine particles - a review, Int. J. Min. Proc., 3 (2), 1976, 103 - 131.
32. TOMLINSON, H.S., and FLEMING, M.G., Flotation rate studies, Proc. 6th. I.M.P.C., Cannes, 1963, Pergamon Press, Oxford, 1965, 563 - 573.
33. GAUDIN, A.M., SCHUHMAN, R., and SCHLECHTEN, A.W., Flotation kinetics. II. The effect of size on the behaviour of galena particles, J. Phys. Chem., 46, 1942, 902 - 918.

34. MORRIS, T.M., Measurement and evaluation of the rate of flotation as a function of particle size, Trans. A.I.M.E., 193, 1952, 794 - 798.
35. BUSHELL, C.H.G., Kinetics of flotation, Trans. A.I.M.E., 223, 1962, 266 - 278.
36. DE BRUYN, P.L., and MODI, H.J., Particle size and flotation rate of quartz, Trans. A.I.M.E., 205, 1956, 415 - 419.
37. MELOY, T.P., The treatment of fine particles during flotation, in 'Froth Flotation - 50th Anniversary Volume', ed. Fuerstenau, D.W., A.I.M.E., New York, 1962, 247 - 257.
38. KELSALL, D.F., STEWART, P.S.B., and TRAHAR, W.J., 'Diagnostic Metallurgy. A systematic method of plant optimisation', A.M.I.R.A. Optimisation and Control, Brisbane, July 1974.
39. KIHLESTEDT, P.G., Particle size distribution and separation results of selective flotation of complex sulphide ores, Proc. 8th. I.M.P.C., Leningrad, 1968, 1, 425 - 431.
40. BAARSON, R.E., RAY, C.L., and TREWEEK, H.B., Plant practice in nonmetallic mineral flotation, in 'Froth Flotation - 50th Anniversary Volume', ed. Fuerstenau, D.W., A.I.M.E., New York, 1962, 427 - 453.
41. ROBERTS, D., Flotation aux amines, des minéraux carbonates de cuivre, non deschlammés, French patent 2,240,296, 1975.
42. KIHLESTEDT, P.G., Flotation of hematite ores with tall oil emulsions, in 'Progress in Mineral Dressing', Trans. Int. Min. Dress. Cong., Stockholm, 1957, Almquist and Wiksell, Stockholm, 1958, 557 - 576.
43. LIN, I.J., and METZER, A., Coadsorption of paraffinic gases in the system quartz dodecylammoniumchloride and its effect on froth flotation, Int. J. Min. Proc., 1, 1974, 319 - 334.
44. GAUDIN, A.M., MIAW, H.L., and SPEDDEN, H.R., Native flotability and crystal structure, Proc. 2nd. International Congress of Surface Activity, 3, London, 1957, 202 - 219.
45. MCCARROL, S.J., Upgrading manganese ores, Trans. A.I.M.E., 199, 1954, 289 - 293.
46. HUTTL, J.B., How Manganese Inc., upgrades complex Three Kids ore, Eng. Min. J., Nov. 1955, 88 - 93, 116.
47. GATES, E.H., Agglomeration flotation of manganese ore, Trans. A.I.M.E., 208, 1957, 1368 - 1372.
48. MILLIKEN, F.R., Metallurgy at National Lead Company, MacIntyre development, Trans. A.I.M.E., 183, 1949, 101 - 115.
49. RUNOLINNA, U., RUINNE, R., and KEIRONEN, S., Agglomeration flotation of ilmenite ore at Otanmaki, Proc. 5th. I.M.P.C., London, 1960, I.M.M. London, 447 - 475.

50. LAPIDOT, M., and MELLGREN, O., Conditioning and flotation of ilmenite ore, Trans. I.M.M., 77, 1968, C149 - C165.
51. KUN LI, LIVINGSTONE, R.W., and LEMKE, L.K., Flotation conditioning of iron ore with petroleum sulphonate, Trans. I.M.M., 70, 1960, 19 - 31.
52. CHI, J.W.H., and YOUNG, E.F., Kinetics of flotation conditioning of a hematite ore, Trans. I.M.M., 72, 1962, 169 - 190.
53. KARJALAHTI, K., Factors affecting the conditioning of an apatite ore for agglomeration flotation, Trans. I.M.M., 81, 1972, C219 - C226.
54. FAHRENWALD, A.W., Emulsion flotation, Min. Congr. J., 43, 1957, 72 - 74.
55. LIVSHITS, A.K., and KUZ'KIN, A.S., Effect of apolar oils on the coalescence rate of air bubbles and the rate of adhesion of an air bubble to mineral, Tsvetn. Metal., 37 (2), 1964, 76 - 77.
56. FARNAND, J.R., SMITH, H.M., and PUDDINGTON, I.E., Spherical agglomeration of solids in liquids suspension, Can. J. Chem. Eng., 39, 1961, 94 - 97.
57. SIRIANNI, A.F., CAPES, C.E., and PUDDINGTON, I.E., Recent experience with the spherical agglomeration process, Can. J. Chem. Eng., 47, 1969, 166 - 170.
58. PUDDINGTON, I.E., and SPARKS, B.D., Spherical agglomeration processes, Min. Sci. Eng., 7 (3), 1975, 282 - 288.
59. FARNAND, J.R., MEADUS, F.W., TYNCHUK, P., and PUDDINGTON, I.E., The application of spherical agglomeration to the fractionation of a tin-containing ore, Can. Metall. Q., 3, 1964, 123 - 135.
60. MEADUS, F.W., NYKYTIUK, A., PUDDINGTON, I.E., and MACLEOD, W.D., The upgrading of tin ore by continuous agglomeration, Can. Min. Metall. Bull., 59, 1966, 968 - 970.
61. FARNAND, J.R., MEADUS, F.W., GOODHUE, E.C., and PUDDINGTON, I.E., The beneficiation of gold ore by oil-phase agglomeration, Can. Min. Metall. Bull., 62, 1969, 1326 - 1329.
62. MEADUS, F.W., PAILLARD, G., SIRIANNI, A.F., and PUDDINGTON, I.E., Fractionating coking coals by spherical agglomeration methods, Can. Min. Metall. Bull., 61, 1968, 736 - 738.
63. FARNAND, J.R., and PUDDINGTON, I.E., Oil-phase agglomeration of germanium-bearing vitrain coal in a shaly sandstone deposit, Can. Min. Metall. Bull., 62, 1969, 267 - 271.
64. SPARKS, B.D., and WONG, R.H.T., Selective spherical agglomeration of ilmenite concentrates, Can. Min. Metall. Bull., 66, 1973, 73 - 77.
65. MEADUS, F.W., and PUDDINGTON, I.E., The beneficiation of barite by agglomeration, Can. Min. Metall. Bull., 66, 1973, 123 - 126.

66. SIRIANNI, A.F., COLEMAN, R.D., GOODHUE, E.C., and PUDDINGTON, I.E., Separation studies of iron ore bodies containing apatite by spherical agglomeration methods, Can. Min. Metall. Bull., 61, 1968, 731 - 735.
67. SPARKS, B.D., and SIRIANNI, A.F., Beneficiation of a phosphoriferous iron ore by agglomeration methods, Int. J. Min. Proc., 1, 1974, 231 - 241.
68. ZUIDERWEG, F.J., and VAN LOOKEREN CAMPAGNE, N., Pelletizing of soot in waste water of oil gasification plants - the Shell pelletizing separation (S.P.S.), Chem. Engr. Lond., 220, 1968, 223 - 227.
69. VON REINDERS, W., Die verteilung eines suspendierten pulvers oder eines Kolloid gelösten stoffes zwischen zwei löslungsmitteln, Kolloid Z., 13, 1913, 235 - 241.
70. SCHULMAN, J.H., and LEJA, J., Control of contact angles at the oil-water-solid interface. Emulsions stabilized by solid particles (BaSO_4), Trans. Far. Soc., 50 (6), 1954, 598 - 605.
71. FINKLE, P., DRAPPER, H.L., and HILDEBRAND, J.H., The theory of emulsification, J. Amer. Chem. Soc., 45, 1923, 2780 - 2788.
72. TAKAKUWA, T., and TAKAMORI, T., Phase inversion method for flotation study, Proc. 6th. I.M.P.C., Cannes, 1963, Pergamon Press, Oxford, 1965, 1 - 8.
73. SHERGOLD, H.L., Two-liquid flotation for the treatment of mineral slimes, Industrie Minérale - Minéralurgie, 3, 1976, 192 - 205.
74. SHERGOLD, H.L., and MELLGREN, O., Concentration of minerals at the oil-water interface: hematite-isooctane-water system in the presence of sodium dodecyl sulphate, Trans. I.M.M., 78, 1969, C121 - C132.
75. SHERGOLD, H.L., and MELLGREN, O., Concentration of minerals at the oil-water interface, Trans. A.I.M.E., 247, 1970, 149 - 159.
76. LAI, R.W.M., and FUERSTENAU, D.W., Liquid-liquid extraction of ultrafine particles, Trans. A.I.M.E., 241, 1968, 549 - 556.
77. RAGHAVAN, S., and FUERSTENAU, D.W., On the wettability and flotation concentration of submicron hematite particles with octylhydroxamate as collector, A.I.Ch.E. Symp. Ser., 71 (150), 1975, 59 - 67.
78. COLEMAN, R.D., SUTHERLAND, J.P., and CAPES, C.E., Reduction of the calcite content of ground shale by liquid-liquid particle transfer, J. Appl. Chem., 17, 1967, 89 - 90.
79. GOOLD, L.A., LOVELL, V.M., and FINKELSTEIN, N.P., Oil-levitation extraction - a variation of flotation, J. South African I.M.M., 132, 1975, 132 - 134.
80. ZAMBRANA, G.Z., MEDINA, R.T., GUTIÉRREZ, G.B., and VARGAS, R.R., Análisis sobre la recuperation de particulas de casiterita menores a 10 micrones, XI Congr. Latinoam. de Química, Santiago de Chile,

Chile, 1973.

81. ZAMBRANA, G.Z., MEDINA, R.T., GUITIÉRREZ, G.B., and VARGAS, R.R., Recovery of minus 10 μ m cassiterite by liquid-liquid extraction, Int. J. Min. Proc., 1, 1974, 335 - 345.
82. YAP, S.N., Adsorption and electrokinetic measurements in cassiterite-aqueous surfactant systems and oil-phase extraction studies, Ph.D. Thesis, Colorado School of Mines, 1975.
83. WINDLE, W., Improvements in or relating to the separation of minerals, British patent, 1,222,508, 1971.
84. OLIVIER, J.P., Process for treating minerals, U.S. patent, 3,432,030, 1969.
85. LOFTHOUSE, H., SHERGOLD, H.L., and WINDLE, N., Improvements in or relating to the treatment of minerals, Patent specif. no. 13174/73, filed in London 19th March, 1973.
86. LANGSTROTH, T.A., Pigment flushing, in 'Pigment Handbook', ed. Patton, T.C., Wiley, New York, 1973, 447 - 455.
87. BLACK, W., Surface-active compounds and their role in pigment dispersion, in 'Dispersion of Powders in Liquids', Applied Science, London, 1973, 132 - 174.
88. MOLLINET, J.L., The rate of surface active agents in processes for dispersing solids in liquid media, Proc. 2nd. International Congress of Surface Activity, 4, London, 1957, 162 - 167.
89. DU PONT and MARTANE, T.A., Improvements in or relating to the production of pigmented compositions, British patent, 546,785, 1942.
90. DU PONT, Improvements in or relating to the production of pigmented compositions in organic vehicles, British patent, 499,334, 1939.
91. BASS, D., Cationic surface-active agents in paint manufacture, Paint Manuf., 27, 1957, 5 - 9.
92. CHATFIELD, H.W., 'The Science of Surface Coatings', Ernest Benn Ltd., London, 1962, p. 320.
93. APPS, E.A., 'Printing Ink Technology', Leonard Hill Ltd., London, 1958, 499.
94. GOMM, A.S., HULL, G., and MOILLIET, J.L., The mechanism of pigment flushing processes, J. Oil Col. Chem. Assoc., 51, 1968, 143 - 160.
95. CHOWDHURY, S., Surface chemical studies of asbestos minerals, Ph.D. Thesis, London University, 1973, pp. 152 - 161.
96. BECHER, P., 'Emulsions: Theory and Practice', A.C.S. Monograph Series, Reinhold Publishing Co., New York, 1965.
97. WELLMAN, V.E., and TARTAR, H.V., A study of factors controlling type of water-soap-oil emulsions, J. Phys. Chem., 34 (2), 1930,

379 - 409.

98. KING, A., Some factors governing the stability of oil-in-water emulsions, Trans. Far. Soc., 37, 1941, 168 - 180.
99. CLOWES, G.H.A., Protoplasmic equilibrium. I. Action of antagonistic electrolytes on emulsions on living cells, J. Phys. Chem., 20, 1916, 407 - 50.
100. HARKINS, W.D., DAVIES, E.C.H., and CLARK, G.L., The orientation of molecules in the surfaces of liquids, the energy relations at surfaces, solubility, adsorption, emulsification, molecular association, and the effect of acids and bases on interfacial tension (Surface energy VI), J. Amer. Chem. Soc., 39, 1917, 541 - 596.
101. BANCROFT, W.D., The theory of emulsification, J. Phys. Chem., 17, 1913, 501 - 520.
102. BANCROFT, W.D., Theory of emulsification, J. Phys. Chem., 19, 1915, 275 - 309.
103. BANCROFT, W.D., and TUCKER, C.W., Gibbs on emulsification, J. Phys. Chem., 31, 1927, 1681 - 1691.
104. SCHULMAN, J.H., and STENHAGEN, E., Molecular interaction in monolayers. III. Complex formation in lipid monolayers, Proc. Roy. Soc. (London), 126B, 1938, 365 - 369.
105. SCHULMAN, J.H., and COCKBAIN, E.G., Molecular interactions at oil-water interfaces. Part I. Molecular complex formation and the stability of oil in water emulsions, Trans. Far. Soc., 36, 1940, 651 - 661.
106. SCHULMAN, J.H., and COCKBAIN, E.G., Molecular interactions at oil-water interfaces. Part II. Phase inversion and stability of water in oil emulsions, Trans. Far. Soc., 36, 1940, 661 - 668.
107. ALEXANDER, A.E., and SCHULMAN, J.H., Molecular interactions at oil-water interfaces. Part III. Interfacial tension measurements, Trans. Far. Soc., 36, 1940, 960 - 964.
108. COCKBAIN, E.G., and McROBERTS, T.S., The stability of elementary emulsion drops and emulsions, J. Colloid Sci., 8, 1953, 440 - 451.
109. ALEXANDER, A.E., Interfacial tension, viscosity and potential changes produced by insoluble monolayers at the oil-water interface, Trans. Far. Soc., 37, 1941, 117 - 121.
110. GILBERT, E.D., The dispersion of self-emulsifiable oils in aqueous solutions, Proc. 2nd. International Congress of Surface Activity, London, 1, 1957, 447 - 456.
111. MACKENZIE, J.M.W., Electrokinetic properties of nujol-flotation collector emulsion drops, Trans. A.I.M.E., 244, 1969, 393 - 400.
112. DAVIES, J.T., and RIDEAL, E.K., 'Interfacial Phenomena', Academic Press, London, 1961.

113. DIBBS, H.P., SIROIS, L.L., and BREDIN, R., Some electrical properties of bubbles and their role in the flotation of quartz, Can. Met. Q., 13 (2), 1974, 395 - 404.
114. VERWEY, E.J.W., Electrical double layer and stability of emulsions, Trans. Far. Soc., 36, 1940, 192 - 203.
115. VAN DEN TEMPEL, N., Stability of oil-in-water emulsions. I. The electrical double layer at the oil-water interface, Rec. Trav. Chim., 72, 1953, 419 - 432.
116. DERJAGUIN, B.V., and LANDAU, L., Theory of stability of strongly charged lyophobic sols and of the adhesion of strongly charged particles in solutions of electrolytes, Acta Physicochim. U.R.S.S., 14, 1941, 633 - 662.
117. VERWEY, E.J.W., and OVERBEEK, J.Th.G., 'Theory of the Stability of Lyophobic Colloids', Elsevier, Amsterdam, 1948.
118. PICKERING, S.U., Discussion of: Hatschek, E., The direct separation of emulsions by filtration and ultrafiltration, J. Soc. Chem. Ind., 29(3), 1910, 125 - 128.
119. BRIGGS, T.R., Emulsions with finely divided solids, Ind. Eng. Chem., 13 (11), 1921, 1008 - 1010.
120. BENNISTER, H.L., KING, A., and THOMAS, K., Stability of emulsions. III. A general survey of solid emulsifying agents with special reference to the hydrous oxides and hydroxides, J. Soc. Chem. Ind., 59, 1940, 226 - 232.
121. MUKERJEE, L.N., and SRIVASTAVA, S.N., Finely divided solids as emulsifiers. Part I. Emulsions stabilised by hydroxides or hydrous oxides of metals, Kolloid Z., 147 (3), 1956, 146 - 152.
122. MUKERJEE, L.N., and SRIVASTAVA, S.N., A study of olive oil emulsions with solid stabilizers, Kolloid Z., 170 (1), 1960, 32 - 35.
123. CHEESEMAN, D.F., and KING, A., The properties of dual emulsions, Trans. Far. Soc., 34, 1938, 594 - 598.
124. EVERY, R.L., WADE, W.H., and HACKERMAN, N., Free energy of adsorption. II. The influence of substrate structure in the systems Al_2O_3 and TiO_2 with n-hexane, CH_3OH and H_2O , J. Phys. Chem., 65 (6), 1961, 937 - 941.
125. AHMED, S.M., and MAKSIMOV, D., Studies of the double layer on cassiterite and rutile, J. Colloid Interface Sci., 29 (1), 1969, 97 - 104.
126. LAI, R.W.M., and FUERSTENAU, D.W., Model for the surface charge of oxides and flotation response, Trans. A.I.M.E., 260, 1976, 104 - 107.
127. PARKS, G.A., Aqueous surface chemistry of oxides and complex oxide minerals, Advances in Chem. Ser., 67, A.C.S., Washington, 1967, 121 - 160.

128. MACKENZIE, J.M.W., Zeta-potential studies in mineral processing: Measurement, techniques and applications, Min. Sci. Eng., 3 (3), 1971, 25 - 43.
129. PARKS, G.A., and DE BRUYN, P.L., The zero point of charge of oxides, J. Phys. Chem., 66 (6), 1962, 967 - 972.
130. cf. KRUYT, H.R., 'Colloid Science', 1, Elsevier, London, 1952, p. 132.
131. GOUY, Constitution of the electric charge at the surface of an electrolyte, J. Physique., 4 (9), 1910, 457 - 467.
132. CHAPMAN, D.L., A contribution to the theory of electrocapillarity, Phil. Mag., 25 (6), 1913, 475 - 481.
133. AVEYARD, R., and HAYDON, D.A., 'An introduction to the principles of surface chemistry', University Press, Cambridge, 1973, p. 43.
134. STERN, O., Zur theorie der electrolytischen doppelschicht, Z. Elektrochem., 30, 1924, 508 - 516.
135. GRAHAME, D.C., The electrical double layer and the theory of electrocapillarity, Chem. Rev., 41, 1947, 441 - 501.
136. BERUDE, Y.G., and DE BRUYN, F.L., Adsorption at the rutile-solution interface. II. Model of the electrochemical double layer, J. Colloid Interface Sci., 28 (1), 1968, 92 - 104.
137. FUERSTENAU, D.W., and HEALY, T.W., Principles of mineral flotation, in 'Adsorptive bubble separation techniques', ed. Lemlich, R., Wiley, New York, 1972, 91 - 131.
138. SOMASUNDARAN, P., HEALY, T.W., and FUERSTENAU, D.W., Surfactant adsorption at the solid-liquid interface - dependence of mechanism on chain length, J. Phys. Chem., 68 (12), 1964, 3562 - 3566.
139. SOMASUNDARAN, P., and FUERSTENAU, D.W., Mechanism of alkyl sulphonate adsorption at the alumina-water interface, J. Phys. Chem., 70 (1), 1966, 90 - 96.
140. MACKENZIE, J.M.W., Interactions between oil drops and mineral surfaces, Trans. A.I.M.E., 247, 1970, 202 - 208.
141. HAN, K.N., HEALY, T.W., and FUERSTENAU, D.W., The mechanism of adsorption of fatty acids and other surfactants at the oxide-water interface, J. Colloid Interface Sci., 44 (3), 1973, 407 - 414.
142. PURCELL, G., and SUN, S.C., Significance of double bonds in fatty acid flotation - an electrokinetic study, Trans. A.I.M.E., 226, 1963, 13 - 16.
143. CASES, J.M., On the normal interaction between adsorbed species and absorbing surface, Trans. A.I.M.E., 247, 1970, 123 - 127.
144. PREDALJ, J.J., and CASES, J.M., Thermodynamics of the adsorption of collectors, Proc. 10th. I.N.P.C., London, 1973, 473 - 493.

145. CASES, J.M., GOUJON, G., and SMANI, S., Adsorption of n-alkylamine chlorides on heterogeneous surfaces, A.I.Ch.E. Symp. Ser., 71, (150), 1975, 100 - 109.
146. FUERSTENAU, D.W., and RAGHAVAN, S., Some aspects of the thermodynamics of flotation, in 'Flotation. A.M. Gaudin Memorial Volume', ed. Fuerstenau, M.C., 1, 1976, 21 - 65.
147. GLEMBOTSKII, V.A., The hydrophobization effect of anionic collectors during flotation, in 'Flotation agents', Israel prog. scientific translations, 1970, 1 - 8.
148. GLEMBOTSKII, V.A., KLASSEN, V.I., and PLAKSIN, I.N., 'Flotation', Primary Sources, New York, 1963.
149. Private communication D. Young (Tioxide International) to Dr. J.A. Kitchener.
150. KUBASCHEWSKI, O., EVANS, E.LL., and ALCOCK, C.B., 'Metallurgical Thermochemistry', Pergamon Press, 1967, p. 428.
151. HUMPHREY, G.L., The heats of formation of TiO , Ti_2O_3 , Ti_3O_5 and TiO_2 from combustion calorimetry, J. Amer. Chem. Soc., 73 (4), 1951, 1587 - 1590.
152. READ, H.H., 'Rutley's Elements of Mineralogy', George Allen & Unwin Ltd., London, 1970, p. 348.
153. BREWER, L., The thermodynamic properties of the oxides and their vapourization processes, Chem. Revs., 52 (1), 1953, 1 - 75.
154. CZANDERNA, A.W., RAO, C.N.R., and HONIG, J.M., The anatase-rutile transition. Part I. Kinetics of the transformation of pure anatase, Trans. Far. Soc., 54 (7), 1958, 1069 - 1073.
155. RAO, C.N.R., YOGANARASIMHAN, S.R., and FAETH, P.A., Studies on the brookite-rutile transformation, Trans. Far. Soc., 57 (3), 1961, 504 - 510.
156. A.S.T.M. Reference 21 - 1276.
157. REHFELD, S.J., Adsorption of sodium dodecyl sulfate at various hydrocarbon-water interfaces, J. Phys. Chem., 71 (3), 1965, 738 - 745.
158. cf. SHINODA, K., NAKAGAWA, T., TAMAMUSHI, B., and ISEMURA, T., 'Colloidal surfactants: some physicochemical properties', Academic Press Inc., London, 1963, p. 7.
159. ELTON, G.A.H., The adsorption of cationic surface-active agents by silica and by octadecane, Proc. 2nd. International Congress of Surface Activity, London, 3, 1957, 161 - 164.
160. KLING, W., and LANGE, H., Interfacial tension of sodium alkyl sulphate solutions and n-heptane, Proc. 2nd. International Congress of Surface Activity, London, 1, 1957, 295 - 303.
161. RAISON, M., The Krafft point of binary mixtures of sodium alkyl sulphates, Proc. 2nd. International Congress of Surface Activity,

- London, 1, 1957, 374 - 379.
162. AVEYARD, R., and HAYDON, D.A., Thermodynamic properties of aliphatic hydrocarbon-water interfaces, Trans. Far. Soc., 61 (10), 1965, 2255 - 2261.
163. LINTON, M., and SUTHERLAND, K.L., Dynamic surface forces, drop circulation and liquid-liquid mass transfer, Proc. 2nd. International Congress of Surface Activity, London, 1, 1957, 494 - 502.
164. TIMMONS, C.O., and ZISMAN, W.A., The relation of initial spreading pressure of polar compounds on water to interfacial tension, work of adhesion and solubility, J. Colloid Interface Sci., 28 (1), 1968, 106 - 117.
165. Handbook of Chemistry and Physics, 53rd. edn., C.R.C. press, 1972 - 73.
166. OVERBEEK, J.Th.G., Electrokinetic phenomena, in 'Colloid Science', ed. Kruyt, H.R., Elsevier Publishing Co., 1, 1952, 194 - 244.
167. HENRY, D.C., The cataphoresis of suspended particles. Part I. The equation of cataphoresis, Proc. Roy. Soc., A133, 1931, 106 - 129.
168. ABRAMSON, H.A., MOYER, L.S., and GORIN, M.A., 'Electrophoresis of proteins and the chemistry of cell surfaces', Rheinhold, New York, 1942, p. 50.
169. HENRY, D.C., The electrophoresis of suspended particles. IV. The surface conductivity effect, Trans. Far. Soc., 44 (2), 1948, 1021 - 1026.
170. OVERBEEK, J.Th.G., Theory of electrophoresis - the relaxation effect, Kolloid Beih., 54, 1943, 287 - 364.
171. BOOTH, F., The cataphoresis of spherical, non-conducting particles in a symmetrical electrolyte, Proc. Roy. Soc., A203, 1950, 514 - 533.
172. WIERSEMA, P.H., LOEB, A.L., and OVERBEEK, J.Th.G., Calculation of the electrophoretic mobility of a spherical colloid particle, J. Colloid Interface Sci., 22 (1), 1966, 78 - 99.
173. KOMOGATA, S., Researches electrotech. lab. Japan, No. 348, 1933, 8 p.
174. MOYER, L.S., and ABRAMSON, H.A., Electrokinetic phenomena. XII. Electroosmotic and electrophoretic mobilities of protein surfaces in dilute salt solutions, J. Gen. Physiol., 19, 1935 - 6, 727 - 738.
175. GREGORY, G.R.F.C., The determination of residual anionic surface-active reagents in mineral flotation liquors, Analyst, 91, 1966, 251 - 257.
176. PEARCE, A.S., and STREAFIELD, E.L., Determination of amines in water, Ger. pat. 1,190,229, 1961, (Analyt. Abs., 12, 1965, 6766).

177. MUKERJEE, P., Use of ionic dyes in the analysis of ionic surfactants and other ionic organic compounds, Anal. Chem., 28, 1956, 870 - 873.
178. GADDUM, J.h., A simple method of measuring surface tension, Proc. Roy. Soc., B109, 1931, 114 - 125.
179. HARKINS, W.D., and BROWN, F.E., The determination of surface tension (free surface energy), and the weight of falling drops. The surface tension of water and benzene by the capillary height method, J. Am. Chem. Soc., 41, 1919, 449 - 524.
180. ADAM, N.K., 'The Physics and Chemistry of Surfaces', Oxford Univ. Press, 1938, p. 413.
181. HARKINS, W.D., Determination of surface and interfacial tension, in 'Physical Methods of Organic Chemistry', 1, ed. Weissberger, A., Interscience, 1949, 355 - 413.
182. WEINER, N.D., PARREIRA, H.C., and ZOGRAFI, G., Interfacial properties of antimicrobial long-chain quaternary ammonium salts, II, J. Pharm. Sci., 55 (2), 1966, 187 - 191.
183. COCKBAIN, E.G., and McMULLEN, A.J., Adsorbed films at oil-water interfaces, Trans. Far. Soc., 47, 1951, 322 - 330.
184. SHERGOLD, H.L., The flotation of ultra-fine particles, Ph.D. Thesis, London University, 1968.
185. CORNELL, R.M., POSNER, A.M., and QUIRK, J.P., A titrimetric and electrophoretic investigation of the p.z.c. and the i.e.p. of pigment rutile, J. Colloid Interface Sci., 53 (1), 1975, 6 - 13.
186. PARFITT, G.D., The surface of titanium dioxide, Prog. Surf. and Membrane Sci., 11, 1976, 181 - 226.
187. TANFORD, C., 'The Hydrophobic Effect', Wiley, New York, 1973.
188. RASTOGI, M.C., and SRIVASTAVA, B.S., Studies on titanium dioxide sols in the presence of surface active agents: Part 1 - pH, conductivity and zeta potential measurements, Indian J. Chem., 11 (9), 1973, 913 - 921.
189. PARFITT, G.D., and WHARTON, D.G., The dispersion of rutile powder in aqueous surfactant solutions, J. Colloid Interface Sci., 38 (2), 1972, 431 - 439.
190. MORIMOTO, T., and SAKAMOTO, M., The electrokinetic potential of titanium dioxide, Bull. Chem. Soc. Japan, 37 (5), 1964, 719 - 723.
191. JACKSON, P., and PARFITT, G.D., unpublished work.
192. WAKAMATSU, T., and FUERSTENAU, D.W., The effect of hydrocarbon chain length on adsorption of sulphonates at the solid/water interface, Adv. Chem. Ser., 79, A.C.S., Washington, 1968, 161 - 172.
193. DASS, S.K., Adsorption of dodecyltrimethylammonium chloride on

- alumina and its relation to oil-water flotation, Trans. I.M.M., 85, 1976, C195 - C199.
194. CASES, J.M., and MUTAFTSCHIEV, B., Adsorption et condensation des chlorhydrates d'alkylamine à l'interface solide-liquide, Surface Sci., 9, 1968, 57 - 72.
195. cf. ADAMSON, A.W., 'Physical Chemistry of Surfaces', Wiley, New York, 1960, p. 403.
196. ROGERS, J., Flotation of soluble salts, Trans. I.M.M., 66, 1957, 439 - 452.
197. GILES, C.H., MACEWAN, T.H., NAKHURA, S.N., and SMITH, D., Studies in adsorption. Part XI. A system of classification of solution isotherms, and its use in diagnosis of adsorption mechanisms and in measurement of specific surface areas of solids, J. Chem. Soc., 3, 1960, 3973 - 3993.
198. FREUNDLICH, H., 'Colloid and Capillary Chemistry', Methuen, London, 1926.
199. DE BRUYN, P.L., Flotation of quartz by cationic collectors, Trans. A.I.M.E., 202, 1955, 291 - 296.
200. JAYCOCK, M.J., and OTTEWILL, R.H., Adsorption of ionic surface active agents by charged solids, Trans. I.M.M., 72, 1963, 497 - 506.
201. FUERSTENAU, D.W., and WAKAMATSU, T., Effect of pH on the adsorption of sodium dodecane-sulphonate at the alumina/water interface, Disc. Far. Soc., 59, 1975, 157 - 168.
202. TER-MINASSIAN SARAGA, L., Discussion of ref. 200, Disc. Far. Soc., 59, 1975, p. 175.
203. OTTEWILL, R.H., RASTOGI, M.C., and WATANABE, A., The stability of hydrophobic sols in the presence of surface-active agents. Part I. Theoretical treatment, Trans. Far. Soc., 56, 1960, 854 - 865.
204. LANGMUIR, I., The adsorption of gases on plane surfaces of glass, mica and platinum, J. Amer. Chem. Soc., 40, 1918, 1361 - 1403.
205. HEJL, V., and SKRIVAN, P., On the bond between iongen collectors and corundum surface, Collect. Czech. Chem. Commun., 34 (12), 1969, 3978 - 3981.
206. MODI, H.J., and FUERSTENAU, D.W., The flotation of corundum - an electrochemical interpretation, Trans. A.I.M.E., 217, 1960, 381 - 387.
207. FUERSTENAU, D.W., and MODI, H.J., Streaming potentials of corundum in aqueous organic electrolyte, J. Electrochem. Soc., 106, 1959, 336 - 341.
208. JAYCOCK, M.J., OTTEWILL, R.H., and RASTOGI, M.C., The adsorption of cationic surface active agents, Proc. 3rd. International Congress of Surface Activity, Cologne, 2, 1960, 283 - 287.

209. TAMAMUSHI, B., and TAMAKI, K., Adsorption of long-chain electrolytes at the solid/liquid interface. Part 2. The adsorption on polar and non-polar adsorbents, Trans. Far. Soc., 55 (6), 1959, 1007 - 1012.
210. POPE, M.I., and SUTTON, D.I., The correlation between froth flotation response and collector adsorption from aqueous solution. Part 1. Titanium dioxide and ferric oxide conditioned in oleate solutions, Powder Tech., 7 (5), 1973, 271 - 279.
211. LEJA, J., Interaction at interfaces in relation to froth flotation, Proc. 2nd. International Congress of Surface Activity, London, 3, 1957, 273 - 296.
212. FRANK, H.S., and EVANS, M.W., Free volume and entropy in condensed systems. III. Entropy in binary liquid mixtures; partial molal entropy in dilute solutions, structure and thermodynamics in aqueous electrolytes, J. Chem. Phys., 13 (11), 1945, 507 - 532.
213. MATIJEVIC, E., and OTTEWILL, R.H., The formation of silver halide sols in the presence of cationic detergents, J. Colloid Sci., 13, 1958, 242 - 256.
214. JOY, A., and WATSON, D., Adsorption of collector and potential-determining ions in flotation of hematite with dodecylamine, Trans. I.M.M., 73, 1963-64, 323 - 334.
215. FUERSTENAU, D.W., and YAMADA, B.J., Neutral molecules in flotation collection, Trans. A.I.M.E., 223, 1962, 50 - 52.
216. DERJAGUIN, B.V., and SHCHERBAKOV, L.M., Effect of surface forces on phase equilibria of polymolecular layers and on the contact angle, Kolloidn. Zh., 23 (1), 1961, 40 - 52.
217. GAUDIN, A.M., WITT, A.F., and BISWAS, A.K., Hysteresis of contact angles in the system organic liquid-water-rutile, Trans. A.I.M.E., 229, 1964, 1 - 5.
218. HUIH, C., and MASON, S.G., Effects of surface roughness on wetting (theoretical), J. Colloid Interface Sci., 60 (1), 1977, 11 - 38.
219. BICKERMAN, J.J., Surface roughness and contact angles, J. Phys. Colloid Chem., 54 (5), 1950, 653 - 658.
220. WENZEL, R.N., Resistance of solid surfaces to wetting by water, Ind. Eng. Chem., 28 (8), 1936, 988 - 994.
221. CASSIE, A.B.D., Contact angles, Disc. Far. Soc., 3, 1948, 11 - 16.
222. GAUDIN, A.M., BANGS, L.B., and WITT, A.F., Hysteresis of contact angles in the system benzene/water/quartz, Proc. 7th. I.M.P.C., New York, 1964, 321 - 328.
223. GAUDIN, A.M., and DECKER, T.G., Contact angles and adsorption in the system quartz-water-dodecane modified by dodecyl ammonium chloride, J. Colloid Interface Sci., 24, 1967, 151 - 158.
224. ROGERS, J., SUTHERLAND, K.L., MARK, E.E., and MARK, I.W.,

- Principles of flotation - paraffin chain salts as flotation reagents, Trans. A.I.M.E., 69, 1946, 287 - 316.
225. EDWARDS, G.R., and EWEERS, W.E., The adsorption of sodium cetyl sulphate on cassiterite, Aust. J. Sci. Res., A4, 1951, 627 - 643.
226. GREBNEV, A.N., STEFANOVSKAYA, L.K., and KOSTAKOVA, M.N., Relation between the hydrocarbon chain length of alkyl sulphates and their flotation properties, Izv. Vysskikh. Uchebn. Zavedenii, Tvetn. Metal., 9 (3), 1966, 12 - 18.
227. SUTHERLAND, K.L., and WARK, I.W., 'Principles of Flotation', Australasian I.M.M., Melbourne, 1955.
228. GAUDIN, A.M., and MORROW, J.G., Adsorption of dodecylammonium acetate on hematite and its flotation effect, Min. Eng., 6, 1954, 1196 - 1202.
229. WADSWORTH, M.E., CONRADY, G.C., and COOK, M.A., Contact angle and surface coverage for potassium ethyl xanthate on galena according to free acid collector theory, J. Phys. Chem., 55, 1951, 1219 - 1230.
230. PHILIPPOFF, W., COOK, S.R.B., and CALDWELL, D.E., Contact angles and surface coverage, Min. Eng., 4, 1952, 283 - 286.
231. BILLET, D.F., and OTTEWILL, R.H., The dependence of contact angle on the adsorption of surface-active agents at the solid-liquid interface, in 'Wetting', S.C.I. monograph, 25, 1967, 253 - 271.
232. TER-MINASSIAN SARAGA, L., Sur une méthode directe d'étude de la densité superficielle des groupes acides à la surface du verre et de la silice vitrifiée, C.R. Acad. Sci. A., 252, 1961, 1596 - 1598.
233. COCKBAIN, E.G., The adsorption of sodium dodecyl sulphate at the oil-water interface and application of Gibb's equation, Trans. Far. Soc., 50 (8), 1954, 874 - 881.
234. MUKERJEE, P., The nature of the association equilibria and hydrophobic bonding in aqueous solutions of association colloids, Adv. Colloid Interface Sci., 1, 1967, 241 - 275.
235. MUKERJEE, P., NYSELS, K.J., and DULIN, D.I., Dilute solutions of amphipathic ions. I. Conductivity of strong salts and dimerization, J. Phys. Chem., 62 (11), 1958, 1390 - 1396.
236. FUOSS, R.M., and ONSAGER, L., Conductance of unassociated electrolytes, J. Phys. Chem., 61 (5), 1957, 668 - 682.
237. PARFITT, G.D., and SMITH, A.L., Conductivity of sodium dodecyl sulphate solutions below the critical micelle concentration, J. Phys. Chem., 66 (5), 1962, 942 - 943.
238. VAN VOORST VADER, F., The pre-association of surfactant ions, Trans. Far. Soc., 57 (3), 1961, 110 - 115.
239. SHEDULOVSKY, L., JAKOB, C.M., and EPSTEIN, M.B., Study of pNa of

- aqueous solutions of sodium decyl, dodecyl and tetradecyl sulfates by e.m.f. measurements, J. Phys. Chem., 67 (10), 1963, 2075 - 2079.
240. FRANKS, F., and SMITH, H.T., The association and hydration of sodium dodecyl sulfate in the submicellar concentration range, J. Phys. Chem., 68 (12), 1964, 3581 - 3584.
241. GILLAP, W.R., WEINER, N.D., and GIRIBALDI, M., Ideal behaviour of sodium alkyl sulphates at various interfaces. Thermodynamics of adsorption at the air/water interface, J. Phys. Chem., 72 (6), 1968, 2218 - 2221.
242. GILLAP, W.R., WEINER, N.D., and GIRIBALDI, M., Ideal behaviour of sodium alkyl sulphates at various interfaces. Thermodynamics of adsorption at the oil/water interface, J. Phys. Chem., 72 (6), 1968, 2222 - 2227.
243. MALAKHOVA, E.E., and ABRAMZON, A.A., Adsorption of surface-active agents at the liquid-liquid interface, Dokl. Akad. Nauk. S.S.R., 180 (5), 1968, 1157 - 1160.
244. AICKIN, R.G., The interfacial tension of sodium secondary alkyl sulphate solutions against oils, J. Soc. Dyers Colourists, 60 (2), 1944, 36 - 40.
245. VON SCHLUGER, M.J., Effect of counter ions on Krafft points and adsorption of n-tetradecyl sulfates, Kolloid-Z.Z. Polym., 233 (1-2), 1969, 979 - 985.
246. WALLACH, J., TER-MINASSIAN-SARAGA, L., and HANSS, M., Dimérisation du bromure d'hexadécyltriméthylammonium (C₁₆Br) étudiée par conductimétrie, C.R. Acad. Sci., C, 279 (3), 1974, 109 - 111.
247. DAVIES, J.T., The application of the Gibb's equation to charged monolayers, and their desorption from the oil-water interface, Trans. Far. Soc., 48, 1952, 1052 - 1061.
248. COCKBAIN, E.G., The adsorption of sodium dodecyl sulphate at the oil-water interface and application of the Gibb's equation, Trans. Far. Soc., 50, 1954, 874 - 881.
249. HAYDON, D.A., and PHILLIPS, J.N., The Gibb's equation and the surface equation of state for soluble ionized monolayers in absence of added electrolyte at the oil/water interface, Trans. Far. Soc., 54 (5), 1958, 698 - 704.
250. VAN VOORST VADER, F., Adsorption of detergents at the liquid-liquid interface (Part 1), Trans. Far. Soc., 56 (7), 1960, 1067 - 1078.
251. HARKINS, W.D., 'The Physical Chemistry of Surface Films', Reinhold, New York, 1952, p. 94.
252. LAVELLE, J.A., Spreading at the solid/oil/water interface, Ph. D. Thesis, Lehigh University, U.S.A., 1968.
253. BARTELL, F.E., and BARTELL, L.S., Quantitative correlation of interfacial free surface energies, J. Amer. Chem. Soc., 56 (11),

1934, '2205 - 2210.

254. OSTERHOF, H.J., and BARTELL, F.E., Three fundamental types of wetting. Adhesion tension as the measure of degree of wetting, J. Phys. Chem., 34, 1930, 1399 - 1411.
255. ZISMAN, W.A., Relation of the equilibrium contact angle to liquid and solid constitution, Adv. Chem. Ser., 43, A.C.S., Washington, 1964, 1.
256. GOOD, R.J., and GIRIFALCO, L.A., A theory for estimation of surface and interfacial energies. III. Estimation of surface energies of solids from contact angle data, J. Phys. Chem., 64 (5), 1960, 561 - 565.
257. DOBIÁŠ, VON B., and SPURNÝ, J., Die benützung von einigen alkyl-sulphaten und o-sulphonaten für die selektive flotation von fluorite und barite, Proc. 3rd. International Congress of Surface Activity, Cologne, 4, 1960, 396 - 403.
258. LAVELLE, J.A., and ZETTLEMOYER, A.C., Estimations of the dispersion and polar force contributions to heats of immersion and interaction energies of organic molecules with rutile and graphon surfaces, J. Phys. Chem., 71 (2), 1967, 414 - 417.
259. DAVIES, J.T., The distribution of ions under a charged monolayer, and a surface equation of state for charged films, Proc. Roy. Soc., A208, 1951, 224 - 247.
260. LIN, I.J., and METZER, A., Adsorption densities on interfaces in three-phase systems, J. Colloid Interface Sci., 40 (2), 1972, 137 - 141.
261. LEJA, J., and POLING, G.W., On the interpretation of contact angle, Proc. 5th. I.M.P.C., London, 1960, I.M.M., London, 325 - 341.
262. MELROSE, J.C., Evidence for solid-fluid interfacial tensions from contact angles, Adv. Chem. Ser., 43, A.C.S., Washington, 1964, 158 - 179.
263. GLEMBOTSKII, V.A., DMITRIEVA, G.M., and SOROKIN, M.M., 'Nonpolar flotation agents', Israel prog. scientific translations, 1970, 114 p.
264. McCLELLAN, A.L., 'Tables of Experimental Dipole Moments', M.H. Freeman & Co., San Fransisco, Calif., 1963.
265. DONAHUE, D.J., and BARTELL, F.E., The boundary tension at water/organic liquid interfaces, J. Phys. Chem., 56 (4), 1952, 480 - 484.
266. STEPHEN, H., and STEPHEN, T., 'Solubilities of Inorganic and Organic Compounds', 1, Macmillan & Co., New York, 1963.
267. SEIDALL, A., 'Solubilities of Organic Compounds', 4, Van Nostrand, New York, 1941.

.